UNIVERSITEIT VAN PRETORIA
UNIVERSITY OF PRETORIA
YUNIBESITHI YA PRETORIA

THE CONTRIBUTION OF MANGANESE OXIDES TO REDOX BUFFERING IN SELECTED SOILS OF THE SOUTH AFRICAN HIGHVELD

by

LEUSHANTHA MUDALY

Submitted in partial fulfilment of the requirements for the degree
MSc. Soil Science
In the Faculty of Natural and Agricultural Sciences
University of Pretoria
Pretoria

Supervisor:	**P.C. de Jager**
Co-supervisors:	**Professor M.V. Fey**
	Dr. J.H. van der Waals

November 2015

DECLARATION

I, Leushantha Mudaly declare that the dissertation, which I hereby submit for the degree MSc. Soil Science at the University of Pretoria, is my own work and has not previously been submitted by me for a degree at this or any other tertiary institution.

SIGNATURE: ..……..

DATE: …….

DEDICATION

In loving memory of my father, Peter Reddy (11.12.1948 – 01.01.2015).

Words will never truly be sufficient to express my love and gratitude for you and all the sacrifices you made for me. You taught me the true meaning of dedication, commitment and hard work. You will continue to live through me everyday through the life lessons and values you instilled in me. I dedicate this to you with all my love...

ACKNOWLEDGEMENTS

The financial assistance of the National Research Foundation (DAAD-NRF) towards this research is hereby acknowledged. Opinions expressed and conclusions arrived at, are those of the author and are not necessarily to be attributed to the DAAD-NRF.
I would also like to extend my thanks and appreciation to Terrasoil and the University of Pretoria for their generous financial contributions to my study.

A warm and heartfelt thank you to the following people who helped me see this study to fruition:
My supervisor, Chris de Jager, for his endless wisdom and guidance throughout my study. Thank you for your meticulous attention to detail and all your encouragement and support throughout the process.
My co-supervisors, Professor Martin Fey and Dr. Johan van der Waals, for their valuable advice and input as well as introducing me to the magical world of manganese.
Professor John Annandale for welcoming me to the University of Pretoria and his tireless encouragement and support ever since.
Ikenna Mbakwe for selflessly providing valuable contributions to this study.
Antoinette Buys for her guidance with SEM as well as the Microscopy and Microanalysis Unit at UP for the use of their facilities.
Jeanette Dykstra and Wiebke Grote for the expertise in XRF and XRD respectively from the Geology department at UP.
Dr. Cathy Clarke for her guidance and the use of equipment at the University of Stellenbosch for part of my study.
PS Rossouw and Dr. Piet-Louis Grundling for their invaluable contribution to this study.
The technical staff at the laboratory in the Department of Plant Production and Soil Science.
The academic staff at the Department of Plant Production and Soil Science for their support and guidance, in particular Dr. Diana Marais.
The departmental secretaries for their willingness to help with all administrative aspects of the project.
My husband, Malan, for his tireless love, support and encouragement especially during the more trying periods of this study.
My mother, Dolly, and sister, Venisha, for their endless love, support and faith in me.

My father, whose pride in me always pushed me to succeed.

Lastly, Bhagawan Sri Sathya Sai Baba for providing the strength and guidance to complete this study.

ABSTRACT

The definition of a wetland places great importance on inundation and saturated soil conditions. The use of redoximorphic features as a soil wetness indicator is widely practiced. The reduction of Fe^{3+} to Fe^{2+}, resulting in the formation of these features, is particularly diagnostic for wetland soils. The problem arises when investigating a soil that shows visible wetness but lacks these redoximorphic features. The interpretation of Fe^{2+} and mottle formation in soils is crucial to correctly assess the hydric status of soils, which has increased the importance of improved delineation guidelines. The study aimed to improve the parameter used to define soil wetness.

Different soils where wetlands had been identified were sampled and their difference in expression of redoximorphic features was investigated. The major difference between these soils was the manganese content, with manganiferous soils lacking the expression of mottles. Results from XRF abd chemical extractions indicated that the dolomites had the highest Mn content while the quartzites and granites had negligible Mn contents. It was not the soils with lower Fe contents that lacked redoximorphic features but rather those with higher Mn activity levels than Fe. Total electron demand (TED) appeared to be a more accurate measure of electron demand in the soils contributed by Mn than manganese electron demand (MED) did. The index of redox buffering was therefore TED as this showed the best correlation with Mn content. The quartzite and granite soils with low Mn contents and low TED exhibited mottling in their morphology. The vertic soils with higher Mn and TED showed very poor mottle expression. The dolomite soils with very high Mn contents and TED values lacked the expected redoximorphic features. The andesite soils collected as a sample of intermediary Mn content greater than the quartzite and granite but less than the vertic and dolomite soils also showed an appreciable TED.

Results from the study show that the dolomite derived soils, with higher Mn contents, have a much higher oxidative capacity compared to the granite and andesite soils, which lead to the conclusion that this was the main factor that prevented the expression of redoximorphic features in the selected soils investigated. It can therefore be concluded that Mn contributes to redox buffering in the soils investigated, preventing mottle expression where it is expected to

occur. These results challenge previous guidelines that use redoximorphic features as signs of wetness indicators to delineate wetlands.

TABLE OF CONTENTS

LIST OF FIGURES

LIST OF TABLES

Chapter one: Introduction and literature review

1.1 Introduction

The delineation of wetlands is a process that is based on the interpretation of various signs of the presence of water in landscapes. These signs include vegetation composition, position in the landscape, soil form and soil wetness indicators. Significant variation regarding the expression of redox morphology in different landscapes has been observed and this aspect introduces a large degree of variability in the interpretation of wetland characteristics and boundaries. Outcomes of wetland delineation exercises are used for administrative, legislative and sometimes criminal prosecution processes. It is therefore imperative that the variable expression of redox morphology in different landscapes be elucidated to improve the empirical underpinning of the regulatory processes dependent on the science. Understanding redoximorphic features is also central to the understanding of pedological processes and soil classification.

Redoximorphic features develop as a result of the reduction or partial reduction of ferric oxides in the soil and their subsequent mobilization and reoxidation. The determinant of signs of wetness is the presence of redoximorphic features in the soil, which manifest as mottles. In the presence of a reductant, which is an element or compound that donates electrons to another species during a redox reaction, Fe^{3+} is reduced to Fe^{2+}. In its reduced form, ferrous iron is mobile and can be transported in solution. Ferrous iron then accumulates in aerobic parts of the soil, where it oxidizes by combining with oxygen and forms spots of various colours. These are known as mottles. The reduction and removal of iron can also cause a colour change at the place where it was removed.

The development of these features, however, is still poorly understood and sometimes these features are conspicuously absent under conditions where they are expected to occur. This leads to the postulation that the redoximorphic features in the soil are being buffered in some way. There is therefore a need to understand what is preventing the appearance of mottles in hydric soils.

The aim of this study is to investigate what causes the buffering of the formation of redoximorphic features in certain hydric soils. Extensive work has been done on the

characteristics of iron oxides, particularly by Schwertmann, however there is a knowledge gap regarding the effects of manganese oxides. Results from this study can hopefully improve guidelines used for wetland delineation in South Africa. This topic also has broader applications in other areas of soil classification and agriculture.

The hypothesis of the study is that soils with high easily reducible Mn contents lack the expression of redoximorphic features. The objectives of the study are to investigate soils derived from different geologies which differ in their expression of mottles. This will be done by examining the relationship between Mn content and redox buffering in these soils.

Chapter one is a literature review and provides a background to the study. Chapter two describes the sites where the samples were taken and includes a basic chemical and physical characterization of the soils sampled. The third chapter looks at where Mn resides in the soils in order to determine its reactivity. Chapter four investigates the differences in electron demand and therefore redox buffer capacity of the different soils. The relationship between certain soil properties and redox buffering is also investigated. Chapter five includes exploratory investigations looking at the influence of drying on Mn solubility and therefore reactivity as well as the effect of matric potential on redox buffering. The last chapter is a synthesis of the findings from the study followed by references. Appendix A to D provides supplementary data for the relevant chapters and references for the appendices follow this.

1.2 Literature review

1.2.1 Introduction

Hydric soils include soils that develop under sufficiently wet conditions to support the growth and regeneration of hydrophytic vegetation. The morphology of a hydromorphic soil is a result of water-related processes. Grey/gley features are produced when the soils are submersed below the water table continually. Redoximorphic features are created when soils are submerged periodically (Fiedler et al., 2007). Oxyaquic conditions, whereby soils are wet but do not develop reducing conditions (Rabenhorst & Parikh, 2000), exist in hydromorphic soils. A wetland soil is similar to a hydromorphic soil with the only difference being that hydromorphic soils may not be subjected to reduction and wetland soils are definitely reduced (Fiedler et al., 2007). According to the National Water Act, Act No. 36 of 1998, wetlands are “land which is transitional between terrestrial and aquatic systems where the water table is usually at or near the surface or the land is periodically covered with shallow

water, and which land in normal circumstances supports or would support vegetation typically adapted to life in saturated soil" (Swanepoel et al., 2008). The emphasis here is on saturated soils and their signatures.

The definition of a wetland is vague and unscientific, lending itself to various interpretations. One particularly unclear term in the definition is the period of saturation because the length (hours, days, weeks) of this period is not specified, which has major practical implications (Bouma, 1983). The length of time would also vary for different soil types, depending on the oxidation capacity of the soil. Over the years however, scientific investigations, legal opinions, and regulatory agencies have focused on vegetative, soil and hydrologic parameters as diagnostic indicators (Faulkner et al., 1989). What is prominent in the wetland definition is the importance of inundation and saturated soil conditions (Faulkner et al., 1989). The use of redoximorphic features as a soil wetness indicator is widely practiced. For some soils, however, mottle interpretation is inadequate, resulting in incorrect evaluations of land use potential (Vepraskas & Bouma, 1976). Redoximorphic features are known to have exceptions to the rule and cannot be applied to every situation (Swanepoel et al., 2008). Determining these soil limitations is very important for interpretive purposes (Bouma, 1983).

In the last few years delineation of wetland areas, as well as wetland environmental issues, such as impacts of mining, urban development and agriculture on wetlands, have become a major concern (Megonigal et al., 1993; Fiedler et al., 2007). The reduction of Fe^{3+} to Fe^{2+} is particularly diagnostic for wetland soils (Faulkner et al., 1989; Swanepoel et al., 2008) with Fe^{2+} resulting in mottle formation used as an important signs of wetness indicator of hydric soils (Megonigal et al., 1993). The interpretation of Fe^{2+} with regards to its re-oxidation and mottle formation in soils is therefore critical to correctly assess the hydric status of soils (Faulkner et al., 1989). It has also increased the importance of improved wetland delineation procedures and guidelines (Fiedler et al., 2007). More significantly it provides insight into the hydrology of the landscape. The correct interpretation of soil morphological features requires an understanding of chemical processes that govern them (Bouma, 1983).

The correct identification of hydric soils goes far beyond the scope of wetlands. There is an urgent need to better understand the soil system in order to practice sustainable and healthy management in an effort to protect the soil itself, as well as the surrounding environment (Stepniewski et al., 2002). It also has importance for the identification of waste disposal sites

(Rabenhorst & Parikh, 2000) and is imperative for construction purposes to ensure minimal impact on the hydrology of the landscape. The use of marginal soils for non-agricultural purposes requires large amounts of money and it is therefore very important to evaluate land use potential of soils adequately. One of the most important soil characteristics to evaluate is soil moisture regime, in particular the degree and duration of saturation (Vepraskas & Bouma, 1976). The verification of the relationship between redoximorphic features and the occurrence and duration of seasonal saturation is also very important to assist land managers and environmental officials with the correct classification of soils and to protect surface and ground water quality (Jacobs et al., 2002). The research from this study also has value in the field of soil geomorphology which expresses the relationship between landscape evolution and soil genesis. It allows geomorphologists to estimate the approximate age of a geomorphic surface in the field as well as soil scientists to indicate drainage conditions and pedogenetic processes (Lin et al., 2005).

There are several soil physical and chemical properties that contribute to the suppression of redoximorphic features where they are expected to exist. These will be addressed in subsequent chapters. There is a knowledge gap, however, when it comes to the role of Mn oxides owing to difficulties in studying Mn mineralogy as well as challenges in accurately quantifying the different Mn species in soil. This is due to their poor crystallinity, low abundance in most soils and their small crystal sizes (Negrac et al., 2005). Manganese^{4+} is the paramount "parking space" for electrons, taking precedence over O_2 because Mn provides O_2, oxidizing O^{2-} in H_2O during photosynthesis to O_2 (zero valent oxygen) (Bartlett, 1988). It plays a strong and active role in soil redox processes (Davison & Woof, 1984; Bartlett, 1988). Manganese provides a poised but sensitive pe environment ready for redox change in either the oxidative or reductive direction (Bartlett, 1988). A study by Dowding & Fey (2007) contributed to speculation that Mn oxides play a role in redox buffering, providing an inertia favouring the persistence of Mn oxides.

1.2.2 Manganese oxides in soils

Manganese is the 12th most abundant element in Earth's crust (about 12 mmol.kg^{-1} Mn) (Gilkes & McKenzie, 1988; Post, 1999; Hardie et al., 2007; Reddy & Delaune, 2008). Manganese can exist in soil solution, sorbed onto mineral surfaces and organic matter or incorporated into organisms, however it is usually a constituent of primary and secondary minerals (Gilkes & McKenzie, 1988; Bartlett 1988). It is commonly found in the fine-grain

fraction of the soils and occurs as dispersed particles, small nodules or concretions, deposited in cracks and veins, coatings on ped surfaces and stains on soil aggregates or associated with inorganic constituents (McKenzie, 1976; Phillips et al., 1998; Negrac et al., 2005). It is an essential constituent in over 250 minerals and is a minor substituent for essential structural ions, such as Fe^{2+} and Mg^{2+}, in several thousand minerals (Gilkes & McKenzie, 1988). Manganese is essential for plant and animal nutrition but can be toxic in high concentrations (McKenzie, 1976; Golden et al., 1993; Pittman, 2005; Nogueira et al., 2007).

Manganese is present in rock and soil minerals as soluble Mn^{2+}, and insoluble Mn^{3+} and Mn^{4+} with the predominant oxidation state being 2+ (Sparrow & Uren, 1987; Gilkes & McKenzie, 1988; Hardie et al., 2007; Nogueira et al., 2007). Manganese^{3+} is extremely reactive and cannot persist for long without being oxidized to Mn^{4+} or reduced to Mn^{2+} (Bartlett, 1988). Under acidic conditions, however, it can persist for longer periods. It is stable in minerals, such as MnOOH and Mn_3O_4, and only slowly reactive when bound to organic acids. One of the most powerful oxidizing agents in soil (only second to the hydroxyl free radical) as well as one of the most powerful reducing agents is Mn^{3+} (Bartlett, 1988). Trivalent Mn can undergo dismutation to generate Mn^{2+} and Mn^{4+} as products (Fujimoto & Sherman, 1948). Manganese in the 3+ and 4+ valencies are generally found as oxides in oxidizing environments in neutral to alkaline conditions when bacterial oxidation is rapid and organic matter reduction is low (McKenzie, 1972; Gilkes & McKenzie, 1988; Golden et al., 1993). The form of Mn^{2+} is dominant under strongly acidic conditions where microbial activity is low and reduction by organic matter is high, and this form of Mn exists in solution (McKenzie, 1972; Gilkes & McKenzie, 1988; Golden et al., 1993).

Manganese in flooded soils exists as water soluble Mn^{2+}, exchangeable Mn^{2+}, reducible Mn^{3+} and/or Mn^{4+}, and residual Mn in soil minerals (Gotoh & Patrick, 1972). Exchangeable Mn^{2+} provides an immediate source of Mn whereas easily reducible Mn^{3+} and Mn^{4+} produce Mn^{2+} after reduction (Dion et al., 1946). Soil Mn has been classified as active, moderately active and inert groups with the active forms being freshly precipitated colloidal fractions (Dion et al., 1946). It is suggested that the various Mn oxides differ in reducibility (Dion et al., 1946).

When the soil experiences waterlogging, a certain amount of Mn will be reduced and dissolved (McKenzie, 1976). During waterlogging, Mn is reduced and becomes mobile. Under aerobic conditions when the soil starts to dry, Mn is oxidized and precipitates around

localized nuclei (McKenzie, 1976). Oxidation of Mn^{2+}, which is rapid, is mainly achieved biologically or by oxygen whereas reduction of the insoluble forms is mostly chemical (McKenzie, 1972; Sparrow & Uren, 1987). High concentrations of Mn^{2+} can result from previous waterlogging or extreme drying in the field (Sparrow & Uren, 1987).

Soil Mn seems to be the key to the spectrum of soil behaviour (Bartlett & James, 1995). Manganese reactions in soils are regulated chemically by thermodynamics and kinetics as well as biologically (Gotoh & Patrick, 1972). The complex interaction of these processes makes it difficult to explain the behaviour of Mn in soil (Gotoh & Patrick, 1972). Manganese oxides are the most effective promoters of oxidation and act as oxidizing agents for many organic and inorganic chemical species (Gilkes & McKenzie, 1988; Negrac et al., 2005). These reactions involve the reduction of Mn^{3+} and/or Mn^{4+}, which is thermodynamically favourable, except at a very acidic pH (Gilkes & McKenzie, 1988).

Manganese in soils is usually present in small amounts (Yaalon et al., 1972), however, their chemical influence is much greater than suggested by this (Bartlett 1988; Post, 1999; Negrac et al., 2005). The high reactivity can be explained by Mn oxide surface characteristics such as the high specific surface area of the microcrystals (± 10 nm) of Mn oxides as well as their high exchange capacity (Gilkes & McKenzie, 1988; Vodyanitskii, 2009), the poor crystallinity of the minerals (McKenzie, 1976; Negrac et al., 2005) and their dynamic redox behaviour in general (Negrac et al., 2005). They also have a low point of zero charge (PZC), which ranges from 1.5 for birnessite to 4.6 in hollandite (Gilkes & McKenzie, 1988) and tends to increase with crystallinity (McKenzie, 1972). At common soil pH values, therefore, minerals develop a high negative surface charge (McKenzie, 1972; Gilkes & McKenzie, 1988) enabling their high sorption capacities (McKenzie, 1972). High sorption capacities can also be explained by the large surface areas of the crystals, contributing to a relatively high CEC of Mn oxides.

The oxides of Mn vary according to the arrangement and linkage of octahedral sheets taking the form of layered, hybrid (mixed-layered) and tunnel structures (Negrac et al., 2005; Vodyanitskii, 2009). A wide range of layer charges and compositions are possible due to the varying redox conditions and chemical constituents available during Mn formation (Negrac et al., 2005). They are mostly amorphous or finely crystalline, however crystalline forms have been reported (McKenzie, 1976). The most common Mn oxide minerals in soils are

birnessite, lithiophorite and hollandite (McKenzie, 1972). The following is a brief description of properties of some of the Mn oxides in soils:

i. **Pyrolusite (MnO_2):** This is most commonly found in ore deposits. It is the most stable form of MnO_2 in the supergene environment. It is commonly found when environmental conditions favour thermodynamic equilibrium.

ii. **Nsutite ($(Mn^{4+},Mn^{2+})(O,OH)_2$):** This is a general name for a family of oxides which occur widely in mineral deposits.

iii. **Birnessite ($(Na,Ca)_{0.5}(Mn^{4+},Mn^{3+})_2O_4 \cdot 1.5H_2O$):** This is a family of disperse forms of Mn oxides. It is one of the most common Mn minerals in soils. It is also found in mineral deposits.

iv. **Lithiophorite ($(Al,Li)MnO_2(OH)_2$):** This is one of the most common Mn minerals found in soils.

v. **Todokorite (Mn_6O_{12}-$3H_2O$):** This is found in soils and ore deposits. It appears to be an intermediate product from the oxidation of lower Mn oxides to pyrolusite.

vi. **Cryptomelane ($K(Mn_7^{4+}Mn^{3+})O_{16}$) and hollandite ($Ba(Mn_6^{4+}Mn_2^{3+})O_{16}$):** This is less common than birnessite and lithiophorite in soils (McKenzie, 1972).

Along with the pure Mn oxides, Mn-containing oxides are found as well (Vodyanitskii, 2009). These minerals are Fe-containing vernadite and Mn-containing ferric minerals such as feroxyhyte, ferrihydrite, and magnetite. The Fe-vernadite and Mn-feroxyhyte are the most common minerals with Mn and Fe existing as impurities respectively (Vodyanitskii, 2009).

Manganese oxides in soils are often closely related to iron oxides in nodules, which generally occur in horizons that undergo seasonal waterlogging (Yaalon et al., 1972; Gilkes & McKenzie, 1988; Phillips et al., 1998). The oxidation of Fe^{2+} occurs faster in the presence of Mn oxides than in pure solution or the presence of Fe oxides (Gilkes & McKenzie, 1988). Studies show that Fe oxides crystallize at sites where Fe and/or Mn oxides are present, however Mn only crystallizes where both Fe and Mn oxides are present (McKenzie, 1976; Gilkes & McKenzie, 1988).

1.2.3 The development of redoximorphic features

The chemistry of living organisms relies heavily on reduction-oxidation (redox) reactions and electron fluxes do not always receive the attention it deserves in many disciplines (Husson, 2013). Oxidation occurs when an atom loses an electron and reduction is the reverse of this chemical process whereby an atom gains an electron (Fiedler et al., 2007). Oxidation favours a lower pH due to the production of protons. Reduction processes on the other hand consume protons, resulting in an increased pH (Frohne et al., 2011).

Soil mineral transformations can be affected by the frequency of changes in redox status (Thompson et al., 2006). Redox reactions stimulate pedogenetic responses, which in turn result in the field identification of and differentiation between hydric and non-hydric soils (Fiedler et al., 2007). The most critical redox reactions occur in soil environments where oxygen (O_2) is partially restricted (Bartlett, 1988). Soil redox reactions control the development of redoximorphic features (van Huyssteen, 2008). Most chemical studies focus on the redox processes that govern iron (Fe) and manganese (Mn) as these elements result in visible redoximorphic features (Bouma, 1983). Redox chemistry controls the precipitation and dissolution of Fe and Mn oxides (Martin, 2005). The combination of redox transformations and transport processes leads to Fe and Mn cycling between aerobic and anaerobic parts of surface sediments (Van Cappellen & Wang, 1996).

Fluctuating water tables resulting from seasonal rainfall variations and evapotranspiration result in alternating oxidizing and reducing conditions (Rabenhorst & Parikh, 2000). These fluctuations cause the Fe coatings on soil particles to alternate between oxidized and reduced forms (Fiedler et al., 2007). Under anaerobic, reducing conditions, ferric iron (Fe^{3+}) residing in oxides are reduced to the soluble form, ferrous iron (Fe^{2+}) (Rabenhorst & Parikh, 2000). Saturation of a few weeks is sufficient for Fe reduction to occur in the presence of sufficient electron donors. Microbial activity controls redox reactions to a large extent in the soil (Fiedler et al., 2007) and is therefore responsible for this reduction. Aerobic microorganisms use O_2 as an electron acceptor in aerobic soils because this releases the most energy. When the soil is saturated however, O_2 is excluded from the soil and facultative anaerobic as well as obligatory anaerobic bacteria take over (Fiedler et al., 2007; van Huyssteen, 2008).

In order for reduction to occur, therefore, the conditions that are necessary are the presence of organic matter, the absence of an O_2 supply, and the presence of anaerobic organisms in an

environment suitable for their growth (Bouma, 1983). Under saturated conditions, water replaces air in macropores, sealing the soil off from the atmosphere. Biological activity rapidly depletes available O_2, creating anaerobic conditions (Faulkner et al., 1989; De Schamphelaire et al., 2007). Anaerobic bacteria are then able to use other electron acceptors, which release increasingly less energy to the microbes and follow a strict sequence for reduction in soils (van Huyssteen, 2008). This sequential order of accepting preferences is NO_3^-> $Mn^{3+/4+}$> Fe^{3+}> SO_4^{2-}> CO_2^-> H_2 (Bouma, 1983; Faulkner et al., 1989; Fiedler & Sommer, 2004; Fiedler et al., 2007; Ferreira et al., 2007). Sequential reduction is predicted by thermodynamics (Ponnamperuma, 1972) and is largely governed by their strength as oxidizing agents in the soils (Faulkner et al., 1989). Generally the electron acceptor with the highest redox potential (Eh) will be reduced first (De Schamphelaire et al., 2007). Oxidation processes follow the reverse order, therefore Fe^{2+}, for example, is oxidized before Mn^{2+} (Bouma, 1983).

In its mobile form, Fe^{2+} can be transported in the soil solution along redox gradients and is lost with outflowing water under reducing conditions (Fiedler & Sommer, 2004) leaving behind Fe depleted zones (Rabenhorst & Parikh, 2000). Once the Fe^{2+}- specific threshold of Eh value is exceeded, Fe becomes immobilized and is transported to an oxidized area where it precipitates (van Huyssteen, 2008) and accumulates (Fiedler & Sommer, 2004) under oxidizing conditions, resulting in Fe enriched zones (Rabenhorst & Parikh, 2000). A redox enriched zone has more Fe than the surrounding matrix (van Huyssteen, 2008).

Depleted zones generally reflect the grey or white colour of the uncoated mineral grains. In extreme cases, Fe oxides are removed completely from the soil, resulting in a depleted, gleyed soil matrix. Ferric Fe is a strong colour agent but ferrous Fe is not (Fiedler & Sommer, 2004). The areas of Fe accumulation, however, appear redder or browner than the soil matrix and are known as mottles or redoximorphic features (Rabenhorst & Parikh, 2000). Manganese oxides are strong soil pigments and give rise to dark brown to black colours. They are less abundant than Fe oxides and therefore often have a minimal effect on soil colour unless they are concentrated as coatings, nodules or concretions (Rabenhorst & Parikh, 2000). Reductive dissolution of Fe^{3+} and $Mn^{3+/4+}$ gives rise to redoximorphic features in the form of mottling and/or gleying (Chadwick & Chorover, 2001). Elemental redistribution is therefore responsible for the formation of redoximorphic features (Fiedler et al., 2007).

The term mottling means “marked with spots of different colour” (Bouma, 1983) and are sometimes referred to as “paints of the earth” (Fiedler et al, 2007). Mottles are “spots, blotches or streaks of subdominant colours” that differ from the soil matrix colour as well as the colour of ped surfaces (Singh & Gilkes, 1996). Mottles can be described as having chromas of ≤ 2, implying saturation for at least some period of the year (Bouma, 1983). Redoximorphic features can take the form of mottles, nodules, concretions and any other morphological features associated with redox reactions involving Fe and Mn (Fiedler et al., 2007). These distinctive colour patterns are used to interpret soil drainage and hydrological conditions (Rabenhorst & Parikh, 2000) and link soil morphology with saturation (van Huyssteen, 2008). These features reflect the effects of soil moisture regime and associated intermittent redox processes over long periods of time (Bouma, 1983).

1.2.4 The use of redoximorphic features as a determinant of signs of wetness and the associated challenges thereof

Direct physical measurements to determine soil moisture regimes can be costly and complex. Monitoring should also ideally be done over several years to gain a good estimate over a wide range of conditions. These challenges are partly the reason for the use of morphological indicators, such as mottles (Bouma, 1983). Soil colour can be very revealing about its character (Rabenhorst & Parikh, 2000) as well as a good general indicator of redox processes (Fiedler & Sommer, 2004). Studies of the relationship between saturation and soil colour have been well documented, with a particular focus on redoximorphic features (Jacobs et al., 2002).

Soil mottles are a great tool to predict soil moisture in undrained soil. The size, abundance and contrast of mottles provide an indication of relative degrees of wetness (Vepraskas & Bouma, 1976) and acts as a measure of pedogenic processes (Singh & Gilkes, 1996). Redoximorphic features have been used as soil wetness indicators for over 30 years (Fiedler & Sommer, 2004). Hydric soils are defined as having formed “under conditions of water saturation, flooding, or ponding long enough during the growing season to develop anaerobic conditions in the upper part” (Fiedler et al., 2007). The identification of hydric soils is often based on soil morphology with the two commonly used characteristics being matrix colours of high values and low chromas and the presence of Fe concentrations (Gotoh & Patrick, 1972).

Soil classification and interpretation, such as wetland delineations, is often linked to the presence and location of redoximorphic features (Rabenhorst & Parikh, 2000). It has been well documented that the use of pedogenic and morphological indicators can lead to erroneous or false conclusions (Fiedler & Sommer, 2004). There have been field cases documented by soil scientists where soils had seasonally high water tables but lacked the redoximorphic features typical of hydric soils (Rabenhorst & Parikh, 2000). In some cases this phenomenon has been attributed to oxyaquic conditions, whereby soils are wet but do not develop reducing conditions (Rabenhorst & Parikh, 2000). It is possible that if the easily reducible Mn content is high or there is low organic matter content and/or low pH, the Eh may remain positive for about six months or longer (Bouma, 1983). Identification and interpretation is therefore complicated due to the complex soil forming processes dominated by redox chemistry (Fiedler & Sommer, 2004).

1.2.5 The prevention of the appearance of redoximorphic features

The presence of Fe^{2+} is used as an indicator of hydric character in soil (Bartlett & James, 1995) and the reduction of Fe^{3+} to Fe^{2+} is particularly diagnostic for wetland soils (Faulkner et al., 1989). The reduction of NO_3^- follows O_2 depletion and this is followed closely by the reduction of Mn^{3+} and/or Mn^{4+}. The reduction of Fe^{3+} only occurs after the preceding elements have been exhausted (Faulkner et al., 1989). The absence of Fe^{2+}, however, does not necessarily mean that the soil is not anaerobic at other times of the year (Faulkner et al., 1989). The formation of redoximorphic features, as well as the intensity of its expression, is site specific and does not always relate to the period of saturation (Fiedler & Sommer, 2004). An important note to bear in mind is that the presence of mottles does indicate wet conditions, however, a lack of mottles does not necessarily imply lack of saturation (Bouma, 1983).

There are several possible explanations for the reticence of certain soils with seasonally high water tables to develop redoximorphic features. They can fall into two categories: **(i)** related to chemical and physical conditions in the soil environment; **(ii)** related to inherent soil properties (Rabenhorst & Parikh, 2000).

i) Related to chemical and physical conditions in the soil environment:

Oxyaquic environments describe soil conditions where soil is wet but not reducing with respect to Fe. These conditions are prevalent when there is either low organic matter content

in the soil, biological activity is limited, or rapid groundwater flow prevents O_2 depletion (Rabenhorst & Parikh, 2000). Another example of the influence of organic matter is that it sometimes coats redoximorphic features (Fiedler & Sommer, 2004). Horizons with redoximorphic features also occur deeper in the soil, where there is a decrease in organic carbon content, which could limit biological reduction of Fe (Jacobs et al., 2002) due to a lack of energy sources (Bouma, 1983). Organic matter therefore plays an important role in controlling the intensity of reduction (Glinski et al., 1992).

Several soil forming factors also influence the development of redoximorphic features. It is unknown, however, how long it takes for colour patterns to respond to changes in soil forming factors as well as to what extent soil colour represents former conditions or how representative it is of current conditions (Franzmeier et al., 1983). A study by Malo et al. (2006) revealed that the properties of temperature, with extreme temperatures inhibiting microbial activity (Swanepoel et al., 2008), and time influence aerobic/anaerobic conditions, which in turn has an effect on the production of Fe^{2+}, and therefore redoximorphic feature formation and matrix colour (Glinski et al., 1992; Malo et al., 2006). Biota is of extreme importance as microbial activity drives reduction in soil. If conditions such as pH and temperature are unsuitable for microbial activity, Fe reduction is limited, resulting in redoximorphic features taking longer to form (Swanepoel et al., 2008).

Other soil conditions can also affect the development of redoximorphic features. Similar morphological features to the one developed by redox processes may also arise from elemental translocations under acidic conditions (Fiedler & Sommer, 2004). In this environment, anaerobic conditions may not exist, however Fe^{2+} is favoured at low pH and therefore the soil morphology may be inconsistent with the landscape, vegetation or hydrology (Swanepoel et al., 2008). An alkaline environment, on the other hand, favours Fe^{3+} over Fe^{2+} and therefore redoximorphic features may be absent under these conditions even if the environment is anaerobic (Swanepoel et al., 2008). The chemical properties of Fe itself, as well as due to the transitory nature of Fe^{2+}, make its use as a hydric soil indicator misleading (Bartlett & James, 1995). Similarly to Mn^{2+}, when a hydric soil begins to dry out, Fe^{2+} is oxidized to Fe^{3+} (Bartlett & James, 1995), which influences the formation of redoximorphic features. On the other hand, there are chemical and mineralogical changes which do not necessarily result in visible features but are also induced by periodic saturation (Bouma, 1983).

ii) Related to inherent soil properties:

In some cases soil parent material plays an important role (Rabenhorst & Parikh, 2000), in particular soil sediment colour. One such inherent property is original sediment colour (Bouma, 1983). Inherited soil colour from parent material used as an indicator can lead to erroneous conclusions (Fiedler & Sommer, 2004). Among these are soils derived from red parent materials, however, not all soils with red parent materials show difficulty in exhibiting redoximorphic features (Rabenhorst & Parikh, 2000).

Another example is the colour of uncoated minerals may be inherently brown, preventing the soil from exhibiting low chroma, grey colours, even once Fe is removed (Rabenhorst & Parikh, 2000). This is not common but can occur when Fe oxides are occluded within mineral grains, such as quartz, or small lithic fragments of shales or silt stones. This isolates Fe from reducing conditions resulting in the soil retaining high chroma colours (Rabenhorst & Parikh, 2000).

Soil parent material can also play a role in redoximorphic feature formation if the original material from which the soil is derived has a low Fe content. If this is the case, the formation of mottles may be few and far between (Swanepoel et al., 2008). Another soil forming factor that plays a role is soil texture. Studies have shown that poorly drained soils coarse textured soils have an absence of low chroma mottles (Swanepoel et al., 2008).

Soil properties also pose a challenge to the use of redoximorphic features as morphological indicators by these features reflecting a relict soil moisture regime that has survived from an earlier period, and not the current one (Bouma, 1983; Fiedler & Sommer, 2004). A relict moisture regime may be associated with a previous climate or undrained soil that was drained by tile drainage (Bouma, 1983). A study by Jacobs et al. (2002) showed the soils in the lower part of the landscape exhibit a relationship between saturation and redoximorphic features. The soils in upland and backslope positions, however, do not have this relationship even though redoximorphic features are evident. This is likely due to the redoximorphic features in these soils being relict, formed before the incision of the landscape.

Another reason may be that some Fe oxides may be more resistant to reduction than others. The most commonly occurring Fe oxide minerals in soils are goethite (α-FeOOH), hematite (α-Fe_2O_3), ferrihydrite ($5Fe_2O_3 \cdot 9H_20$) and lepidocrocite (γ-FeOOH). Thermodynamics reveal

that the solubility products of goethite and hematite are very similar, both having pK values in the range of 42.2 – 44. Ferrihydrite (pK = 37 – 39.4) and lepidocrocite (40.6 – 42.5), however, have pK values orders of magnitude lower. It is therefore expected that goethite and hematite are the most common Fe oxides found in soils as they are the more stable phases (Barrow & Torrent, 1987; Rabenhorst & Parikh, 2000). Goethite and hematite are generally found in highly weathered soils of tropical and sub-tropical regions (Singh & Gilkes, 1992). It has been shown by Fey (1981) that aluminium (Al) substitution in these two minerals lowers their propensity for reduction and solubilisation. The dissolution of Fe oxides decreases as Al–substitution increases (Fritsch et al., 2005). Goethite can accommodate about 33 mol percent aluminium (Al) in its structure while hematite can incorporate about half of this, accommodating about 16 mol percent (Barrow & Torrent, 1987; Rabenhorst & Parikh, 2000; Kusuyama et al., 2002; Fritsch et al., 2005). Several studies have investigated the phenomenon of normally occurring goethites being less susceptible to reduction than hematites (Fey 1981; Rabenhorst & Parikh, 2000; Fritsch et al., 2005), which consequently results in pedogenic yellowing of red soil material (Fey 1981; Fritsch et al., 2005).

The substitution of Al for Fe in Fe oxides is well documented (Schulze, 1984; Schwertmann 1991; Singh & Gilkes, 1992). The Al^{3+} ion (0.53 Angstrom) is slightly smaller than the Fe^{3+} ion (0.65 Angstrom), therefore, the average size of the unit cell is reduced when Al substitutes for Fe (Schulze, 1984; Singh & Gilkes, 1992). Substitution of Al for Fe is more common in upper soil horizons where Fe oxide particles are smaller as opposed to the larger crystal sizes of Fe oxides found at depth (Fritsch et al., 2005). This substitution influences the crystallization as well as the chemical properties of the mineral (Schwertmann, 1991; Kusuyama et al., 2002). Aluminium release from Al-substituted Fe oxides inhibits the activity of Fe-reducing bacteria, which promote Fe oxide dissolution under reducing conditions (Fritsch et al., 2005).

Apart from Al substitution stabilizing the crystal structure of Fe oxides against reduction, goethite, and therefore Al substitution, appears to concentrate in mottles relative to the soil matrix. The dominance of goethite over hematite in mottles is favoured by low pH, the presence of organic compounds in the soil solution and the high H_2O activity. Goethite is also favoured over hematite in the presence of Al^{3+} because Al in the soil solution can bring ferrihydrite back into solution, which allows nucleation and polymerisation of aluminous

goethite (Singh & Gilkes, 1996). A study conducted by Singh & Gilkes (1996) showed that there was a higher citrate-bicarbonate-dithionite extractable Al content in mottles than the surrounding matrix, which is explained by the higher goethite content in mottles. This leads to a large extent of Al substitution in goethite in mottles (Singh & Gilkes, 1996). Red mottles are seen in more oxygenated environments where less reduction occurs (Barrow & Torrent, 1987).

There are several external factors that could also be responsible for the disconnect between soil colour patterns and period of saturation. These include soil disturbances such as forest clearance and plowing, which can both alter morphological properties by changing vegetation. Landscape hydrology may also be altered by dams, agricultural drainage systems, highway drains as well as other drainage systems (Franzmeier et al., 1983).

1.2.6 Redox buffering

A mixture of redox states is generally encountered in a non-equilibrium redox system (Bartlett & James, 1995). When a change in the external environment does not result in an expected pedogenic change, such as the formation or disappearance of mottles, soil is said to be in a state known as pedogenic inertia. As referenced by Chadwick and Chorover (2001), Bryan and Teakle define pedogenic inertia as "the case where a pedogenic process, as established, continues in spite of changes in the pedogenic environment to one that should not favour its continuation".

Redox buffering, also known as redox resistance and redox poise, is an indicator of redox buffering capacity, which is the resistance of a soil system to changes in redox potential. It can be chemically measured as the time required, under water saturated conditions, to lower the redox potential of a soil to a given value (Stepniewski et al., 2002). It can also be measured as the quantity of strong reductant required to reduce redox potential (Eh) by one volt (Stepniewski et al., 2005) or the resistance to change in potential upon the addition of a small quantity of oxidant or reductant (Ponnamperuma, 1972; Fiedler et al., 2007). Redox buffering increases with the total concentration of oxidant plus reductant, and for a fixed total concentration it is maximum when the ratio of oxidant to reductant is 1 (Ponnamperuma, 1972; Fiedler et al., 2007). A soil's capacity to buffer redox changes determines the rate and extent of the soil morphological response to an influx of electrons (Chadwick & Chorover,

2001). There is no known chemical measurement relating redox buffering to electron demand and this study aims to introduce such a measurement.

1.2.7 The role of manganese in buffering Fe reduction and ferrous iron accumulation

Since Al substitution has such a great effect on the stability of Fe oxides, it is possible that it can exhibit the same influence on Mn oxides, which may lead to the stabilization of Mn oxides against reduction. Apart from this phenomenon, it is also possible for Mn to substitute for Fe in goethite structures (Singh & Gilkes, 1996; Kusuyama et al., 2002). Manganese in the 2+ state and Fe^{2+} have similar ionic radii (0.82 and 0.78 Angstrom respectively), and can readily substitute for one another (Neue & Bloom, 1987).

Manganese 3+/4+ is a powerful oxidant and studies have revealed that oxidation of added Mn was proportional to Mn oxides. It was hypothesized that oxidation was autocatalytic, involving Mn^{2+} oxidation by existing Mn oxide surfaces (Bartlett, 1988). Mn oxides generally have a low point of zero charge (PZC), which ranges from 1.5 to 4.5 for Mn oxides (Murray, 1974; McKenzie, 1981; Negrac et al., 2005). A surface is positively charged at a pH below PZC and negative at a pH above PZC (Murray, 1974) with cation adsorption favoured at pH values higher than PZC and anion adsorption favoured at a pH lower than PZC (Gadde & Laitinen, 1974). Manganese oxides therefore generally have a negative charge in the pH range of most soils (Negrac et al., 2005) and have a strong tendency to adsorb Mn^{2+} cations and other heavy metals (Bartlett, 1988). Manganese oxides have a much higher affinity for Mn^{2+} than any other divalent cations and it has been postulated that specific adsorption is accountable for this high affinity (Tu et al., 1994).

This could have a dual effect on Fe reduction and the development of redoximorphic features in soils. Firstly, if Mn^{2+} is continually reoxidized and not lost from the system, it will not be depleted, resulting in a buffering of Fe reduction as Fe reduction cannot take place until Mn^{2+} is removed, following the sequential order of reduction (Lovley & Phillips, 1988; Faulkner et al., 1989). Manganese reduction can therefore inhibit Fe reduction (Thamdrup et al., 1994). Secondly, reduced Fe^{2+} can be re-oxidized on Mn oxide surfaces (Ponnamperuma, 1972), thereby preventing their mobilization to oxidized parts of the soil where they can precipitate to form mottles. This was substantiated by an investigation conducted by Lovley & Phillips (1988) which revealed that Mn^{4+} oxidation of Fe^{2+} is the limiting factor to the accumulation of Fe^{2+} where Mn^{4+} reduction occurs. The reaction not only prevents the production of Fe^{2+}

in Mn oxide-containing sediments, but also oxidizes Fe^{2+} that has migrated from the zone of Fe^{3+} reduction (Lovley & Phillips 1988). Previous studies by these authors have also shown that Fe^{3+} reducing bacteria reduce the amorphous Fe oxide fraction in soil and amorphous Fe^{3+} is produced by $Mn^{3+/4+}$ oxidation of Fe^{2+}.

It has also been shown that due to the fact that Fe^{2+} is oxidized more rapidly in the presence of MnO_2, it has a tendency to deposit on the remaining Mn oxides rather than the Fe oxides (McKenzie, 1976; Gilkes & McKenzie, 1988; Negrac et al., 2005). This could leave Fe^{2+} trapped in Mn oxides, rather than Fe oxides, which influences Fe oxide reduction. An Mn oxide coating on soil particles could exist on the exterior of a soil ped for a long period of time without oxidizing the adsorbed Fe^{2+} within the ped (Bartlett & James, 1995). This again possibly leaves Fe^{2+} trapped in and on Mn oxides, influencing the overall Fe oxide reduction behaviour in soil. It has also been suggested that as the soil starts to dry out, the oxidation potential increases and the mixed oxides catalyse the oxidation of Mn and Fe (Gilkes & McKenzie, 1988). This leads to preferential deposition on oxide surfaces instead of somewhere else in the soil matrix (Gilkes & McKenzie, 1988). This would result in decreased mottle formation.

Several studies have shown the suppression of Fe uptake, Fe^{2+} in particular, in the presence of Mn oxides. An investigation by Fujimoto and Sherman (1948) revealed that pineapple growth was adversely affected by high Mn content not because of Mn toxicity but rather because of Mn-induced Fe deficiency. A study by Myers & Nealson (1988) suggested that Fe^{2+} did not accumulate in the presence of Mn oxides. Another study by Golden et al. (1993) showed that the Wahiawa soil in Hawaii, which has Mn minerals dispersed throughout the soil in high concentrations, shows no response to soil applied Fe^{2+} fertilization due to the oxidative and physiological effects of Mn. This particular study showed that lithiophorite (an Mn oxide) was coated with Fe oxides on the nodule surface, suggesting that Fe^{2+} entering the soil through weathering or fertilization may be oxidized by the Mn oxide surface, thereby creating a protective Fe-oxide surface coating (Golden et al., 1993). This could be further exacerbated by the fact that Mn is mobilized under less reducing conditions than Fe (Fiedler & Sommer, 2004), therefore, Mn can be reduced and reoxidized before Fe can be released. Iron reduction can possibly be further buffered in this way.

Looking at the sequential order of reduction, the presence of nitrates delays the reduction of Mn and Fe oxides (Glinski et al., 1992). Manganese, however, appears to "work its magic" in nitrogen (N) dynamics as well. One molecule of hydroxylamine, which is an intermediary product in the process of denitrification, is oxidized by six molecules of Mn^{3+}, thereby producing nitrite (NO_2^-) as the major product of oxidation (Bartlett, 1988). Mn oxides are responsible for the non-microbial conversion of NO_2^- to NO_3^- and studies have revealed that synthetic MnO_2 readily oxidizes NO_2^- to NO_3^-. The oxidation of NO_2^-, formation of NO_3^-, and MnO_2 reduction were stoichiometrically related regardless of the presence of O_2. This explains the low amount of NO_2^- despite low numbers of *Nitrobacter* (which are bacteria responsible for converting nitrites to nitrates) and an environment unsuitable for their growth (Bartlett, 1988). Reactions therefore show that Mn can possibly retard, prevent, stimulate, or cause denitrification (Bartlett, 1988). Another study conducted by Davison & Woof (1984) on a Rostherne Mere lake in the UK showed an accumulation of Mn^{2+} for 4-5 months, which is not uncommon, but what was unusual was the absence of Fe^{2+} during this period. The lake remains at the Mn stage and appears to be a finely poised system showing Mn reduction and the initial stages of denitrification (Davison & Woof, 1984). It is clear that the effect Mn has on N results in redox buffering by preventing the depletion of NO_3^- and thereby preventing the reduction of Mn and Fe oxides.

1.3 Summary

Redoximorphic features are expressed differently in different soil types and their expression, or lack thereof, can be influenced by several soil properties. From the review of literature it appears that Mn plays a significant role in the buffering and influencing of redox processes, and therefore redox morphology, in soils. The effect of Mn on the influencing of Fe redox processes and its expression in soils has a significant influence on the understanding of soil related wetland indicators. It therefore is a critical component requiring elucidation for the establishment of an empirical foundation for regulatory processes and decisions.

Chapter two: Site description and soil properties

2.1 Introduction

Samples were collected from different areas in the Pretoria, Centurion and Midrand region. All of the areas sampled are influenced by varying geologies, as indicated in Figure 2.1. Samples were collected moving down the catena at the quartzite, dolomite and granite sites in order to investigate differences in redox buffering at different positions of the landscape. Catenary sequences are useful to study element mobility (Childs & Leslie, 1977). In the presence of Fe and Mn oxides, the study of inter-element relationships involving Fe and Mn is permitted (Childs & Leslie, 1977). Besides the study by Childs & Leslie (1977), a study by Boero & Schwertmann (1987) also proved useful in studying soil material in a catenary sequence by variations in Fe and Mn dynamics. Mn appears to be a good indicator of soil forming processes in topographic sequences (Yaalon et al., 1972).

Specific sites were chosen with wetlands present, making these soils ideal for comparison of the presence or absence of redoximorphic features at different sites with similar hydrology. The andesite and basalt samples were taken as individual samples, not in a catenary sequence, to use as comparative geologies with suspected varying Mn contents. This was important as the study aims to link changes in expression of redoximorphic features in soil derived from different geologies with varying Mn content. A more detailed description of each site is provided below. Figure 2.1 is a map indicating the sites at which the samples were taken. Results for the chemical and physical characterization of these soils are provided in the soil properties section of this chapter. Mineralogical characterization of the soils can be viewed in Appendix C.

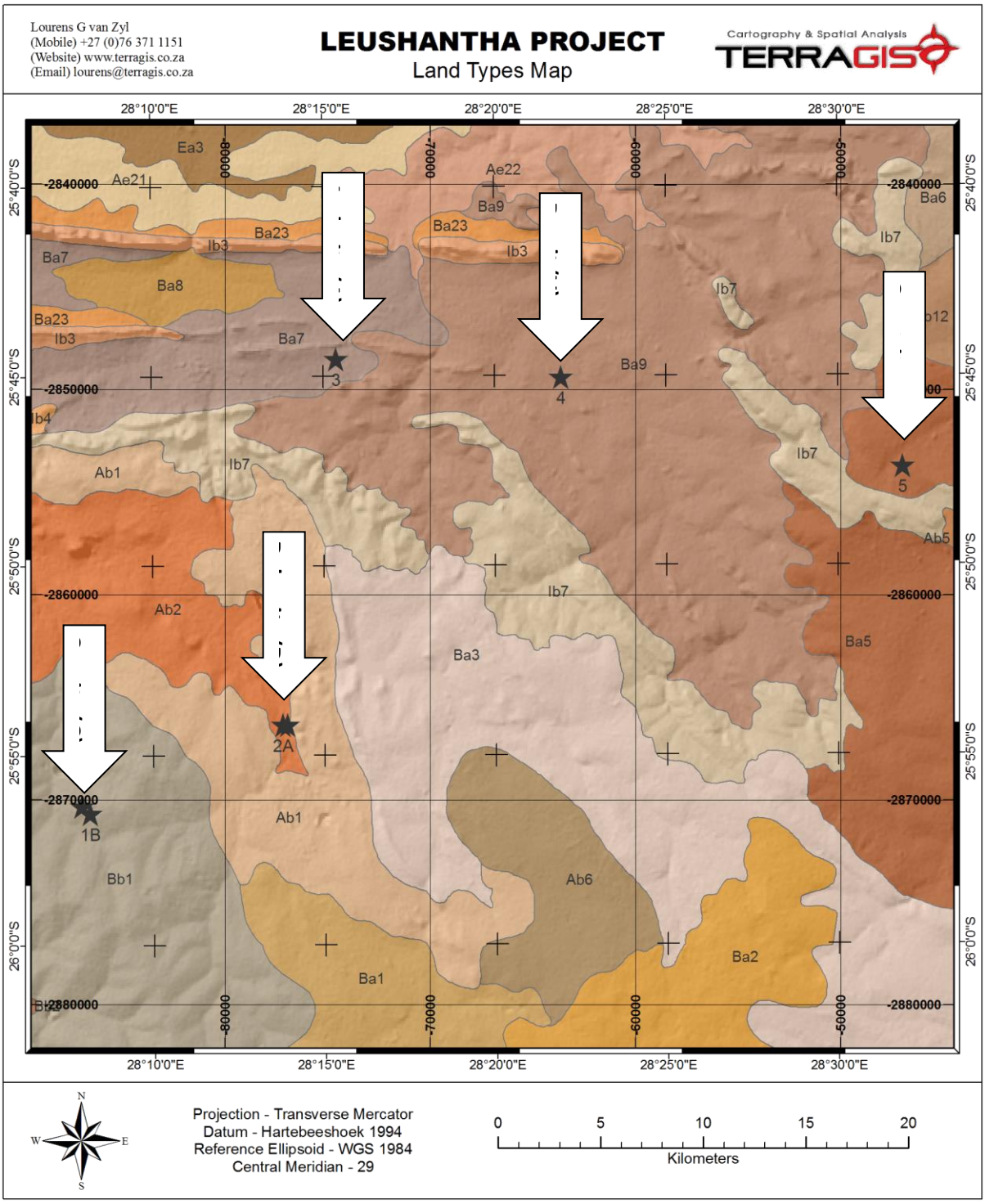

Figure 2.1: Map indicating sampling sites

2.2 Site descriptions

2.2.1 Site Q

Soils collected at this site are derived from quartzite. The soil at the top of the catena was a deep red colour, which became yellow as the position shifted further down the landscape and finally a bleached and gleyed soil was visible at the bottom of the landscape close to the

wetland as depicted in Figure A1 in Appendix A. This soil type was relevant to the study as it is seen as a model site with redoximorphic features, as shown in Figure A2, Appendix A, appearing at site Q_Mid as expected for the hydrology of the landscape, indicating a fluctuating water table. This landscape is typical of the plinthic catena found in the South African Highveld. Table 2.1 provides the position in the landscape where the samples were collected and the classification.

Table 2.1: Description of site Q

Sample	Position in the landscape	Depth (cm)	Horizon classification	Soil classification (SA Taxonomy)
Q_Crest_A	Crest	0-20	Orthic A	Hutton
Q_Crest_B1		*40-60	Red apedal B	
Q_Crest_B2		1.2-1.5	Red apedal B	
Q_Mid_A	Midslope	0-20	Orthic A	Avalon
Q_Mid_B1		40-60	Yellow-brown apedal B	
Q_Mid_B2		60-80	Soft plinthic B	
Q_Foot_A	Footslope	10-40	E	Kroonstad
Q_Foot_B		40-70	G (with mottles)	
Q_Bot_A	Valley bottom	0-10	Orthic A	

*Gaps in depth, e.g. between 20-40cm, were left in order to avoid mixing of horizons when horizon differentiation was difficult

Wetland description

The study site is located within the headwaters of a channelled valley-bottom wetland complex with extensive seep zones. This section is 92.5 ha. The soils indicate that seeps are seasonally wet whilst the valley-bottom section of this wetland complex is permanently wet. The system is transected by various roads (Figure 2.4). Dams occur in various sections of the valley-bottom with some drains evident. Cultivation occurs in parts of the seep zone. Delineation was done by onscreen digitizing with Google Earth (GE) Pro (2004 image). The headwater section of this much larger wetland complex was selected based on the slope change along the Thalweg of the valley-bottom (Figure 2.2).

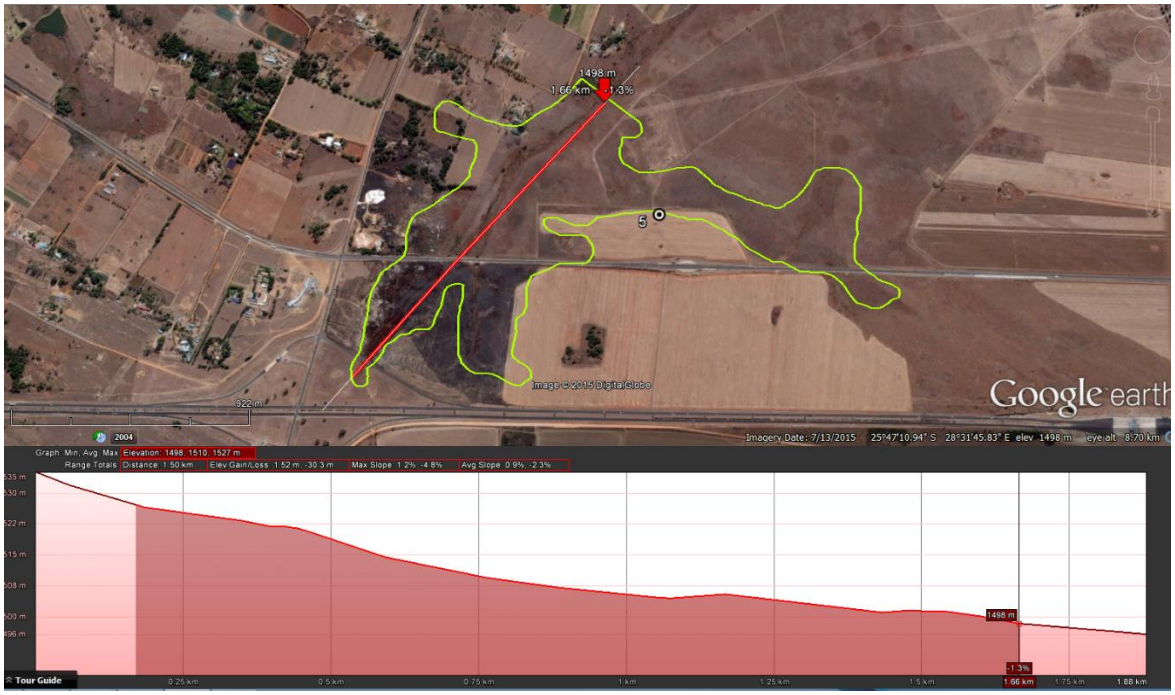

Figure 1.2: Wetland boundaries (green line) and slope along its Thalweg (red line)

2.2.2 Site V

These soils are basalt derived vertic soils. A small area was sampled and the samples were taken in close proximity of each other. The samples differed in colour with one being black and the other brown. Both samples were taken close to a wetland. Samples could only be collected to a depth of 20 cm before rock was encountered. Rock samples were not collected. Upon visual and textural examination in the field, the soils exhibited a high clay content, as expected for vertic soils, and had very poor expression of redoximorphic features. The samples were sticky to the touch and stained the fingers when manipulated. The vertic soils were chosen as a variation in soil type. Table 2.2 provides the position in the landscape where the samples were collected and the classification.

Table 2.2: Description of site V

Sample	Position in the landscape	Depth (cm)	Horizon classification	Soil classification (SA Taxonomy)
V_Black	Valley bottom	0-20 Below	Vertic A Hard rock	Arcadia
V_Brown	Valley bottom	0-20 Below	Vertic A Hard rock	Arcadia

Wetland description

The study site is a seep located within the headwaters of a channelled valley-bottom wetland complex. This section is 3 ha. Imagery and the presence of a dam filled with water throughout the year over the past 5 years indicate that the wetland is permanently wet (Figure 2.3). The system is transected by various roads (Figure 2.3). Dams occur in various sections of the system with infilling and light industrial development around the study site. The delineation was done by onscreen digitizing with GE Pro (2015 image). This seep zone in the headwater section of a much larger wetland complex was selected based on the road intersection and the dam (Figure 2.3).

Figure 2.3: Wetland boundaries (green line) and slope along its Thalweg (red line)

2.2.3 Site G

Soils were collected in Midrand at the Halfway House granite dome. The catena is similar to that of the quartzite derived soil with the exception of the mottling occurring at the bottom of the landscape closer to the wetland, whereas in the quartzite derived soils, mottling occurred higher up in the landscape. This soil type was chosen due to the presence of expected redoximorphic features, depicted in Figure A3 in Appendix A. Table 2.3 provides a description and classification of the samples.

Table 2.3: Description of site G

Sample	Position in the landscape	Depth (cm)	Horizon classification	Soil classification (SA Taxonomy)
G_Crest_A	Crest	0-20	Orthic A (appeared bleached, however a Munsell colour of 7.5YR 4/6 was noted, which does not fall within the bleached colours category)	Hutton
G_Crest_B		20-50	Red apedal B	
G_Mid_A	Midslope	0-20	Orthic A	Clovelly
G_Mid_B		20-50	Yellow-brown apedal B	
G_Bot_A	Valley bottom	0-20	Orthic A (Fe accumulation around roots – indicating reduced conditions during some periods of the year)	Longlands
G_Bot_B1		20-40	E	
G_Bot_B2		20-40	Soft plinthic (going into a G)	

Wetland description

The study site is a seep located within the headwaters of a channelled valley-bottom wetland complex. This section is 19 ha. Soils indicate that the wetland is seasonally wet with permanently wet zones in places. The system is transected by various roads (Figure 2.4). Excavation of the abandoned Pan-African parliament occurs in various sections of the system with infilling and commercial light industrial development around the study site. The delineation was done by on-screen digitizing with GE Pro (2007 winter image).

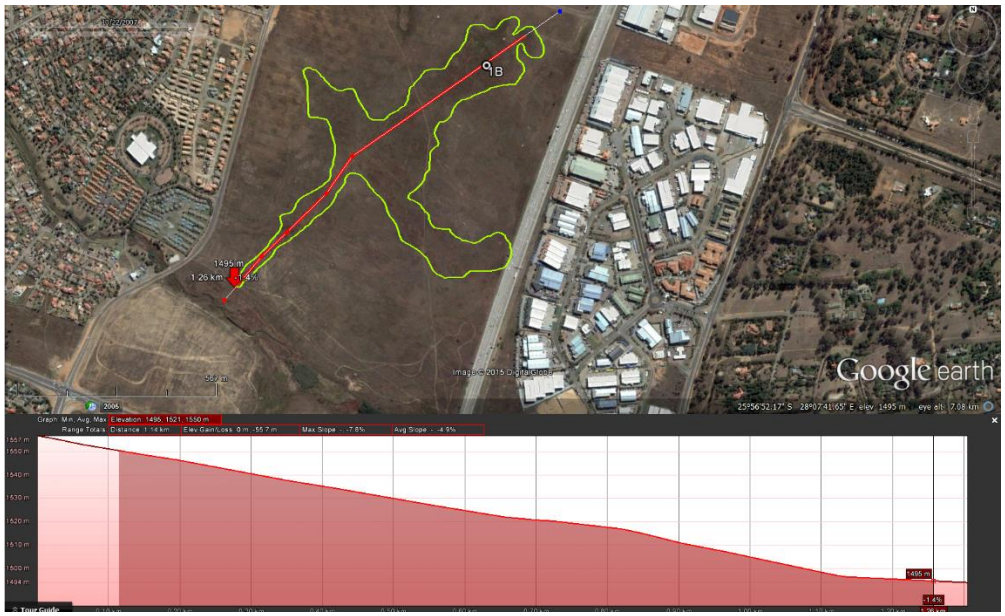

Figure 2.4: Wetland boundaries (green line) and slope along its Thalweg (red line)

2.2.4 Site D

The dolomite derived soils are manganiferous soils, chocolate brown in colour, as demonstrated in Figure A4 in Appendix A. Ferromanganese wad was visible at the site of sampling. Samples were collected in the upper part of the landscape as well as further down near the wetland. Samples could only be collected to a depth of 20 cm before hard rock was encountered. Vegetation on the site was indicative of a wetland, however redoximorphic features were absent. The lack of mottling where it was expected to occur in this soil was the reason this site was selected. Table 2.4 provides the position in the landscape where the samples were collected and the classification.

Table 2.4: Description of site D

Sample	Position in the landscape	Depth (cm)	Horizon classification	Soil classification (SA Taxonomy)
D_Crest_A	Crest	0-20 Below	Orthic A Hard rock	Mispah
D_Bot_A	Valley bottom	0-20 Below	Orthic A Hard rock	Mispah

Wetland description

The study site is within a narrow seep located at the edge of a channelled valley-bottom wetland with a distinct riparian zone. This section is linked to a meander and is 11 ha. Vegetation (Figure 2.5) indicates that the seep zone is seasonally wet with permanently wet zones closer to the stream channel (Figure 2.6). The system was previously cultivated and a furrow runs through the study site (Figure 2.7) and recently deposited debris indicates the extent of not only flooding but also catchment changes. Delineation was done by onscreen digitizing with GE Pro (2008 winter image). The wetland was delineated within a meander on the eastern banks of the system.

Figure 2.5: *Imperata cylindrica* on site indicates temporary to seasonal wetness

Figure 2.6: Soils indicate surface deposition of silt (grey) on a seasonal basis and Mn (black) movement indicating mobilization of Mn with increase in water downslope

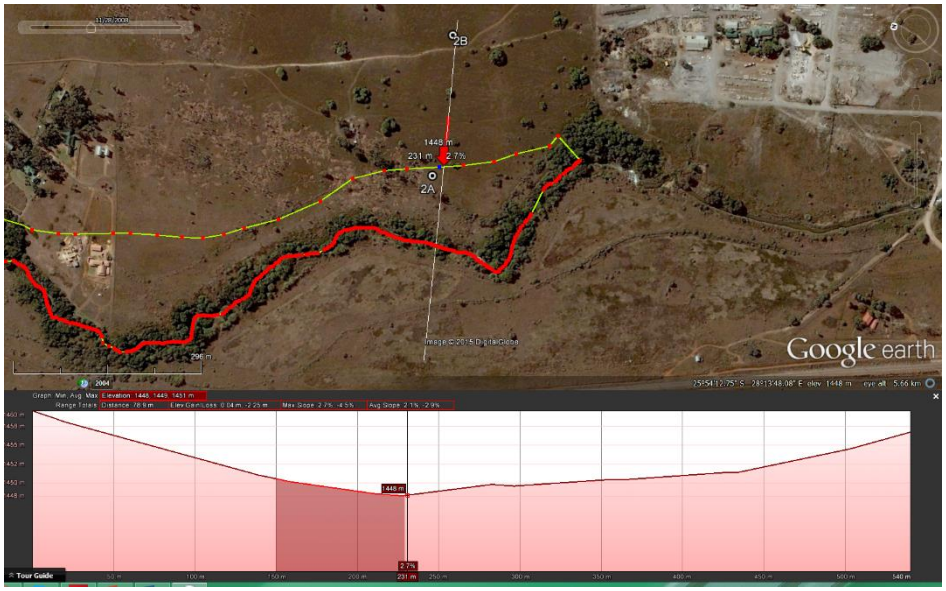

Figure 2.7: Wetland boundaries (green line) and slope along its Thalweg (red line)

2.2.5 Site A

These soils were collected at the Hatfield Experimental Farm in Pretoria and are derived from andesite. The surface of the soil was dry and had visible cracks (refer to Figure A5(a) in Appendix A) indicative of the clays present in the soil (mineralogy provided in chapter three). This is a red soil as seen in Figure A5(b). The first 30 cm was a red-brown colour and appeared to exhibit a high clay content, making sampling with an auger difficult. The next 30 cm showed a deepening of the red colour of the soil and a few Mn concretions were visible. In the following 30 cm, a considerably higher concentration of Mn concretions was present. At 80 cm a pebble layer was encountered and no further samples could be taken. Sampling at this site was not taken close to a wetland, however this soil type was chosen for the study because it was expected to have an appreciable Mn content, based on the general expectation that ultramafic and mafic rocks should inherently have a higher concentration of Mn (Alexander et al., 2007) as well as the visual observation of black Mn concretions on the soil surface. Table 2.5 provides the position in the landscape where the samples were collected and the classification.

Table 2.5: Description of site A

Sample	Position in the landscape	Depth (cm)	Horizon classification	Soil classification (SA Taxonomy)
A_Mid_A	Midslope	0-30	Orthic A	Hutton
A_Mid_B1		30-50	Red apedal B	
A_Mid_B2		50-80	Red apedal B	

2.2.6 Manganese wad

Psilomelane is an Mn-containing mineral in ferromanganic soil nodules and is also known as wad or black ocher (Vodyanitskii, 2009). It is also a general name for individual Mn oxides (Vodyanitskii, 2009). The ferromanganese wad used in this study originated from the alteration of the Permian Karoo strata (Pack et al., 2000). It is a finely laminated and friable substance mainly composed of Fe and Mn oxyhydroxides, containing 77–91 wt. percent Fe_2O_3 + MnO (Pack et al., 2000). A scanning electron microscopy investigation of the wad was conducted and can be perused in the Appendix D.

Ferromanganese wad was supplied by Metmin Ltd., a company that mines the wad in Ventersdorp for uranium extraction (refer to Figure A6 in Appendix A). This wad was used as a control sample as it is a pure mineral and exhibits an extremely high Fe and Mn content. These elements are of particular interest in this study as the reduction of Fe leads to mottle formation and the study looks at the role Mn possibly plays in buffering redox reactions, potentially preventing mottle formation.

2.3 Soil properties

2.3.1 Chemical soil properties

2.3.1.1 Methods and materials

Walkley-Black

An addition of 10 ml of 0.167 M $K_2Cr_2O_7$ to 1 g soil (0.5 g for soils with expected high organic carbon) was followed by the addition of 20 ml of concentrated H_2SO_4. Samples were agitated and left to cool before the addition of 150 ml deionized water and 10 ml of concentrated ortho-phosphoric acid. Ferroin indicator was added and samples were titrated with 0.5 M Fe_2SO_4 until the end point was reached, indicated by a colour change from green to maroon (Nelson & Sommers, 1996; Non-Affiliated Soil Analysis Work Committee, 1990a).

Cation exchange capacity

The unbuffered method for cation exchange capacity usually makes use of ammonium (e.g. NH_4Cl) in the equilibrating solution and potassium (e.g. KNO_3) to serve the purpose of ammonium being analysed for (Courchesne & Turmel, 2007). The method used for this study used potassium in the equilibrating solution (KCl) and ammonium in the extracting solution (NH_4Cl) and instead of NH_4^+ being analysed, K^+ was analysed by ICP-AES. The

instrument used was the Spectro Genesis FEE ICP-AES. This method is demonstrated by Zelazny et al. (1996) for point of net zero charge where potassium is replaced by ammonium and potassium is the cation that is analysed (Zelazny et al., 1996). The method was carried out this way because the determination of potassium with an ICP-AES is vastly more accurate than an ammonium determination using this instrument.

To 5 g of soil, 30 ml of 0.2 M KCl was added. Samples were agitated and centrifuged, after which the clear supernatants were discarded. This process was repeated four times over. Samples were then washed three times with 30 ml of 0.04 M KCl. The supernatants were discarded after each wash and the samples were weighed after the final wash in order to determine the volume of the entrained solution. The washed samples each received 30 ml of 0.2 M ammonium chloride. Samples were then agitated and centrifuged and the supernatants were collected in 250 ml volumetric flasks. This process was repeated four times further. The solution was analysed for K^+ after the final washing (Zelazny et al., 1996).

Exchangeable iron, aluminium, manganese, calcium, magnesium and sodium

An aliquot of 25 ml of 1 M KCl was added to 5 g of soil. Samples were agitated, centrifuged and membrane filtered (0.45 um) after which the filtrates were acidified to pH < 3 with 65% HNO_3. Samples were then analysed using ICP-AES (Bertsch & Bloom, 1996).

Titratable acidity

Samples of 5 g were agitated with 35 ml of 1 M KCl. The suspensions were membrane filtered (0.45 um) and the soil was washed twice with 15 ml 1 M KCl. Filtrates were titrated with 0.1 M NaOH to determine total exchangeable acidity (Fey 2010, adapted from Mclean 1965).

Soil pH

To 10 g of soil, 25 ml of 1 M KCl was added. Samples were agitated and left to stand for an hour before pH readings were taken. The procedure was repeated using deionized water in place of KCl as the medium, keeping the soil to solution ratio 1:2.5 (Non-Affiliated Soil Analysis Work Committee, 1990b).

The results provided in Table 2.6 will be used in subsequent chapters in order to draw comparisons and are linked with other chemically determined parameters.

Table 2.6: Soil chemical properties

Sample	Organic carbon (%)	CEC ($cmol_c.kg^{-1}$ soil)	Exchangeable cations ($mmol.kg^{-1}$ soil)						Soil pH		Titratable acidity ($mmol_c.kg^{-1}$ soil)
			Al	Fe	Mn	Ca	Mg	Na	pH_{water}	pH_{KCl}	
Q_Crest_A	0.54	5.22	1.47	< MDL	0.18	1.29	0.48	0.14	4.70	3.88	9.01
Q_Crest_B1	0.31	5.45	0.11	< MDL	0.07	3.51	1.54	0.09	5.12	4.68	2.07
Q_Crest_B2	0.15	5.60	0.04	< MDL	0.06	0.76	2.68	0.11	5.21	4.91	< MDL
Q_Mid_A	0.52	4.65	0.31	< MDL	0.31	2.87	1.57	0.10	5.58	4.26	2.34
Q_Mid_B1	0.33	6.27	< MDL	< MDL	0.09	5.00	2.86	0.05	6.12	5.05	< MDL
Q_Mid_B2	0.30	6.53	< MDL	< MDL	0.09	5.37	4.06	0.03	6.16	5.41	< MDL
Q_Foot_A	0.33	4.38	0.52	< MDL	0.01	1.14	1.02	0.02	5.71	4.15	3.50
Q_Foot_B	0.21	6.31	0.09	< MDL	0.01	2.15	4.29	0.03	5.87	4.57	0.50
Q_Bot_A	2.39	10.2	0.04	< MDL	0.11	7.28	5.76	0.06	5.68	4.63	0.33
V_Black	0.45	56.0	< MDL	< MDL	< MDL	57.6	97.9	0.54	8.42	7.28	0.33
V_Brown	1.73	45.9	< MDL	< MDL	< MDL	64.0	59.6	0.09	8.09	7.07	< MDL
G_Crest_A	0.68	6.09	0.35	< MDL	0.08	1.87	0.74	0.06	5.76	4.26	4.67
G_Crest_B	0.47	6.49	0.94	< MDL	0.07	1.90	0.64	1.77	5.08	4.17	8.34
G_Mid_A	0.40	4.64	0.87	< MDL	0.13	1.18	0.45	0.01	5.33	4.18	5.00
G_Mid_B	0.41	4.86	1.13	< MDL	0.13	1.16	0.33	0.01	4.99	4.10	6.00
G_Bot_A	0.45	4.25	1.09	0.02	0.02	0.78	0.26	0.03	5.00	3.92	6.67
G_Bot_B1	0.28	3.96	1.10	0.01	< MDL	0.51	0.16	0.03	5.55	4.00	6.34
G_Bot_B2	0.28	5.64	1.72	< MDL	0.01	0.83	0.33	0.09	5.62	3.94	9.68
D_Crest_A	0.72	11.4	1.82	0.09	0.48	10.3	3.59	0.49	6.56	5.84	< MDL
D_Bot_A	1.03	12.2	1.82	0.08	0.55	10.1	3.82	1.88	6.55	5.50	< MDL
A_Mid_A	1.08	13.0	< MDL	< MDL	0.27	19.4	12.8	0.01	6.35	5.10	< MDL
A_Mid_B1	0.97	12.0	< MDL	< MDL	0.09	21.0	13.5	0.04	6.66	5.68	< MDL
A_Mid_B2	0.77	13.6	< MDL	< MDL	0.06	20.1	16.1	0.06	6.85	5.78	< MDL
Mn wad	0.02	6.38	1.83	0.09	0.48	2.31	1.33	0.73	6.62	5.67	< MDL

< MDL = Below method detection limit

2.3.2 Physical soil properties

2.3.2.1 Methods and materials

Soil colour

The colour of the soil samples was determined visually using a Munsell Colour Chart.

Soil texture pre-treatments

- ***Removal of carbonates and soluble salts***

To a sample of 40 g, 25 ml of deionized water was added followed by 10 ml of 1 M pH 5 NaOAc. The samples were then agitated and centrifuged, with the clear supernatants being discarded. Soils were washed twice more with 50 ml deionized water (Grossman & Reinsch, 2002).

- ***Removal of organic matter***

After the removal of carbonates, 25 ml of deionized water was added to the samples before they were agitated. Samples received 5 ml of hydrogen peroxide and were heated to 90ºC for the evaporation of excess water. The peroxide and heat treatment was repeated three more times (Grossman & Reinsch, 2002).

- ***Removal of iron oxides***

After the removal of organic matter, 150 ml of citrate bicarbonate buffer (refer to CBD method in Chapter three for constituents of this buffer) was added to the samples. Samples were agitated, followed by the addition of 3 g of sodium dithionite. Samples were heated to 80ºC and stirred intermittently for 20 minutes. Samples were then centrifuged and the clear supernatants discarded. All samples were washed twice with deionized water (Grossman & Reinsch, 2002; Non-Affiliated Soil Analysis Work Committee, 1990c).

Soil texture determination

Following the pre-treatment of the samples, 10 ml of calgon dispersing solution (made up of 0.58 M sodium hexametaphosphate and 0.07 M sodium carbonate) was added to each. Deionized water was added to all of the samples to make the volume up to 150 ml. Samples were transferred to a dispersion cup and mixed with an electric mixer. Dispersed samples were passed through a 0.053 mm sieve until the percolate was clear, in order to separate the silt and clay fractions from the sand (Non-Affiliated Soil Analysis Work Committee, 1990c).

- ***Clay determination***

The clay and silt fractions were made up to 1 L with deionized water. A blank was made up of calgon dispersing solution and deionized water. Samples were mixed thoroughly by inserting a plunger with upward and downward movements several times. Hydrometer readings of the samples and blank were taken at 30 s, 1 min, 3 min, 10 min, 30 min, 60 min, 90 min, 120 min, 8 hrs, 16 hrs and 24 hrs (Grossman & Reinsch, 2002).

- ***Sand determination***

The fraction that did not pass through the 53 um sieve was transferred to a beaker and placed in the oven to dry overnight at 105ºC. The dried samples were passed through a nest of sieves that were ordered as 1000, 500, 250, 106 and 53 um. Fractions from each sieve were collected wand weighed separately (Grossman & Reinsch, 2002).

- ***Silt determination***

The silt fraction was calculated by the difference between the clay and sand fractions.

2.3.2.2 Results and discussion

Similarly to the soil chemical properties, the analysis was done in order to provide an overall view of the soil physical characteristics (Table 2.7). These results are used in subsequent chapters and are linked to other chemically determined parameters.

Table 2.7: Soil physical characteristics

Sample	Soil colour		Soil texture			
	Dry	Moist	Sand	Silt	Clay	Texture
Q_Crest_A	7.5YR 4/6	5YR ¾	82.4	1.3	16.3	Sandy loam
Q_Crest_B1	5YR 4/6	2.5YR 3/6	66.2	5	28.8	Sandy clay loam
Q_Crest_B2	5YR 4/6	5YR ¾	65	3.7	31.3	Sandy clay loam
Q_Mid_A	7.5YR 5/4	7.5YR 3/4	80	2.5	17.5	Sandy loam
Q_Mid_B1	10YR 5/6	7.5YR 4/6	70	6.3	23.7	Sandy clay loam
Q_Mid_B2	10YR 5/4	10YR 3/6	67.5	6.2	26.3	Sandy clay loam
Q_Foot_A	2.5Y 6/1	2.5Y 4/2	81.3	3.7	15	Sandy loam
Q_Foot_B	2.5 Y 6/2	10YR 5/2	65	5	30	Sandy clay loam
Q_Bot_A	10YR 4/1	2.5Y 3/1	82.4	3.8	13.8	Sandy loam
V_Black	2.5Y 4/1	2.5Y 2.5/1	30	12.5	57.5	Clay
V_Brown	10YR 3/1	2.5Y 2.5/1	45	11.3	43.7	Clay
G_Crest_A	7.5YR 4/6	7.5YR 3/4	71.3	3.7	25	Sandy clay loam
G_Crest_B	2.5YR 4/6	2.5YR 3/6	58.7	5	36.3	Sandy clay
G_Mid_A	10YR 6/4	10YR ¾	77.4	3.8	18.8	Sandy loam
G_Mid_B	10YR 5/4	10YR ¾	72.4	6.3	21.3	Sandy clay loam
G_Bot_A	10YR 5/2	10YR 4/2	82.5	2.5	15	Sandy loam
G_Bot_B1	10YR 5/2	10YR 4/2	81.3	5	13.7	Sandy loam
G_Bot_B2	10YR 6/4	10YR 5/2	66.3	5	28.7	Sandy clay loam
D_Crest_A	7.5YR 2.5/3	10YR 2/2	76.3	10	13.7	Sandy loam
D_Bot_A	7.5YR 3/3	10YR 2/2	68.8	8.7	22.5	Sandy clay loam
A_Mid_A	2.5YR 4/8	5YR ¾	38.8	6.2	55	Clay
A_Mid_B1	2.5YR 4/8	5YR ¾	8.8	8.7	82.5	Clay
A_Mid_B2	5YR 4/6	5YR ¾	6.3	7.4	86.3	Clay

2.4 Summary

Soils were sampled in different areas in the Highveld. Samples were taken down a catenary sequence in order to later investigate the difference in redox buffering at different landscape positions. All samples, apart from andesite, were collected at wetland sites. Redoximorphic features were clearly expressed in the quartzite and granite soils, which is expected from typical soils situated in these landscapes with a fluctuating water table. The vertic soils however, had very poor expression of mottles and, even more surprising, the dolomite soils completely lacked redoximorphic features where they were expected to occur.

Chapter three: Manganese extractability in the various soils

3.1 Introduction

Soil characterization was conducted in order to determine the reactivity / solubility and quantities of Mn, Fe and Al. This in turn would highlight the propensity of the Mn to be oxidized or reduced. The Fe and Al contents were determined in order to investigate their interaction with Mn and the effect it may have on the oxidizing ability of Mn oxides as well as Mn reactivity.

X-ray Fluorescence (XRF) was conducted for the determination of total Mn, Fe and Al contents. The choice of the most appropriate method to determine total elemental content is at the discretion of the analyst however the two most commonly used methods in laboratories are XRF and acid digestions (Rayment & Lyons, 2011). XRF is a technique for multi-element determination and is widely used for the assessment for total elemental concentrations in soil (Towett et al., 2013). Analysis by XRF provides a good estimate of total elemental content in all chemical forms, including those in the silicate lattices (Baize, 2009).

Selected samples were subjected to two different methods that are both generally assumed to provide similar elemental contents. The dithionite citrate method was developed as a simpler procedure to the citrate-bicarbonate-dithionite method developed by Mehra & Jackson (1960) while providing very similar results. The citrate-bicarbonate-dithionite method was developed by Mehra & Jackson and is useful for the solubilisation of oxides and hydroxides of Fe, Al and Mn. According to literature, the methods should be analogous and similar results for the extractable elements using dithionite citrate and citrate-bicarbonate-dithionite should be obtained (Courchesne & Turmel, 2007), however this is likely to depend largely on the mineralogy of the soil.

Ammonium oxalate was used to extract the amorphous and poorly crystalline fraction of the elements in the soils that are more susceptible to soil reactions, in particular, redox reactions. Elements that are held more tightly within the crystal structure are less likely to participate in chemical reactions. The metals residing in amorphous and poorly crystalline minerals, however, will participate in redox reactions much more readily because non-crystalline

oxides are less stable than their crystalline counterparts (Ottow, 1981). Crystalline oxides are more resistant to attack than non-crystalline oxides and hydroxides (Kersten & Forstner, 1990). Amorphous oxides are also more chemically reactive due to the characteristics of their specific surface area (Relic et al., 2005).

The Mn fraction in the 3+ and 4+ states (the easily reducible fraction) was determined by an acid hydroxylamine extract. Mn in these forms are present in oxides and have a strong oxidizing tendency. The amount of easily reducible Mn in the soils was determined in order to test the hypothesis that soils with a greater Mn content, in particular a larger easily reducible Mn fraction, are the ones that lend to greater redox buffering. The alternate hypothesis is that soils with high Mn contents do not lead to greater redox buffering. This could be true if the Mn in the soils is in the soluble form instead of the easily reducible form or if the easily reducible forms of Mn are in a coordinative environment that makes it less redox reactive.

Mineral composition influences many chemical characteristics of soil, including buffering properties. X-ray diffraction was conducted on the samples in order to determine the mineralogy of the soils, with the main focus being Mn oxides in order to investigate how the mineral make-up relates to Mn reactivity. These minerals are important as they act as the supply of Mn for redox reactions (McKenzie, 1989). It was expected that the Mn minerals detected would be in oxide rather than hydroxide forms due to the fact that Mn^{2+} is poorly hydrolyzed (Vodyanitskii, 2009), however it was expected that most Mn would be in the easily reducible forms and not the soluble form.

3.2 Methods and materials

3.2.1 X-ray fluorescence

Samples were milled in a tungsten-carbide milling pot to obtain particle sizes below 75 um. Loss on ignition (LOI) values were determined by drying the samples at 100˚C and roasting them at 1000˚C. From these samples, 1 g of sample was mixed with 6 g of lithium tetraborate flux and fused at 1050˚C to form a stable fused glass bead. The samples were then mixed with PVA binder and pressed in an aluminium cup at 10 tons for trace metal analysis. The Thermo Fisher ARL Performa's Sequential XRF with OXSAS software was used for analysis (Loubser & Verryn, 2008).

3.2.2 Dithionite citrate

The principle behind this method is that the dithionite causes reduction, resulting in the dissolution of the metal oxides susceptible to redox promoted dissolution (Pansu & Gautheyrou, 2007). Dithionite is quite stable as a dry solid but decomposes in aqueous solutions. The mechanism of reduction is as follows (Varadachari et al., 2006):

Oxidation half-reaction:

$$S_2O_4^{2-}(aq) + 2H_2O(l) \rightarrow 2HSO_3^-(aq) + 2H^+(aq) + 2e^- \quad (1)$$

Reduction half-reaction:

$$S_2O_4^{2-}(aq) + 2H^+(aq) + 2e^- \rightarrow S_2O_3^{2-}(aq) + H_2O(l) \quad (2)$$

Overall reaction:

$$2S_2O_4^{2-}(aq) + H_2O(l) \rightarrow S_2O_3^{2-}(aq) + 2HSO_3^-(aq) \quad (3)$$

Dithionite is an active reducer below a pH of 9 – 10 (Pansu & Gautheyrou, 2007). The sodium citrate buffers the solution pH close to 7, which avoids the precipitation of iron sulphide compounds (Varadachari et al., 2006; Courchesne & Turmel, 2007). In this way, extracted phases are maintained in solution (Pansu & Gautheyrou, 2007). The optimum pH for reduction is 7 - 8 because precipitation of colloidal sulphur occurs at a pH below 6.5. This results in a suspension in the extract which makes measurement by absorption spectrometry difficult. The buffered medium avoids this phenomenon.

Due to the instability of dithionite solutions and their ability to undergo rapid decomposition (Varadachari et al., 2006), a fresh solution was prepared and used immediately in order to prevent inconsistent results. A 25 ml aliquot of 0.68 M sodium citrate solution was added to 0.5 g of soil, after which 0.4 g of dithionite was added. Samples were shaken for 16 hours and centrifuged thereafter. The isolated supernatants were membrane filtered using 0.45 um pore size filter paper and analysed using inductively-coupled plasma atomic emission spectroscopy (ICP-AES).

3.2.3 Citrate-bicarbonate-dithionite

Similar to the dithionite citrate (DC) method, dithionite is the reductant, however in this method sodium bicarbonate acts as the buffering agent. Reducible elements, such as Mn, Fe and Al, are reduced and maintained in solution by complexation with citric acid in a system buffered at pH 7.3. The buffering inhibits sulphur precipitation (Pansu & Gautheyrou, 2007).

The strong chelating action of citrate on ferrous Fe prevents reprecipitation of FeS at the near-neutral pH of this extraction (Shang & Zelazny, 2008).

A citrate-bicarbonate buffer (constituting 0.3 M sodium citrate and 1 M sodium bicarbonate) was added to 10 g of soil to reach a solution volume of approximately 37.5 ml. Samples were agitated before the addition of 0.75 g sodium dithionite to each. Samples were then placed in a water bath at 80°C and stirred intermittently for 20 minutes (Grossman & Reinsch, 2002). The elevated temperature of 80°C limits the decomposition of the dithionite. This elevated temperature also serves to accelerate the reaction and limit the appearance of any colloidal sulphur that and FeS that may have precipitated (Pansu & Gautheyrou, 2007). Van Hoff's rule states that chemical reactions increase by a rate of two to threefold for every 10°C increase in temperature (Rabenhorst & Parikh, 2000). Samples were centrifuged and filtered (0.45 um) before being analysed for Fe, Al and Mn by ICP-AES (Grossman & Reinsch, 2002).

3.2.4 Acid ammonium oxalate

The acid ammonium oxalate (in the dark) extraction is useful for the determination of amorphous and very poorly crystalline metal forms in the soil. The reaction is carried out in the absence of light to avoid photodecomposition (Courchesne & Turmel, 2007) of the oxalate solution as well as the dissolution of crystalline Fe oxides (Kersten & Forstner, 1990). The two mechanisms responsible for dissolution of elements in an acid oxalate solution under darkness are protonation and complexation (Shang & Zelazny, 2008).

A volume of 20 ml of acid ammonium oxalate solution (a mixture of 0.2 M ammonium oxalate solution and 0.2 M oxalic acid solution at a ratio of 1.3:1, adjusted to pH 3) was added to 0.5 g of soil. Oxalate has a strong complexing ability at pH 3, which allows the extraction of the elements (Shang & Zelazny, 2008). Samples were agitated for 4 hours after which they were centrifuged. The extracts were membrane filtered using 0.45 um pore size filter paper and thereafter analysed using ICP-AES (Courchesne & Turmel, 2007).

3.2.5 Acid hydroxylamine

An acid hydroxylamine (HA) extraction was the appropriate method for the determination of the easily reducible Mn fraction of the soils. The amount of Fe and Al extracted was also measured in order to look at their association with Mn oxides. A hydroxylamine extract that

is acidified preferentially reduces Mn oxides whereas an oxalate extract that is buffered is selective for Fe oxide reduction (Relic et al., 2005). The citrate-bicarbonate-dithionite (CBD) method possibly extracts Mn as an oxide. The CBD extractable Mn values are usually higher than the hydroxylamine extractable values, indicating that some Mn may be removed from the structure of primary minerals (Phillips et al., 1998). The Mn-HA values are therefore more reliable than the Mn-CBD values (Phillips et al., 1998).

It is for the above mentioned reasons that the hydroxylamine method was chosen for its ability to selectively dissolve manganese oxides while minimizing the dissolution of iron oxides, based on the different behaviours of Mn and Fe oxides towards reduction under various conditions (Phillips et al., 1998). This solution effectively extracts Mn from ferromanganese nodules and Mn oxide coatings (Phillips et al., 1998). The principle of this method is based on dissolution kinetics of Fe and Mn oxides and hydroxides in the presence of hydroxylamine hydrochloride under specified experimental conditions, i.e. The concentration of the hydroxylamine extract, acidity, agitation time and sample : extractant ratio (Shang & Zelazny, 2008). The method provides more accurate results for amorphous and poorly crystalline Mn materials than crystalline oxides (Shang & Zelazny, 2008).

The mechanism for this reaction involves the reduction of Mn^{3+} and Mn^{4+} to Mn^{2+} (Neamen et al., 2004). The reaction for the reduction of Mn^{4+} is:

$Mn^{4+}O_2(c) + 2NH_3OH^+ \rightarrow Mn^{2+} + N_2(g) + 4H_2O$

The reaction for the reduction of Mn^{3+} is:

$Mn^{3+}{}_2O_3(c) + 2NH_3OH^+ + 2H^+ \rightarrow Mn^{2+} + N_2(g) + 5H_2O$

The experimental procedure was as follows. To 0.5 g of soil, 25 ml of hydroxylamine hydrochloride solution (0.1 M $NH_2OH{\cdot}HCl$ in 0.01 M HNO_3) was added. Samples were shaken for 30 minutes after which they were centrifuged. Supernatants were membrane filtered and analysed by ICP-AES (Gambrell, 1996).

3.2.5.1 Manganese speciation

The major Mn species extracted with acid hydroxylamine extraction are Mn^{3+} and Mn^{4+}, however a fraction of Mn^{2+}gets extracted along with this. In order to obtain a more accurate estimation of easily reducible Mn, a KCl extract and acid hydroxylamine extract were conducted using the same volume of extractant as the acid hydroxylamine method (25 ml) but

an increased mass of soil (1 g). This was done so that the KCl and hydroxylamine extracts now had equal quantities of extracting solution and soil (unlike the original methods) in order to avoid any error in results due to unequal soil to solution ratios. The remainder of the method remained the same as the acid hydroxylamine (Gambrell, 1996) and exchangeable Fe, Al and Mn (Bertsch & Bloom, 1996). All values were converted to a mass concentration ($mmol.kg^{-1}$) and the KCl extractable Mn was subtracted from the hydroxylamine extractable Mn.

3.3 Results and discussion

3.3.1 Understanding the reactivity of Mn in the various soils using XRF and chemical extractions

There are two experimental ways to characterize free oxides in soils (Jeanroy et al., 1991). The first is a chemical method relying on solubility and the second is a physical method involving clay mineralogy (Jeanroy et al., 1991). Selected samples were used for the chemical extractions as it was assumed they provide an estimate of total contents. Initially these samples were subjected to chemical extraction in order to compare the results obtained with the results from XRF in an attempt to determine the most appropriate method for the determination of total Mn, Fe and Al. A further review of literature, however, as well as results from analysis, show that the DC and CBD provide an estimate of the fraction of Mn, Fe and Al residing in the oxides and hydroxides of the various soils. Redox stable matrices, such as clay minerals, appear to be resistant to attack by these extractants. Pansu & Gautheyrou (2007) also suggest that the CBD method solubilises oxides and hydroxides, while leaving clays unaffected. Results from these chemical extracts could therefore be used to determine the fraction of the elements that reside in oxides and hydroxides in these soils. Understanding where the elements reside, Mn in particular, in the soils investigated is important in order to determine their redox stability or reactivity. The samples were selected according to their varying Mn contents, according to XRF, with the dolomite sample having the highest content, andesite samples having less and granite samples the least. Results from this analysis were used to express the amorphous and easily reducible elemental contents as a fraction of their respective total contents. This gives an indication of the fraction of the elements that are redox active in the soils.

3.3.1.1 X-Ray fluorescence

Table 3.1 shows the total amount of Mn, Fe and Al determined by XRF (refer to Appendix B Table B1 for other elements detected in the samples). The results indicate that the andesite (A) and vertic (V) samples had the highest Al contents, which is explained by their high clay contents (refer to Chapter two, Table 2.7). Similar to Al, the andesite sample also had the highest Fe content, which can also be attributed to the clay content as seen in Figure 3.1. It appears that the clay minerals provided the surface area for Fe oxides to precipitate on. Both Al and Fe show a strong correlation with clay content. Something interesting to note for Fe is that the quartzite (Q), granite (G) and dolomite (D) samples were taken from different positions in the landscape and for all of these samples Fe content appeared to decrease in the samples taken in lower positions in the landscape. These three sites have wetlands present and the loss of iron downslope could be attributed to increased reduction in these positions, resulting in loss of Fe. Aluminium on the other hand increased downslope for the quartzite and dolomite samples, and increased in the granite samples. A trend noticed is that both Fe and Al tend to increase with depth in the soil profiles. This is the result of illuviation and is most likely linked to clay content.

Table 3.1: Total elemental contents (mmol.kg^{-1}) for all soils as determined by XRF and elemental ratios as indices of relative enrichment

Sample	Al	Fe	Mn	Fe:Al	Mn:Al	Mn:Fe
Q_Crest_A	453	172	2.07	1:2.64	1:219	1:82.8
Q_Crest_B1	683	250	2.54	1:2.73	1:269	1:98.7
Q_Crest_B2	795	295	3.30	1:2.69	1:241	1:89.5
Q_Mid_A	379	93.5	3.02	1:4.06	1:126	1:31.0
Q_Mid_B1	604	121	2.65	1:4.98	1:228	1:45.8
Q_Mid_B2	751	201	3.24	1:3.73	1:232	1:62.1
Q_Foot_A	324	43.5	1.06	1:7.45	1:307	1:41.1
Q_Foot_B	718	78.0	1.41	1:9.20	1:509	1:55.3
Q_Bot_A	246	69.2	2.28	1:3.56	1:108	1:30.3
V_Black	1362	769	43.5	1:1.77	1:31.3	1:17.7
V_Brown	1219	901	72.0	1:1.35	1:16.9	1:12.5
G_Crest_A	1028	122	3.04	1:8.42	1:338	1:40.1
G_Crest_B	1311	172	2.90	1:7.64	1:452	1:59.1
G_Mid_A	636	92.3	2.52	1:6.89	1:252	1:36.6
G_Mid_B	742	116	3.37	1:6.40	1:220	1:34.4
G_Bot_A	421	42.7	0.44	1:9.87	1:964	1:97.7
G_Bot_B1	750	88.1	0.42	1:8.51	1:1773	1:208
G_Bot_B2	460	40.3	0.14	1:11.4	1:3263	1:286
D_Crest_A	514	322	276	1:1.60	1:1.86	1:1.16
D_Bot_A	821	261	112	1:3.15	1:7.32	1:2.33
A_Mid_A	1610	798	21.0	1:2.02	1:76.5	1:38.0
A_Mid_B1	2273	1034	17.8	1:2.20	1:128	1:58.1
A_Mid_B2	2412	1061	19.0	1:2.27	1:127	1:56.0
Mn wad	273	3619	2388	1:0.08	1:0.11	1:1.52

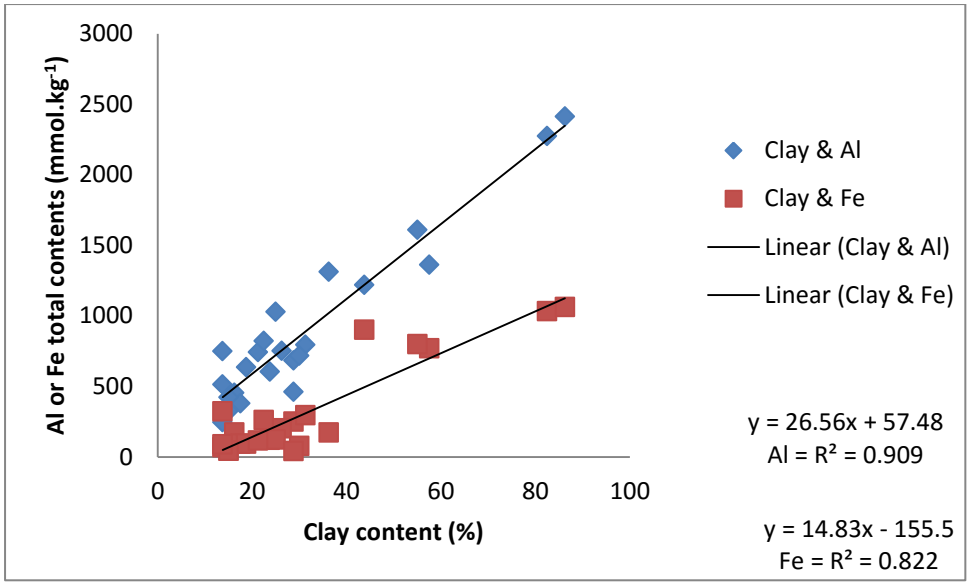

Figure 3.1: Relationship between clay content and Fe and Al

With regards to the Mn content in all the soils, the dolomite samples had the highest Mn content by far, best shown by the Mn:Fe molar ratio (Table 3.1) that was almost equimolar for D_Crest_A (1:1.16) and approximately a 1:2 ratio for D_Bot_A. This was closer to the Mn wad than any other soil. The brown vertic showed the closest Mn enrichment after the dolomites (1:12.5). This was, however, still an order of a magnitude smaller compared to the D_Crest_A soil. The andesite samples showed a lower Mn content than the dolomite and vertic samples but a much higher enrichment in Al and Fe. The quartzite and granite samples had much lower Mn contents than the other soils (lower than 5 mmol.kg^{-1} of soil). An interesting observation was made for the quartzite and granite soils. The quartzite soils showed an enrichment of Mn and less Fe downslope. The opposite was seen for the granite soils, which showed an enrichment of Fe and less Mn downslope. This suggests that Mn is more susceptible to reduction and loss in the granite soils than quartzite soils.

The high value of Mn in the dolomite soil, as detected by XRF, is expected due to the geology of the soil. Results for the Mn wad, which revealed a high Fe and Mn content, is in accordance with the study by Hawker and Thompson (1988). The reason for the difference in Mn content can be linked to parent material. Manganese rich parent materials give rise to Mn-rich soils. The main parent materials of dolomite and basalt are known to accommodate Mn minerals, producing Mn-rich soil. Parent material such as granite, with little Mn present in it, produce well drained, quartz-rich soil, which is poor in Mn, upon weathering (Yaalon et al., 1972). The trend observed is that, apart from quartzite Mn tends to decrease with depth

and decrease downslope. This opposes the findings however of Childs & Leslie (1977) and Yaalon et al. (1972) which showed an accumulation of Mn downslope under the influence of weathering. These studies however did not reveal if this was total Mn content or just the soluble or easily reducible fractions. Many factors can influence Mn distribution such as parent material, geomorphic processes, and soil moisture regime (Yaalon et al., 1972).

The high Mn content, as detected by XRF, in the vertic and andesite could be attributed to the higher clay content in these soils, apart from their original parent material. Increased clay contents can retard the loss of Mn by weathering (Discussion with PC de Jager). A study conducted by Reddy & Perkins (1976) showed that Mn can be fixed by clay minerals. This is explained by possible mechanisms such as precipitation, fixation in the clay lattice wedge zones and sorption on exchange sites. The association between Mn and clay content can be seen from the XRF analysis (Table 3.1) which shows a much higher Mn content for the dolomite soils, vertic and andesite soils. The vertic and andesite soils in particular had the highest clay contents as demonstrated in Table 2.7. Similar results were found by Harris & Adams (1966) who suggest that Mn resides primarily in the clay fraction. A study by Yaalon et al (1972), however, disputes this with their results finding that Mn was mainly in the non-clay fraction. It is important to bear in mind that the type of clay also controls Mn availability in soils (Rajakumar et al., 1996).

3.3.1.2 Chemical extractions - dithionite citrate and citrate-bicarbonate-dithionite

Extraction with dithionite citrate (DC) and citrate-bicarbonate-dithionite (CBD) indicated that the andesite samples had the highest Al and Fe contents (Table 3.2). This is consistent with the fact that it is derived from mafic rock with a high clay forming potential (refer to Table 2.7 for clay content), rich in ferrous Fe and Mg (as indicated by exchangeable Mg in Table 2.6). The dolomite soils (that do not exhibit mottles) had a strikingly higher Mn content than any of the other soils. The andesite samples had an appreciable Mn content and the granite samples (that have mottles present in the morphology) had a negligible Mn content. The results from these extracts for the selected samples followed the same trend as XRF for the Al, Fe and Mn contents.

Table 3.2: Dithionite citrate and citrate-bicarbonate-dithionite extractable Al, Fe and Mn ($mmol.kg^{-1}$)

	Al	Fe	Mn

Sample	DC	CBD	DC	CBD	DC	CBD
G_Bot_A	9.99	0.78	0.73	1.46	< MDL	< MDL
G_Bot_B1	9.33	0.66	0.54	1.14	< MDL	< MDL
G_Bot_B2	12.5	1.03	1.16	2.43	< MDL	< MDL
D_Bot_A	19.2	2.95	234	283	51.7	7.79
A_Mid_A	47.1	3.18	1404	625	9.19	0.80
A_Mid_B1	79.2	4.44	1847	572	7.51	0.66
A_Mid_B2	93.1	4.51	1927	627	8.55	0.66

3.3.1.3 Comparison of XRF with chemical extractions and determination of where elements reside in the soil

The Al determined by XRF for all samples was much higher than that chemically extracted by DC and CBD. This indicates that the Al in all the soils is predominantly in the clay minerals and therefore detected by XRF. The Fe extracted from the granite (G_Bot) samples chemically was much lower than the Fe determined by XRF. The amount of Fe chemically extracted from G_Bot_A and G_Bot_B2 was less than 2.5 mmol.kg^{-1} but XRF showed an Fe content of over 40 mmol.kg^{-1}. Sample G_Bot_B1 had less than 1.5 mmol.kg^{-1} Fe chemically extracted while XRF showed an Fe content over 80 mmol.kg^{-1}. The Fe in these samples is therefore associated with the clay fraction. This could be explained by the soft plinthic character of the G_Bot sample. The Fe in these samples appears to be fairly redox stable. The dolomite sample (D_Bot_A) showed similar Fe contents from XRF and both chemical analyses (DC and CBD), indicating that Fe in this sample resides in oxides in the soil. It is important to note that it is well supported in literature that CBD treatment does not always provide complete dissolution of Fe (Varadachari et al., 2006). Dissolution of goethite, hematite and amorphous ferric oxide using this method have been shown to be incomplete with one study suggesting that hematite was only dissolved to the extent of 50% (Varadachari et al., 2006). This is contrary to the method proposed by Mehra & Jackson (1960) who found the method to be efficient in dissolving crystalline hematite at pH 7.3 (near neutral) maintained by an $NaHCO_3$ buffer (Varadachari et al., 2006). In this case, however, since similar results are obtained by XRF and chemically, it can be assumed that almost complete dissolution of free oxides took place. The andesite samples had a much higher DC extractable Fe content than that detected by XRF, and therefore it can be assumed that Fe in the andesite samples resides in oxides.

The Mn content for all samples was higher as determined by XRF than chemically extracted. The CBD extractable Mn content was 7.79 mmol.kg^{-1}, DC extractable Mn was 51.7 mmol.kg^{-}

[1] and XRF showed an Mn content of 112 mmol.kg^{-1}. The Mn in all the samples therefore appears to be associated with clay minerals in these soils, or in crystal structures that make electron transfer difficult. The CBD method extracted a lower quantity of all the elements for most of the samples than DC, with the exception being Fe in the granite soils. These two extractions will be the subject of further comparison and discussion in Chapter five.

Comparison of the chemical extractions and XRF indicate that Al, Fe and Mn are extracted to a different extent for each method. Table 3.3 indicates the significance of the difference between Mn contents using the three different methods (the significant differences for Fe and Al are provided in the Appendix B in Tables B2 and B3). These differences show that XRF does not extract similar contents to the chemical extractants and that DC and CBD are not analogous methods for all soils as DC extracts significantly higher elemental contents than CBD. This could be attributed to the lower pH of the DC extraction solution as well as the lower soil to extract ratio of the DC extract resulting in an excess of reductant for the soil to react with. The extractability of the elements using these two extractants will also largely depend on the geology of the soils and the extent of weathering that the soils have been subjected to. The two chemical extracts appear to be ineffective in extracting Mn, Fe and Al from clay minerals and preferentially reduce oxides and hydroxides while XRF is able to determine elements in oxides, hydroxides and clay minerals. From this point forward, therefore, total elemental contents were taken as determined by XRF.

Table 3.3: Significance of differences in Mn content between XRF, DC and CBD

Sample	p-Values from T-Test for Significant Differences between Mn Contents		
	XRF & DC	XRF & CBD	DC & CBD
G_Bot_A	$2.74*10^{-08**}$	$6.12*10^{-07**}$	0.04^{**}
G_Bot_B1	$2.36*10^{-08**}$	$9.59*10^{-09**}$	0.42
G_Bot_B2	$4.25*10^{-08**}$	$2.36*10^{-09**}$	$7.57*10^{-03**}$
D_Bot_A	$5.2*10^{-04**}$	$2.84*10^{-06**}$	$7.74*10^{-04**}$
A_Mid_A	$1.99*10^{-04**}$	$2.58*10^{-06**}$	$2.71*10^{-04**}$
A_Mid_B1	$8.15*10^{-04**}$	$2.41*10^{-06**}$	$1.98*10^{-03**}$
A_Mid_B2	$1.17*10^{-04**}$	$1.83*10^{-07**}$	$2.32*10^{-04**}$

* = Significant difference ($\alpha = 0.01$)
** = Highly significant difference ($\alpha = 0.05$)

Since Mn and its influence on redox chemistry are the main focus of this study, differences in the amounts of Mn determined by XRF and the chemical extractions are shown in Table 3.4. Results revealed that the dolomite soil, with the highest Mn content, had the largest difference in Mn content measured. This is clear from a comparison of the differences in Mn

content as determined for all three methods. It can therefore be seen that the Mn is somehow being buffered from reduction in the chemical extractions, particularly the CBD method where the largest difference is observed between XRF and CBD. The large amount of Mn that could not be removed by reduction is an indication of the high quantity of Mn that is redox stable. It also appeared that the higher the Mn content in the soil, the larger the difference observed between XRF and the chemical extracts as well as between the two chemical extracts.

Table 3.4: Comparison of differences in Mn content between XRF and the chemical extractions (mmol.kg^{-1} soil)

Sample	XRF - DC	DC - CBD	XRF – CBD
G_Bot_A	0.44	<0.01	0.43
G_Bot_B1	0.42	<0.01	0.42
G_Bot_B2	0.14	<0.01	0.14
D_Bot_A	60.5	43.9	104
A_Mid_A	11.8	8.39	20.2
A_Mid_B1	10.3	6.85	17.1
A_Mid_B2	10.4	7.89	18.3

3.3.2 Amorphous elemental content

The results as depicted in Table 3.5 show that the andesite and vertic soils had the highest amorphous Al content. This is the same trend as that observed for the total Al contents and is expected due to the high clay content of these soils. The brown vertic had the highest amorphous Fe content followed by the andesite and dolomite soils. This is different to the total Fe content, which was highest for the andesite samples as determined by XRF. This indicates that the Fe in the brown vertic is more amorphous and less associated with the clay minerals in the soil. The dolomite soils had by far the highest amorphous Mn content followed by the brown vertic and the andesite samples. This followed the same trend as the total Mn contents determined by XRF. The amorphous Mn content in the wad was much lower than in the dolomite sample despite the fact that the wad contained a higher total Mn content than the dolomite samples. It therefore appears that Mn occurring in soils naturally is much more amorphous than that found in purer minerals.

Table 3.5: Amorphous elemental contents (oxalate extractable) and the fraction of amorphous metal content over total metal content as determined by XRF

Sample	Amorphous elemental content (mmol.kg^{-1})	Fraction of amorphous metal content over total metal content (%)

	Al	Fe	Mn	Al	Fe	Mn
Q_Crest_A	15.7	9.68	0.32	3.46	5.64	15.6
Q_Crest_B1	23.1	10.3	0.23	3.37	4.12	8.90
Q_Crest_B2	20.3	12.7	0.16	2.55	4.29	4.95
Q_Mid_A	10.4	4.32	0.91	2.73	4.62	30.2
Q_Mid_B1	13.9	5.19	0.55	2.31	4.28	20.6
Q_Mid_B2	14.6	8.16	0.91	1.95	4.05	28.1
Q_Foot_A	6.24	5.69	< MDL	1.93	13.1	0
Q_Foot_B	11.8	9.14	< MDL	1.64	11.7	0
Q_Bot_A	8.74	37.4	0.84	3.55	54.1	36.8
V_Black	46.5	37.1	7.06	3.41	4.82	16.2
V_Brown	54.8	101	30.7	4.50	11.3	42.6
G_Crest_A	22.4	7.96	1.01	2.18	6.52	33.2
G_Crest_B	29.1	8.31	0.43	2.22	4.84	14.8
G_Mid_A	13.0	4.62	0.84	2.04	5.01	33.2
G_Mid_B	15.6	5.41	0.98	2.10	4.67	29.1
G_Bot_A	8.52	10.4	0.01	2.02	24.2	2.85
G_Bot_B1	7.50	4.85	< MDL	1.00	5.51	0
G_Bot_B2	16.1	14.8	< MDL	3.51	36.7	0
D_Crest_A	35.3	37.8	87.8	6.88	11.7	31.8
D_Bot_A	38.1	40.1	82.0	4.64	15.4	73.0
A_Mid_A	41.8	54.7	12.5	2.59	6.85	59.3
A_Mid_B1	61.7	62.8	8.68	2.71	6.07	48.9
A_Mid_B2	63.7	66.2	9.48	2.64	6.24	50.0
Mn wad	27.1	72.7	17.0	9.94	2.01	0.71

The trend observed is that the amorphous Al and Fe contents in the soils (except quartzite samples) tend to increase with depth in the soil horizons. It is possible that due to the sandy nature of the quartzite soils, much of the Al and Fe leached out of the profiles. The Mn content is too low for a noticeable trend in most soils and the dolomite samples are too shallow to see a trend with depth. Looking at the andesite soils however it can be distinguished that Mn increases with depth, following the trend of Al and Fe for the granite samples. Looking at element mobility in the catenary sequence no real trend for the elements can be discerned.

A relationship appears to exist between amorphous Al and total Fe, as seen in Figure 3.2, indicating that much of the Fe is associated with the Al in the soil. This association is well documented. The isomorphic substitution of Al for Fe in goethite and to a lesser extent hematite (Tardy & Nahon, 1985) results in structural modifications (Schwertmann, 2008). This ionic substitution is made possible due to the similar size of Fe^{3+} and Al^{3+} with Al^{3+} having a slightly smaller ionic radius (0.53 *Å*) than Fe^{3+} (0.65 *Å*) (Schulze, 1984). This substitution of Al for Fe tends to increase the stability of the modified mineral (Fey, 1981). The results from the oxalate extract reveal that the soils with higher Mn contents tend to have

higher Al contents. It could therefore be possible that the Al in these soils could be substituted for Fe or Mn in the minerals, since both Fe and Mn have identical ionic radii of 0.645*Å (*Abdel-Khalek et al., 2008*)*. It could therefore be possible that Al has the same stabilizing effect on the Mn oxides as they do on the Fe oxides. This would retard the reduction of Mn^{2+} which would in turn prevent Fe^{2+} from being reduced. A comparison of amorphous Al and total Mn, similar to that depicted in Figure 3.2, revealed a correlation coefficient of 0.13 for all the samples and 0.51 when taking only the samples with appreciable Mn contents (V, D and A) into consideration. The relationship between amorphous Al and total Mn therefore appears to be weak. The correlation between amorphous Al and amorphous Mn was very similar, revealing a correlation coefficient of 0.16. Chapter four further investigates the influence of Al, Fe and Mn on redox buffering.

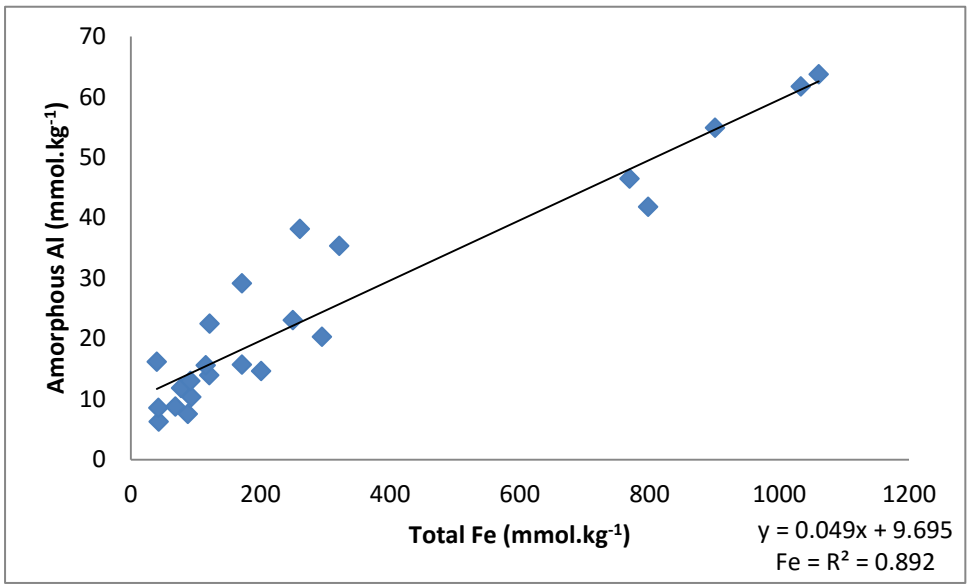

Figure 3.2: Relationship between amorphous Al and total Fe

Something that was observed upon comparing the DC and CBD extractable contents (Table 3.2) with oxalate extractable elemental contents is that for some samples the amorphous content measured was higher (e.g. D_Crest_A had an amorphous Al content of 35 $mmol.kg^{-1}$ soil and a total content extracted by DC of 25 $mmol.kg^{-1}$). The possible explanation for this is that the ammonium oxalate extract solution pH is 3 (conducive to redox and proton promoted dissolution), whereas the DC and CBD extracts are buffered at neutral pH (7 – 7.3) to ensure that reductive dissolution is the main mechanism of dissolution (Arshad, et al., 1971). The lower pH of the oxalate extract also induces stronger reducing conditions, leading to an increased extraction of the metals. The contrast appears more stark with CBD than DC.

A possible reason could be that oxalate extracts a larger amount of Fe from soil clay and silt fractions than CBD does and studies have also shown that Fe removal from nodules is more efficient with oxalate than CBD (Varadachari et al., 2006). This could be true for Al and Mn as well.

The fraction of amorphous metal content over the total metal content was compared in order to determine to the percentage of the metals existing in the amorphous phase in these soils. This can be expressed as the particular element's activity level, for example Fe activity level is expressed as oxalate-extractable Fe over dithionite-extractable Fe (Frohne et al., 2011). The results are given in Table 3.5. With regards to amorphous Al, it appears that a relatively small fraction was amorphous in all of the samples. The D_Crest_A sample had the highest Al content and this was only 7%. The Al therefore seems to be well incorporated in the crystal structure of the associated minerals of these soils.

The Q_Bot_A sample had by far the highest amorphous Fe fraction, and therefore Fe activity level, followed by the G_Bot_B2 sample. It can therefore be elucidated that the higher the water content in the soil (the closer the sample is to the wetland), the higher the fraction of amorphous Fe is relative to the total content and therefore Fe activity level. This is expected as the fluctuating water table leads to a reducing environment in which Fe^{3+}, which sits in the crystal structure, is reduced to the amorphous form of Fe^{2+} (Reddy & DeLaune, 2008).The soluble Fe^{2+} re-oxidizes under aerobic conditions, forming less crystalline ferric oxides. The amorphous Fe content increased from the D_Crest to D_Bot sample further downslope, indicating reducing conditions where D_Bot was sampled. The fraction of amorphous Fe and Al appeared to increase in the dolomite (D_Crest) sample as well as the wad. These are the samples with the higher Mn contents. It is therefore possible that Mn oxides are able to re-oxidize soluble Al and Fe and incorporate them into their crystal structures very weakly.

The trend observed for Mn for most of the samples is that the fraction of amorphous Mn in relation to the total content of the metal was much higher than that of Fe and Al, indicating that this element has the highest activity level. Mn in these samples is mostly amorphous, which concurs with a study by Singh & Gilkes (1996). This can be explained by the poor crystallinity of Mn oxides (Post, 1999). Interestingly, the only samples that had negligible amorphous Mn contents are those that exhibit redoximorphic features, i.e. the Q_Foot and

G_Bot samples that were taken near the wetlands. The wad had a very low Mn activity level despite its high total content.

The enrichment of Mn in the dolomite samples was calculated in order to better understand their high activity levels. The same was done for the Mn wad sample to investigate the reason for its conspicuously low Mn activity level. The dominant elements in the dolomite and wad samples were Al, Fe and Mn and therefore Mn enrichment was calculated as [(Mn/Al+Fe+Mn)*100]. The calculations were first done using total elemental contents as determined by XRF. The D_Crest and D_Bot samples had an Mn enrichment of 25% and 9% respectively with dominant element in these samples being Al. The Mn wad had an Mn enrichment of 38%, having Fe as the dominant element. These results did not explain the high Mn activity of the dolomite samples and the low activity of the wad, therefore the calculations were redone using the amorphous elemental contents, which is the more reactive fraction. It was clear for the dolomites that the dominant amorphous element was Mn. The Mn enrichment values for the D_Crest and D_Bot samples were 55% and 52% respectively. This explains the high Mn activity levels in these soils. Interestingly, the wad had an Mn enrichment of only 15% with the amorphous fraction of this sample being dominated by Fe. This explains the low Mn activity level of the wad.

Results indicate that the amorphous Fe contents is much higher in the dolomite, andesite and vertic soils (all samples with high Mn contents according to results from XRF and chemical extractions) than the granite and quartzite (low Mn content soils according to characterization by XRF and chemical extractions). It was observed that the soils with the lower total and oxalate extractable Fe, Mn and Al contents were the soils that exhibit mottling in the morphology. These soils therefore experience poor buffering to reduction. It also seems that soils with a higher Mn activity level than Fe (the dolomites) are the soils that lack redoximorphic features. This further suggests that there is buffering of the expression of redoximorphic features in manganiferous soils.

3.3.3 Easily reducible manganese

The easily reducible forms of manganese in the soil are Mn^{3+} and Mn^{4+}. It is these forms of Mn that act as oxidizing agents in the soil (Bartlett, 1988). The method that was used was specific for the dissolution of Mn oxides with minimal dissolution of other minerals, however

it can be seen in Table 3.6 that a considerable amount of Al, and to a lesser extent Fe, was extracted using this method. The low amount of Fe extracted is in accordance with a study conducted by Relic et al. (2005) in which very small quantities of Fe was extracted by hydroxylamine. This investigation revealed that about 8% of amorphous oxyhydroxides and less than 1% of magnetite, goethite and hematite are extracted by hydroxylamine. A study by Lovley & Phillips (1987) however explains the increased amount of Fe extracted from the Q_Bot_A, V_Brown, and both D samples. This investigation elucidated that a 0.25 M hydroxylamine hydrochloride extract is the more preferred method for the determination of amorphous Fe (III) oxides in soils to ammonium oxalate (Lovley & Phillips, 1987) because under reducing conditions, hydroxylamine reduces Fe^{3+} to Fe^{2+} (Wallmann et al., 1993). The concentration of the hydroxylamine hydrochloride used in the method for these soils is 0.1 M therefore a higher concentration would have likely resulted in a higher quantity of Fe being extracted.

Nevertheless, since the method was intended for the reduction of Mn oxides and acid hydroxylamine is specific for the determination of easily reducible Mn, the method was not modified and the results obtained for Mn is the main focus of the investigation. A critical review of literature suggests that Mn contents vary between the air-dried and field moist states and more representative values are obtained by examining the soil in the field moist state. A number of studies have revealed that Mn^{2+} increases upon drying (Ross et al., 2001; Bartlett & James, 1980) and easily reducible Mn decreases (Berndt, 1988) indicating that drying favours reduction. All Mn determinations were therefore conducted on field moist samples so that the chemical nature of the Mn oxides was not changed by drying. The influence of drying on the solubility of Mn in the soils used in this study will be further explored in Chapter five.

Table 6.6: Hydroxylamine extractable elemental contents and fraction of easily reducible Mn over total Mn content as determined by XRF

Sample	Hydroxylamine extractable elemental content ($mmol.kg^{-1}$)			Fraction of easily reducible Mn over total Mn content (%)
	Al	Fe	Mn	
Q_Crest_A	4.55	0.61	0.47	20.3

Q_Crest_B1	3.89	0.17	0.23	9.55
Q_Crest_B2	4.06	0.33	0.18	4.70
Q_Mid_A	3.11	0.78	0.80	31.2
Q_Mid_B1	2.07	0.47	0.68	31.9
Q_Mid_B2	2.09	0.58	0.51	19.9
Q_Foot_A	2.09	1.72	0.02	3.24
Q_Foot_B	1.81	0.39	0.03	2.23
Q_Bot_A	3.13	7.20	0.93	51.9
V_Black	0.24	0.44	10.3	2.67
V_Brown	4.96	4.62	23.9	12.5
G_Crest_A	6.00	0.80	0.95	34.9
G_Crest_B	7.02	0.40	0.49	18.4
G_Mid_A	4.05	0.79	0.82	41.5
G_Mid_B	4.28	0.54	0.61	20.1
G_Bot_A	3.06	1.39	0.01	4.68
G_Bot_B1	1.80	0.66	< MDL	0.78
G_Bot_B2	2.65	1.01	< MDL	2.45
D_Crest_A	13.4	13.3	132	34.5
D_Bot_A	11.8	11.7	90.5	63.4
A_Mid_A	3.80	1.50	10.8	42.9
A_Mid_B1	5.40	1.25	6.95	25.6
A_Mid_B2	5.18	1.38	6.58	32.2

Table 3.6 demonstrates that results are similar to that of the amorphous Mn content of the soil, with the dolomite soils having the highest easily reducible Mn content from all the soils (between 80-90 mmol Mn per kg soil). The vertics and andesite soils had a lower easily reducible Mn content than the dolomites but higher than the quartzite and granite samples. The quartzite and granite soils had very low, almost negligible, easily reducible Mn contents having values of less than or equal to 1 $mmol.kg^{-1}$ soil. Only soil samples were subjected to this extraction and therefore the wad was not analysed. It is clear from this experiment that the easily reducible Mn was low in soils that expressed mottles in their morphology.

The trend observed is that easily reducible Mn tends to decrease with depth, showing lower values in the subsoils than the A horizons for the samples. This could be due to reduction by organic matter in the topsoils resulting in higher amounts of soluble Mn in A horizons. Looking at the soils taken in a catenary sequence (quartzite, granite and dolomite) easily reducible Mn tends to decrease downslope. This could be a result of soluble Mn being more mobile and more easily transported downslope than easily reducible forms. This opposes the findings of Phillips et al. (1998) which revealed that lower hydroxylamine extractable Mn values were found in summit samples than samples taken downslope. This follows the theory that Mn transported in soil solution tends to settle in leached, partially weathered bedrock where the water table is present (Phillips et al., 1998).

A link has been established between hydroxylamine reducible Fe^{3+} and microbially reduced Fe^{3+} (Lovley & Phillips, 1987; Cummings et al., 1999). Amorphous and poorly crystalline Fe is the most important phase for microbial Fe reduction (De Schamphelaire et al., 2007). It would therefore have been expected that these soils would have prominent mottle expression. What is observed, however, is that the V_Brown and dolomite samples with the higher Fe extracted also had the highest easily reducible Mn extracted and it is in these samples that the morphology lacks redoximorphic features. The Q_Bot_A sample had a considerably high hydroxylamine extractable Fe content compared to the other samples, however this can be explained by the high organic carbon content in this soil which serves as a source of electrons for reduction processes. The Q_Foot and G_Bot samples, however had lower easily reducible Fe contents, and incidentally the lowest easily reducible Mn contents, and these are the soils that exhibit redoximorphic features.

The fraction of easily reducible Mn over total Mn is expressed in Table 3.6. This was done because Mn oxides with a greater fraction of easily reducible Mn have a greater oxidizing capacity (Davison & Woof, 1984). The D_Bot_A sample (which did not express mottles) had the highest percentage of easily reducible Mn in relation to total Mn while the samples that showed the lowest fractions were the granite and quartzite samples (G_Bot and Q_Foot) taken near the wetland (exhibiting redoximorphic features). This infers that the dolomite soils appear to have the greatest oxidizing capacity while the quartzite and granite soils appear to have weak oxidizing capacities. A trend observed for the hydroxylamine extractable Mn expressed as a fraction of the total Mn content (Table 3.6) is similar to that obtained for easily reducible Mn in the samples (Table 3.6).

The relationship between total Mn (as determined by XRF) and easily reducible Mn was also investigated. A high degree of correlation between the two indicates that most of the Mn present is redox reactive (Davison & Woof, 1984). The results are given in Figure 3.3. The graph shows a strong correlation between the two indicating that in these soils, Mn is redox reactive.

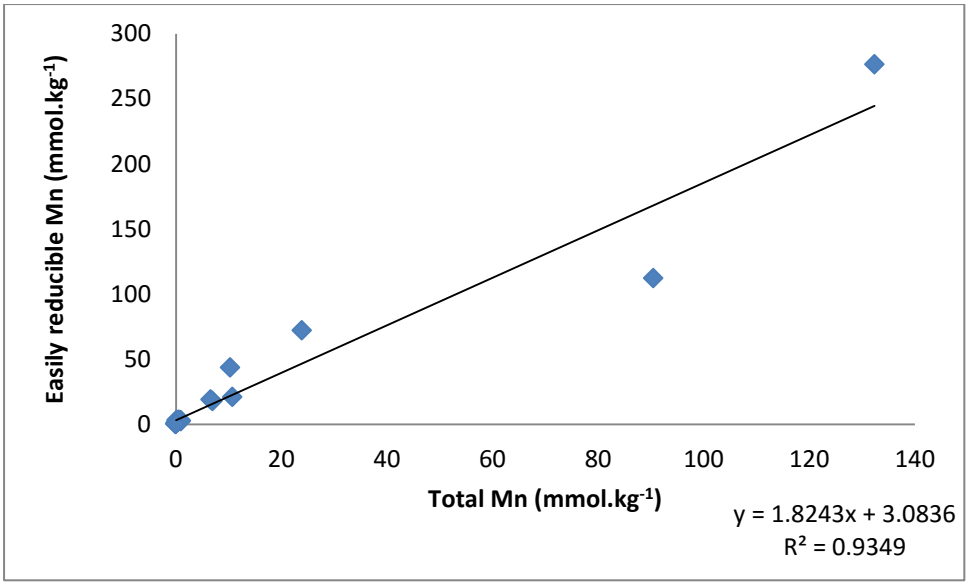

Figure 3.3: Relationship between total Mn and easily reducible Mn

3.3.3.1 Manganese Speciation

The manganese extracted with the acid hydroxylamine extraction is mainly in the 3+ and 4+ states. A complexity of Mn crystal chemistry, however, is the various valencies that Mn can exist in, making it difficult to determine the proportions of Mn^{4+}, Mn^{3+} and Mn^{2+} (Post, 1999). It was therefore suspected that an amount of Mn^{2+} was also extracted in the acid hydroxylamine extraction. This made it necessary to determine what quantity of the extracted Mn was attributed to Mn^{2+} in order to isolate Mn^{3+}/Mn^{4+}. What was observed, however, is that only a very small amount of exchangeable Mn (in the form of Mn^{2+}) was extracted (Table 3.9). All samples had less than 0.5 mmol.kg^{-1} exchangeable Mn. It was therefore unnecessary to perform any recalculations on the results obtained from the acid hydroxylamine extract as the Mn^{2+} was effectively negligible and it can be assumed that the contribution of exchangeable Mn to the easily reducible Mn extracted was negligible.

Table 3.7: Manganese speciation derived from easily reducible and exchangeable content

Sample	Hydroxylamine (Mn^{2+}, Mn^{3+}, Mn^{4+})	KCl(Mn^{2+})	Easily reducible Mn(Mn^{3+}, Mn^{4+})
Q_Crest_A	0.43	0.01	0.42
Q_Crest_B1	0.24	< MDL	0.24
Q_Crest_B2	0.16	0.01	0.15
Q_Mid_A	0.98	0.04	0.94
Q_Mid_B1	0.85	< MDL	0.85
Q_Mid_B2	0.65	< MDL	0.65
Q_Foot_A	0.04	< MDL	0.03
Q_Foot_B	0.03	< MDL	0.03
Q_Bot_A	1.19	< MDL	1.19
V_Black	1.17	< MDL	1.16
V_Brown	9.01	< MDL	9.01
G_Crest_A	1.07	0.01	1.06
G_Crest_B	0.54	0.01	0.54
G_Mid_A	1.06	0.01	1.05
G_Mid_B	0.69	0.01	0.68
G_Bot_A	0.02	< MDL	0.02
G_Bot_B1	0	< MDL	< MDL
G_Bot_B2	0.01	< MDL	< MDL
D_Crest_A	95.2	< MDL	95.2
D_Bot_A	71.1	< MDL	71.1
A_Mid_A	9.03	< MDL	9.03
A_Mid_B1	4.55	< MDL	4.55
A_Mid_B2	6.10	< MDL	6.10

3.4 Summary

The results for total elemental contents using XRF show that the andesite samples have the highest Al and Fe contents, which appears to be linked to the high clay content of this soil. The dolomite soil (which has no mottles present in the morphology) has the highest total Mn content. The vertic and andesite soils have less Mn than the dolomite samples but more than the quartzite and granite samples which have negligible Mn contents (and exhibit mottles).

Elemental extractions by DC and CBD on selected samples show the same trend as XRF for these samples. Quantitative comparisons of the elements as determined by XRF (which estimates elemental contents from oxides, hydroxides and clay minerals) and extracted chemically (selective for extraction from oxides and hydroxides) reveal that Al and Mn seem to be associated more with the clay fraction while Fe appears to reside in soil oxides and hydroxides. Although literature suggests that DC and CBD should give similar results, this study finds that this is not always true. In this study, with the exception of Fe for the granite samples, CBD extracts lower quantities of Mn, Fe and Al than DC does.

A study of the amorphous fraction of the soil reveals a strong correlation between total Fe and amorphous Al in the soils. It is seen that Fe and Al contents increase in the dolomite samples and wad, which led to the assumption that there was an association of not only the Mn oxides with Fe but with Al as well. It was therefore postulated that a similar stabilizing effect to that of Al and Fe could exist between Al and Mn due to the similar ionic size of Fe and Mn. A low correlation coefficient was observed between the two elements, however this does not rule out the possibility of Mn substitution having a stabilizing effect on Fe oxides.

An expression of the amorphous contents of the elements over their total contents show that a higher fraction of Mn was amorphous compared to Fe and Al and that Al is well incorporated in the crystal structure. The highest amorphous Fe contents were found in the dolomite, vertic and andesite samples (which also have higher Mn contents) with lower contents found in the quartzite and granite samples (which have negligible Mn). It would therefore be expected that the samples with higher amorphous Fe contents are more susceptible to attack by strong reductants, however it was the samples with the lower amorphous Fe contents that exhibited redoximorphic features. Soils with higher Mn activity levels than Fe are the soils that lack redoximorphic features. High Mn activity levels of the dolomites can be explained by the samples being highly enriched in Mn (approximately 50% Mn enrichment). It therefore appears that a buffering mechanism is at play, preventing the reduction of the amorphous Fe in the high Mn content soils.

The easily reducible Mn contents for all the soils follows the same trend as the Mn contents determined by XRF, DC, CBD and ammonium oxalate. The easily reducible Mn contents decreases in the samples that express mottles in their morphology and are higher in the samples that lack redoximorphic features. Soils with lower hydroxylamine extractable Fe (and lower hydroxylamine extractable Mn) were the soils that exhibited mottling. A high correlation between easily reducible and total Mn content indicate that the Mn in the samples is redox reactive and therefore willing to participate in redox reactions. These results again suggest that redox reactions are buffered in some way in hydric soils with high Mn contents.

Chapter four: The redox buffering capabilities of the selected soils

4.1 Introduction

Manganese in the form of oxides (Mn^{3+} and Mn^{4+}) is the "paramount parking place for electrons", even above oxygen, because the release of O_2 in soil, water and air is only made possible by the oxidation of O^{2-} in water by Mn during photosynthesis (Bartlett, 1988). Mn^{3+} and/or Mn^{4+} play a pivotal role in redox processes and its quantification as well as the determination of the forms it exists in (which infers the crystallinity of Mn in the sample and therefore reactivity) is important. It is expected that soils with a higher Mn^{3+} and/or Mn^{4+} content have a higher oxidizing tendency than reducing and therefore buffer reduction. Strongly buffered soils have a lower propensity to donate electrons than weakly buffered ones do. Soils, therefore, naturally have different electron accepting and donating tendencies.

Redox status can be classed into four soil conditions; oxidizing (>400mV; O_2 predominant), weakly reducing (400 to 200mV; O_2, nitrate, and $Mn^{3+/4+}$ reduced), moderately reducing (200 to -100mV; Fe^{3+} reducing) and strongly reducing (<100mV; sulphate and CO_2 reduced) (Mansfeldt, 2003; Husson, 2013). There are six redox status categories (Bartlett & James, 1995).

1. **Superoxic:** Very highly oxidized soils with a prevalence of Mn oxides and Mn^{3+} or oxygen free radicals.
2. **Manoxic:** Highly oxidizing soil systems that are well drained and lack gley mottles throughout the profile
3. **Suboxic:** These are oxidizing soils that contain nitrates. The reducing tendency is balanced by oxidizing propensity.
4. **Redoxic:** The balanced reducing and oxidizing tendencies favour reduction. There is an absence of Fe^{2+} and presence of Fe^{3+} in recently oxidized forms.
5. **Anoxic:** The presence of Fe^{2+} is diagnostic in these highly reduced soils and nitrates are absent.
6. **Sulfidic:** These are very strongly reducing soils. Oxygen is absent and sulphides are prevalent.

In order to test the different propensities of soils to donate or accept electrons, redox measurements for the selected soils of this study had to be tested. The conventional method

of measuring anaerobic conditions is by measuring redox potential (Eh) (Fiedler et al., 2007). There is a need however to improve the assessment of these conditions in order to identify hydric soils and wetlands (Fiedler et al., 2007). The results from the measurement of redox potential, have limited use (Bartlett, 1988) with Eh measurements being difficult to reproduce and interpret (Husson, 2013). Thermodynamic equilibrium is almost never reached in natural soil systems and the heterogeneity and thermodynamic instability, which occurs when chemical equilibrium is not achieved, of these systems results in the measured redox potential being a mixed potential (Bartlett & James, 1995; Dowley et al., 1998). Another reason that the direct measurement of electron activity by reduction potential (Eh) is not always practical is due to low concentrations of dissolved electrons (Lindberg & Runnels, 1984; Herbel et al., 2007) or the presence of multiple redox species (Striggow, 2013). It is also possible that some redox species that are strong oxidants or reductants are trapped in crystal structures and weaker oxidants and reductants in solution are given the opportunity to participate in redox reactions much faster. Another flaw of Eh measurements is that the oxidized species of N, S, Mn, Fe, C and H, which are all major components of partially oxidized soils, will not influence measured potentials because they are not electroactive (Bartlett & James, 1995). Exclusion of these species makes these measurements confusing and of little value (Bartlett & James, 1995).

Problems with Eh measurements are also often encountered with the platinum (Pt) electrode due to the difficulty in obtaining accurate readings (Alloway, 1995). The measurement of pH relies on solution H^+ activity, however Eh measurements rely on electron transfer (not activity) and depends on the Pt electrode being inert. This quality is negatively influenced in the presence of dissolved O_2 due to the reaction of the oxygen with the surface of the Pt^0 surface of the electrode, oxidised to Pt^{2+}. The result of this is the reduced sensitivity of electrode response from the electron transfer between the redox-sensitive species in solution. Measurements with Pt electrodes under aerobic conditions are also an unreliable indicator of redox status due to the response of the electrodes to pH when dissolved oxygen is dominant in these environments (Essington, 2004) as well as the low concentration of redox couples in well aerated soils (Dowley et al., 1998). These electrodes are also very sensitive to calibration as well as polarization of the electrode, which could cause erroneous results (Pansu & Gautheyrou, 2006). Another challenge is that exchange current densities could be insufficient, leading to inaccurate electrode responses for many redox couples (Herbel et al., 2007) or the exchange current may be too low to establish an Eh measurement (Lindberg &

Runnels, 1984). Problems can also arise with the installation of Pt electrodes in soils over a long period of time, such as poisoning and contamination that occurs when the electrode becomes coated with substances that affect the measured electrode, and electrode breakdown, which is caused by electrode rupture or waterproof resin leakage under saturated water conditions (Mansfeldt, 2003). These can lead to unreliable measurements.

With the above-mentioned challenges taken into consideration, it was decided to conduct the redox studies for the selected soils by chemical analysis in order to assess the ability of the soils to act as electron acceptors. There are limited documented soil chemistry tests for redox determinations. Two of the few that can be applied are manganese and total electron demand. Manganese electron demand (MED) and total electron demand (TED) are both tests to measure the oxidizing capacity of soil. Unlike the Cr oxidation test, the measured values are unaffected by the activities of the reductants in the soil to a large extent (Bartlett, 1988). This is because iodide cannot be further reduced but chromate ($Cr_2O_7^{2-}$) where Cr has a valency of 6+, can be reduced to Cr^{3+}.

The understanding of the principle behind this method is important in order to interpret the analysis. The test for electron demand is based on an iodometric redox titration, which is one of the most accurate volumetric redox measurements (Barreiro & Naves, 2007). This involves the titration of iodine with sodium thiosulphate using starch as an indicator to detect the colour change. During the reaction, iodide (I^-) is oxidized to iodine (I_2) by an analyte (such as MnO_4^- and MnO_2, which are electron acceptors) (Barreiro & Naves, 2007). The reactions would look as follows:

$$6I^- + 2MnO_4^- + 4H_2O \rightarrow I_2 + MnO_2 + 8OH^-$$

$$2I^- + MnO_2 + 4H^+ \rightarrow I_2 + Mn^{2+} + 2H_2O$$

The iodine that is generated is then reduced by the titrant, thiosulfate ($S_2O_3^{2-}$) by the following reaction:

$$I_2 + 2S_2O_3^{2-} \rightarrow 2I^- + S_4O_6^{2-}$$

Iodine develops a deep blue colour with starch and the colour disappears once all of the iodine is removed. This iodometric titration is conducted at a pH between 3 and 5 (Barreiro & Naves, 2007). In the absence of iodine, the solution remains colourless.

4.2 Methods and materials

4.2.1 Manganese electron demand

Intermittent agitation of 2 g field moist soil (0.5 g for high Mn content soils, i.e. dolomite and Mn wad) with 12 ml pH 4 0.6 M NH_4OAc, which buffers the solution at a pH of 4,and 4 ml 0.2 M KI, was performed for 18 hours. In many anoxic environments, acetate is an important electron donor that supports reductive processes (Yoon et al., 2013). A study by He et al. (2002) revealed that acetate was the electron donor for the reductive dechlorination of cis-1,2-dichloroethene and another study by Yoon et al. (2013) showed that denitrifying *Shewanella* spp. used acetate as an electron donor. In this method, however, the ammonium acetate is used to buffer the pH of the solution. The samples were centrifuged and membrane filtered (0.45 um). Starch solution (0.3 g starch boiled in 50 ml deionized water) was added as an indicator and samples were titrated to a colourless endpoint with 2 mM $Na_2S_2O_3$ (Bartlett & Bruce, 1996).

4.2.2 Total electron demand

A volume of 4 ml 0.2 M KI followed by 12 ml 0.1 M HCl was added to 2 g field moist soil (0.5 g for high Mn content soils, i.e. dolomite and Mn wad). Samples were centrifuged and membrane filtered. Starch solution indicator was added to extractants, after which these were titrated to a colourless endpoint with 2 mM $Na_2S_2O_3$ (Bartlett, 1988).

4.3 Results and discussion

It is expected that for soils with a net oxidizing tendency, more iodide will be oxidized to iodine because strongly redox buffered soils have a lower propensity to accept electrons than weakly buffered ones do. Soils with a stronger reducing tendency are more willing to accept and donate electrons.

4.3.1 Manganese electron demand (MED) and total electron demand (TED)

4.3.1.1 Manganese electron demand

MED aims to isolate the contribution of Mn oxides to the oxidizing ability of the soil and is generally the preferred measure of the role of Mn oxides in reactions of soil. This is because in addition to Mn oxides, TED also measures the role of Fe^{3+}. The results of MED can be seen in Table 4.1. An increase of MED with Mn is indicative of oxidized levels of Mn in the samples (Bartlett, 1988). A restricted O_2 environment tends to show an increase in MED

(Bartlett, 1988). This can be explained by the O free radicals, which are generated as a result of partial reduction of O_2, providing a mechanism for the oxidation of Mn and the freshening of MnO_2 surfaces (Bartlett, 1988). The only samples with any measurable MED were the wad, dolomite samples and the A_Mid_B2. The Mn wad had by far the highest MED, due to it having a much higher total Mn content (2388 $mmol.kg^{-1}$) than the soils. This MED was very high despite the fact that the amorphous fraction of Mn as well as the easily reducible fraction of Mn was lower than the dolomite soils. The dolomite soils, which had the highest Mn content from all the soil samples as determined by XRF (D_Crest = 276 $mmol.kg^{-1}$, D_Bot = 112 $mmol.kg^{-1}$), had the highest MED values, which are still considerably low taking into account the high total Mn content of these soils. The MED per mass of Mn was investigated (Table 4.1). Values are represented in umol and not mmol in order to show the differences more clearly. It was expected that the wad and dolomite samples would have the highest MED per mass Mn in the soil. What was observed, however, is that all the soil samples with measurable MED had very similar values for MED per mass of Mn in the soil. The Mn wad had a vastly higher MED than the dolomite soil, and had double the value for MED per mass Mn in soil.

The rest of the samples (quartzite, granite, vertic and andesite A and B1 horizons) showed no colour reaction and therefore no MED could be determined from these soils and was assumed to be negligible. The vertic samples (in particular the V_Brown vertic) had the second highest Mn content as determined by XRF (V_Black = 44 $mmol.kg^{-1}$ and V_Brown = 72 $mmol.kg^{-1}$), however, no MED was detected. The andesite samples followed the vertic samples in Mn quantity determined by XRF with all of them having similar Mn quantities (21, 18 and 19 $mmol.kg^{-1}$ for the topsoil, B1 and B2 horizons respectively) but only the B2 horizon (19 $mmol.kg^{-1}$) had a measurable MED.

Table 4.1: MED and TED (mmol $e^-.kg^{-1}$ soil) and MED and TED per mass of total Mn and total Fe+Mn (umol e^-.umol Mn/Mn+Fe) in the soil as determined by XRF

Sample	MED	MED per mass Mn	TED	TED per mass Fe+Mn
Q_Crest_A			0.93	5.38
Q_Crest_B1			0.59	2.32
Q_Crest_B2			0.66	2.21
Q_Mid_A			1.78	18.4
Q_Mid_B1			2.12	17.1
Q_Mid_B2			1.72	8.39
Q_Foot_A			0.90	20.3
Q_Foot_B			0.37	4.64
Q_Bot_A			3.46	48.4
V_Black			6.85	8.43
V_Brown			29.2	30.0
G_Crest_A			1.92	15.3
G_Crest_B			1.32	7.57
G_Mid_A			2.10	22.2
G_Mid_B			1.40	11.8
G_Bot_A			0.55	12.6
G_Bot_B1			0.30	3.43
G_Bot_B2			0.31	7.73
D_Crest_A	2.86	10.3	146	243
D_Bot_A	0.85	7.59	129	347
A_Mid_A			13.6	16.7
A_Mid_B1			9.54	9.07
A_Mid_B2	0.20	10.4	9.95	9.22
Mn wad	46.8	19.6	387	64.5

Considering the results from the previous chapter for the total Mn contents and easily reducible Mn contents, the dolomites had the highest, followed by the andesites and vertics. The A_Mid_B2, however, is the only andesite sample that had a measurable MED. The possible reason why this horizon had a measurable MED could be due to the large amount of Mn concretions in its horizon, and these features could possibly be newly formed and therefore more susceptible to redox reactions.

Looking at the vertic samples, the fraction of amorphous Mn in the V_Brown sample was 42% and therefore a measurable MED was expected. The fraction of amorphous Mn over total Mn for the V_Black was only 16%, as calculated in Chapter three, which indicates that Mn is well incorporated in crystal structures, possibly making them unavailable for participation in redox reactions. This would account for why this sample did not have measureable MED. Looking at the easily reducible Mn contents for both of these soils the V_Black had 10 and V_Brown had 24 mmol.kg^{-1} soil. It was therefore again expected that the brown vertic at least would show an MED.

Other reasons why the samples with considerable Mn contents (the vertics and andesite topsoil and B1 horizons) did not measure any MED values could be due to Mn in these samples being present in the form of impurities in the crystal structures of Fe oxides, making them poorer electron acceptors. Another possibility is that the high clay content of these soils had a stabilising effect on the Mn oxides and inhibits its participation in redox reactions and therefore its oxidizing capabilities. It is also possible that the higher organic matter content in the A and B1 horizons reduced $Mn^{3+/4+}$ to Mn^{2+} making the MED negligible.

Errors in the method could have also been encountered. This is suspected because the MED values that were detected for the samples, particularly the dolomite samples, were quite low when you take into consideration the high amount of Mn, in particular easily reducible Mn, in these samples. It is possible that this method is not suitable for old, highly weathered soils. The concentration of KI that is stipulated and thus used for this method is 0.2 M, however, this may not have been concentrated enough to avoid volatilization of iodine. The method used by Dowding (2004) made use of 0.5 M KI, which may have overcome this challenge. In the method used in this study, an attempt was made to concentrate the reagents and ensure a greater excess of iodide by decreasing the amount of soil used for the high Mn content soils. A mass of 0.5 g was used instead of the 2 g outlined in the method. This was another modification to the original method that was carried out by Dowding (2004). The use of high concentrations of KI could result in a decrease in sensitivity, however the use of too little soil can have the same effect (Communication with PC de Jager). There are therefore pros and cons to both methods of concentrating the reagents.

Experimental error could have also resulted in the soils showing a low MED despite their high Mn contents. It is possible that this method may not be effective in measuring MED in soils with high Fe contents. Both the dolomites and andesites had high Fe contents, and showed low MED values despite their high Mn contents, particularly the dolomites. It is possible that the Fe oxides in high Fe containing samples interfere with the results by adsorbing iodide that has been reduced from iodine during the reaction. Iodide can be sorbed by organic matter as well as Al and Fe oxides, however this is pH dependent (Whitehead, 1973). Iodide is sorbed by soil organic matter under basic conditions and Fe and Al oxides under acidic conditions (Couture & Seitz, 1983). Iodide can be adsorbed on sesquioxides at a pH below 6 (Nath et al., 2010).

4.3.1.2 Total electron demand

The method for TED is very similar to MED with the major difference being that pH 4 NH_4OAc is used for MED which is absent in TED and HCl is incorporated in the TED method. The TED solution is acidified to a pH of about 1, which exposes the samples to more mineral dissolution, thus accessing Mn that resides deeper in the crystal structures. Reduction is also favoured to a larger extent than TED at this decreased pH. The effect of pH also extends to the difference in sorption of iodide by Fe and Al oxides. Sorption of iodide is pH dependent and a study by Kennedy et al. (2011) showed that sorption of I^- was strongly immobilized at pH 2.5. Sorption mainly occurred at pH 4 and iodide remained strongly sorbed to a pH of about 9 (Kennedy et al., 2011). Thus the phenomenon of I^- sorption by Fe and Al oxides occurs at the pH of the MED method but should not occur at the pH of the TED method. Another difference is that the time between extraction and titration is critical for this method due to the slow oxidation of iodine by O_2 at low pH and this could lead to inflated TED values if the time limit is not strictly adhered to (Bartlett, 1999).

In contrast to MED, all samples had a measurable TED as seen in Table 4.1. This is expected because this method is a measure of all oxidizing agents, including Fe^{3+} (Bartlett, 1988). The TED per mass Fe+Mn in the soil was measured and results are represented in Table 4.1. The dolomite soils had a much greater Mn reactivity per mass Fe+Mn compared to any of the other soil samples, as well as the wad. This can be explained by results form Chapter three that revealed that the dolomite samples have an approximately 50% Mn enrichment whereas the wad has an Mn enrichment of only 15%.

It appeared that TED decreased downslope for the granite and dolomite samples. This is probably linked to the decrease in Fe downslope as indicated by Table 3.1. For the dolomite samples, the trend can be explained by the lower Mn content downslope (as indicated in Table 3.1). An increase in TED is observed downslope for the quartzite samples, again linked to the higher organic material however this is now downslope.

The wad had the highest TED, as expected due to its high Fe and Mn content. The soil samples that had the highest TED were the dolomites and brown vertic samples. These had the highest Mn contents and the vertic have very poor mottle expression while the dolomite does not exhibit redoximorphic features in its morphology. The granite and quartzite samples had very low TED values. It was expected that Q_Crest would show a higher TED due to the

high total Fe content particularly in the subsoils (ranging between 250 and 300 mmol.kg^{-1}). The amorphous Fe contents, however, were much lower (between 9 and 13 mmol.kg^{-1}). Figure 4.1 shows the strong correlation between Mn and TED. The slope suggests that one mole of Mn "demands" 0.59 moles of electrons, in the presence of the dolomite samples and reduces to 0.35 in its absence. The correlation coefficient, however, remains virtually the same. This is attributed to the much higher easily reducible Mn content in the dolomite samples (90.5 and 132 mmol.kg^{-1} for the D_Bot and D_Crest samples respectively) with the next highest easily reducible Mn content being 10.8 mmol.kg^{-1} for the A_Mid_A sample. In order to investigate the role that Mn plays in redox chemistry of the soil as well as the influence that Fe and Al have on Mn, TED was correlated with the various extractants discussed in Chapter three.

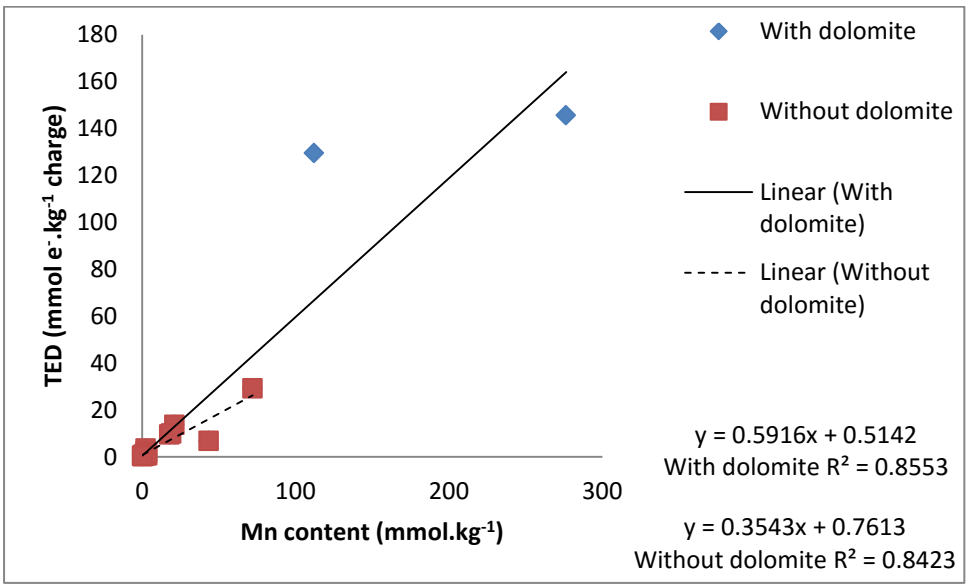

Figure 4.1: Correlation between Mn content determined by XRF and TED

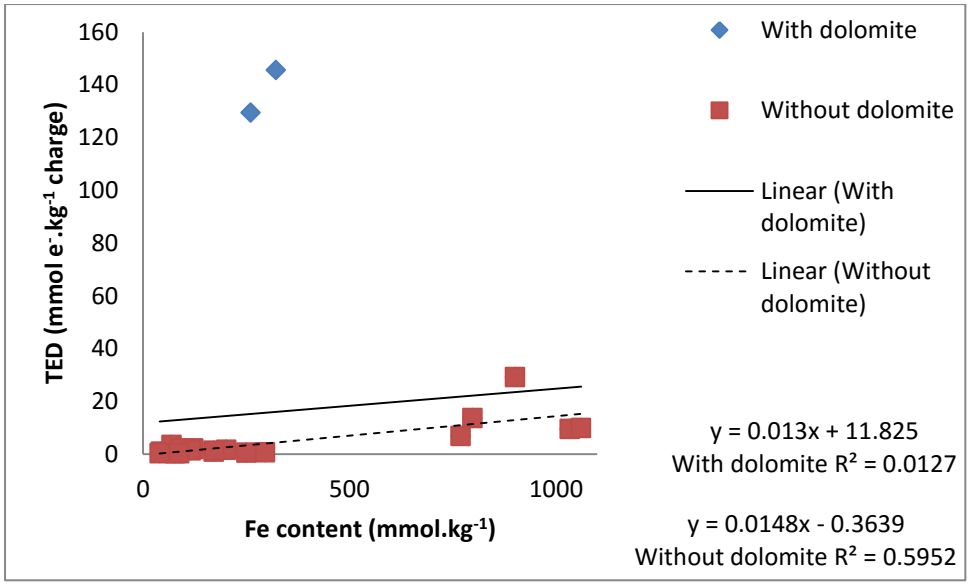

Figure 4.2: Correlation between Fe content determined by XRF and TED

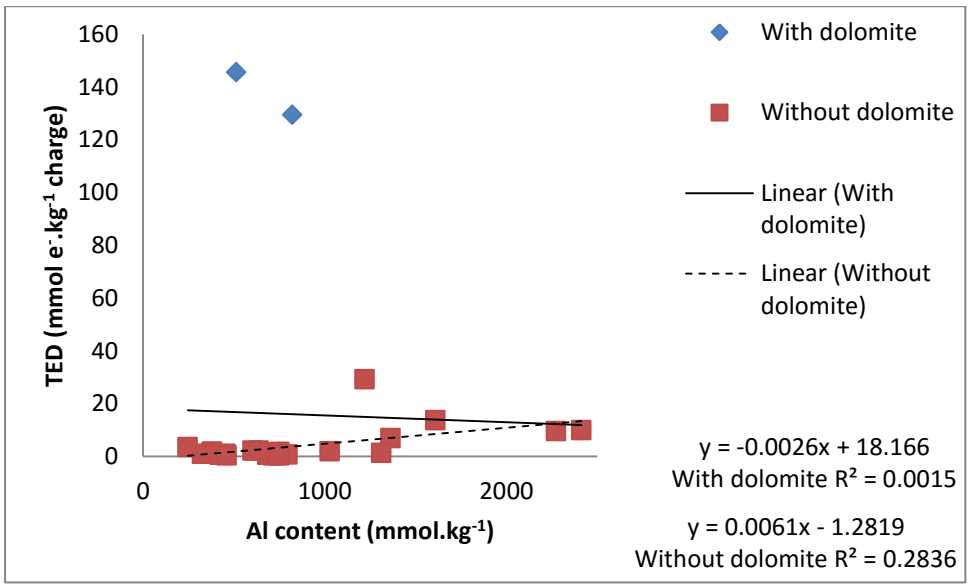

Figure 4.3: Correlation between Al content determined by XRF and TED

Figure 4.1 above indicates that there is a strong correlation between total Mn content and TED (R^2 value of 0.85). The relationship between Fe and Al respectively and TED were also evaluated, which is shown in Figures 4.2 and 4.3, and the graphs show that there are much weaker relationships between Fe and TED as well as Al and TED (both have R^2 values ≤ 0.01 when dolomite is included). From the graphs, however, it was observed that the dolomite samples had much higher TED values for these samples. They are not considered outliers because they had similar Al and Fe contents to other samples, however the TED appeared to have a stronger relationship with the high Mn contents of these samples. These two samples (D_Crest_A and D_Bot_A) were therefore removed from the analysis and correlation graphs

were re-evaluated. The results show that the correlation between Mn content and TED remained little affected when omitting the dolomite samples. The relationship between Fe and TED, however, appeared to strengthen considerably in the absence of dolomite, while Al still showed very little to no correlation with TED. This suggests that a relationship between Fe content and TED does exist, however the influence of Fe on TED appears to be concealed in the presence of high Mn contents in the soil.

The strength of the relationship between TED and Mn was tested by adding the XRF total Al+Mn, Fe+Mn and lastly Al+Fe+Mn to see if the relationship strengthens or weakens. The results however showed a weak if any relationship. The correlation coefficients were again higher in the absence of dolomite and therefore those figures, as a best case scenario, are reported here. The relationship between TED and Mn+Al showed an R^2 value of 0.3. The correlation coefficient TED with Mn+Fe was 0.62 and the coefficient for Mn+Al+Fe was 0.42. It therefore appears that the addition of Fe and Al lowers the strength of the relationship of total Mn with TED. Aluminium in particular appears to decrease electron demand.

A similar trend to that of XRF was seen when drawing the same comparisons between these elements and TED using the ammonium oxalate, DC and CBD extracts. The graphs of the oxalate extract are given below (Figures 4.4-4.6). Graphs of the DC and CBD extracts were constructed in the same way and the results thereof are represented in Table 4.2. For the correlation between amorphous Mn content and TED, a positive correlation was expected because the oxalate extract isolates the redox active Mn better. The R^2 values (Figure 4.4) indicates the strong linear correlation between the two both in the presence and absence of the dolomite soils. The relationship between Fe and Al and TED respectively showed the same trend as the total contents. Amorphous Fe explains a large amount of the variation in the absence of dolomite, however Mn^{4+} was the stronger electron acceptor when present in appreciable amounts (Figure 4.5). A very poor correlation was observed between amorphous Al content both in the presence and absence of the dolomite samples, however the relationship is somewhat strengthened in the absence of the dolomite samples (Figure 4.6).

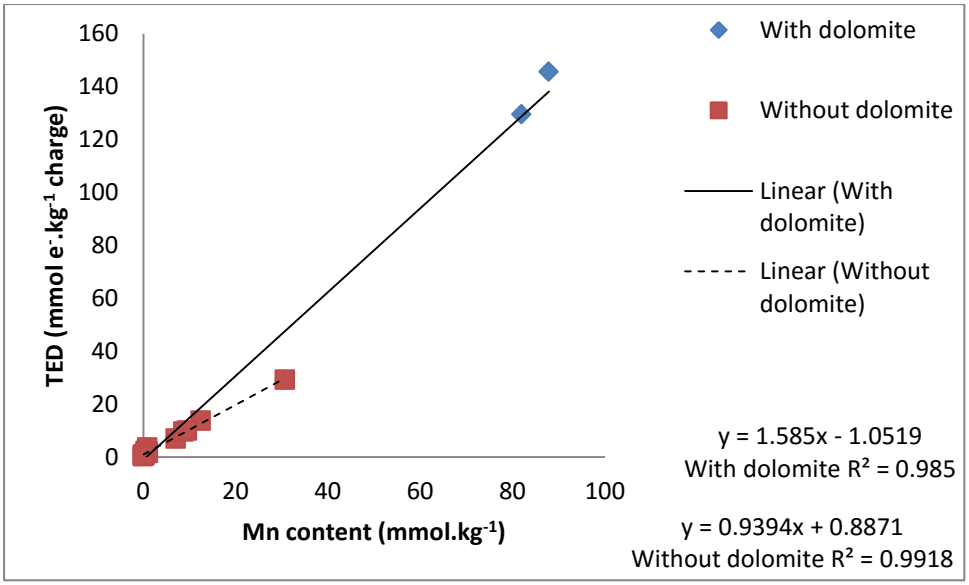

Figure 4.4: Correlation between amorphous Mn and TED

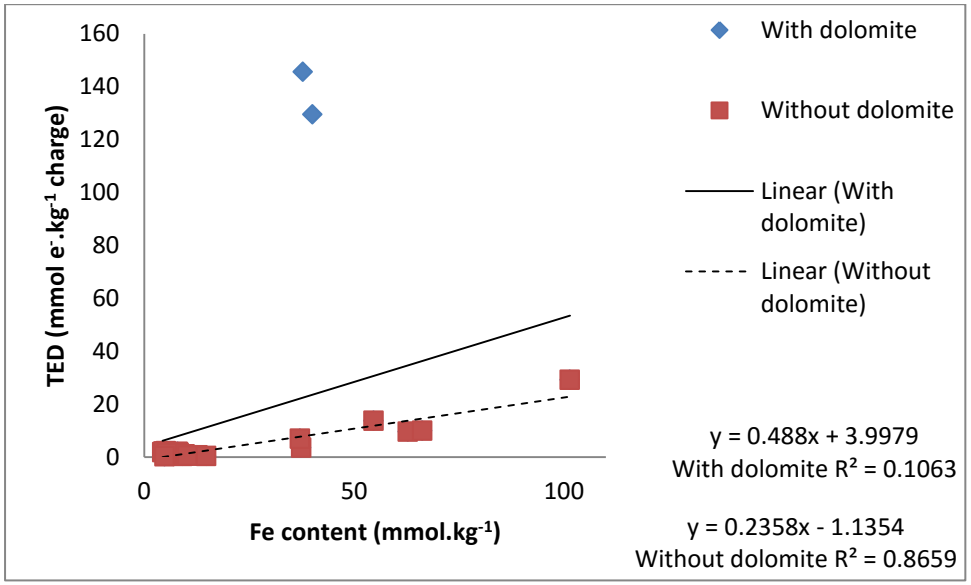

Figure 4.5: Correlation between amorphous Fe and TED

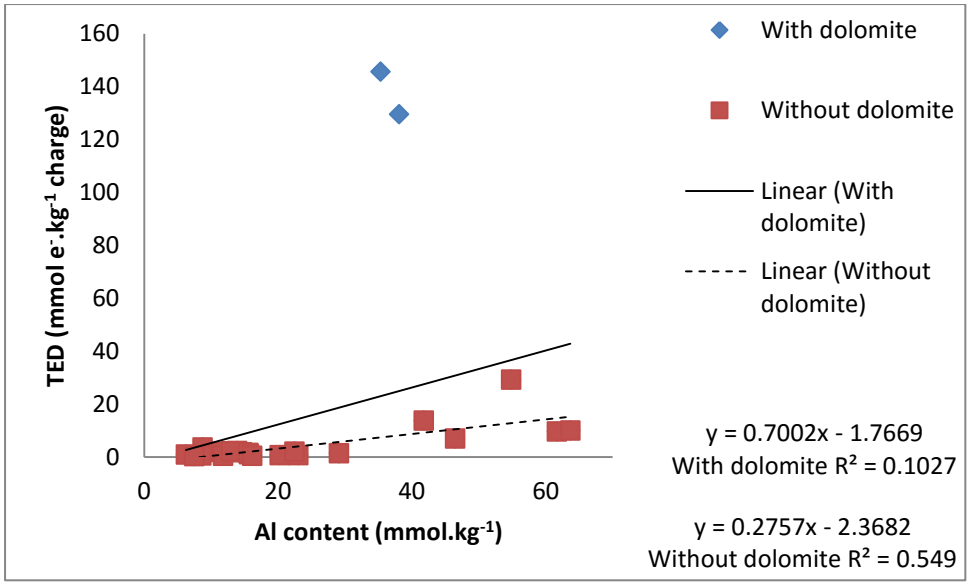

Figure 4.6: Correlation between amorphous Al and TED

The results in Table 4.2 show that the correlation between the extractable Mn and TED is strong and coefficients were very similar for all extracts, however, the relationship between extractable Fe and Al respectively with TED strengthens in the absence of the manganiferous dolomite soils. This follows the trend of electron acceptors as Fe acts as an electron acceptor in the absence of Mn. The DC extract showed stronger relationships for Fe and Al with TED than the CBD extract, probably due to the higher amount of Fe and Al that was extracted by DC.

Table 4.2: Linear correlation coefficients (R^2) describing the relationship between chemically extracted Mn, Fe and Al with TED

Soil property	R^2 in the presence of dolomite samples	Regression line equation (with dolomite)	R^2 in the absence of dolomite samples	Regression line equation (without dolomite)
Dithionite citrate extractable Mn	0.94	y = 1.76x + 1.10	0.98	y = 1.26x + 0.53
Dithionite citrate extractable Fe	0.02	y = -0.01x + 37.5	0.85	y = 0.006x + 0.91
Dithionite citrate extractable Al	0.01	y = -0.19x + 37.6	0.68	y = 0.13x + 0.09
CBD extractable Mn	1	y = 16.6x – 0.27	0.99	y = 15.7x + 0.05
CBD extractable Fe	<0.01	y = 0.001x + 16.0	0.45	y = 0.01x - 0.19
CBD extractable Al	<0.01	y = -1.24x + 20.9	0.023	y = 0.36x + 2.78

The fraction of Mn that is expected to contribute most to the electron demand is the easily reducible fraction. Therefore the correlation between easily reducible Mn and TED was drawn, as depicted in Figure 4.7. Results show a strong linear correlation between the two. The regression equations suggest that the relationship between Mn and TED is almost unity, approximately 1 mole Mn "demands" 1 mole of electrons. In contrast to other comparisons drawn in the presence and absence of the dolomite samples, the strength of this relationship seems to be enhanced in the presence of the dolomite samples.

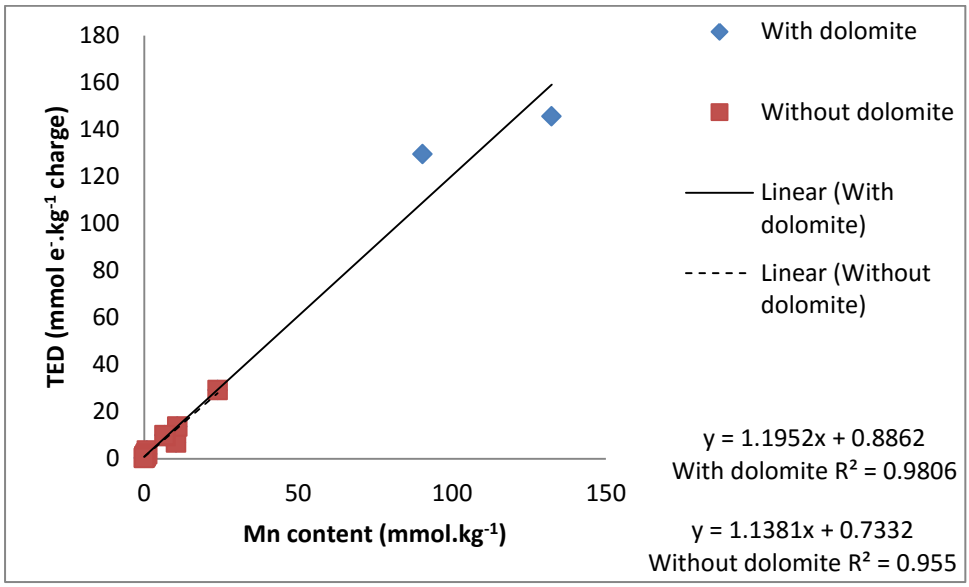

Figure 4.7: Correlation between easily reducible Mn and TED

From the information gathered, it was deduced that Mn is the largest role player in TED. It is for this reason that TED is henceforth used as the indicator / index of manganese electron demand and not MED. The shortage of samples that have any measureable MED also made it impossible to draw comparisons from. A trend that is observed is that the higher the TED, the lower the expression of mottles in the soils. The dolomite and vertic soils were sampled at hydric parts of the landscape and exhibited no mottle expression. The dolomite and vertic samples taken at wetland sites, as well as the andesite sample, which all had higher Mn contents than the quartzite and granite samples, had the highest TED while the granite and quartzite samples, which were both taken at wetland sites, had the lowest TED but expressed mottles in their morphology.

The results obtained from the TED study were then further investigated. There did not appear to be a trend in terms of landscape position and TED. In general, the topsoils had

higher TED values than the subsoils for the various soils. This could possibly be linked to the higher organic matter content in the topsoils causing Mn and Fe to form poorly ordered crystals, making these elements readily available to participate in redox reactions. The quartzite and granite showed the lowest TED values. These samples therefore have the lowest redox buffer capacity and also happen to be the ones occurring closest to the wetland. All of these samples exhibited redoximorphic features.

4.3.2 Relationship between soil properties and redox buffering

After investigating the role of Mn on redox buffering of the selected soils, it was necessary to look at various soil properties and the role that they may play in redox buffering of the soil. This was done in an effort to establish if other soil properties, along with Mn, contribute to redox buffering in these soils. Several soil properties were compared to TED, the results of which are discussed below.

4.3.2.1 The influence of the exchange complex on redox buffer capacity

The composition of the soil's exchange complex can play an important role in redox buffering. This may be an indirect influence due to its role in pH buffering. The relationship between TED and the properties of total exchangeable acidity as well as cation exchange capacity were investigated in order to study this effect. With regards to exchangeable acidity, it was expected that if the exchangeable acidity is high, it is likely that the soil's ability to buffer a decrease in pH is low. This would lead to acidification of the soil, under which conditions oxidation would be less favoured. This in turn would result in a low TED and therefore low redox buffering capacity. If the exchangeable acidity is low, the soil is expected to buffer the decrease in pH by absorbing protons. This would result in a higher redox buffer capacity of the soil.

The results in Figure 4.8, however, demonstrate a very low R^2 value indicating very little correlation between exchangeable acidity and redox buffering of these soils. The correlation coefficient was recalculated in the absence of the dolomite samples and the relationship remained very poor. What is important to note, however, is that the soils with the highest TED had virtually no titratable acidity.

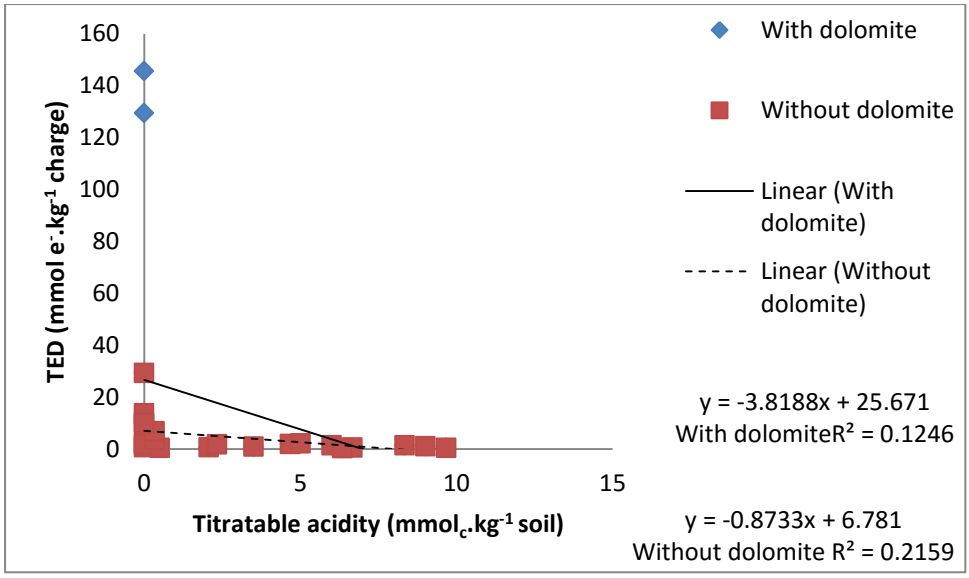

Figure 4.8: Correlation between titratable acidity and TED

Similarly to acidity, graphs were constructed to investigate the relationships between TED and CEC. Cation exchange capacity (CEC), is a measure of the amount of cations that can be held and exchanged per unit mass of soil (White, 2006). It is commonly observed that soils with a higher CEC exhibit a greater pH buffer capacity (Brady & Weil, 2002; McCauley et al., 2009). With CEC having such an impact on pH buffering in soil, it was therefore expected that CEC would play a major role in redox buffering since pH and oxidation-reduction go hand in hand in soil systems. The postulation was that the higher the CEC, the higher the buffer capacity of the soils due to the increase in Mn and Fe that can be held on the exchange complex to contribute to an increase in redox buffering. This will depend on the form of Mn on the exchange complex, for example Mn in the form of Mn^{2+} will not have much effect on electron demand. The correlation coefficient depicted in Figure 4.9 indicates that CEC at best only explains 50% of the variation observed, which is not a very strong relationship.

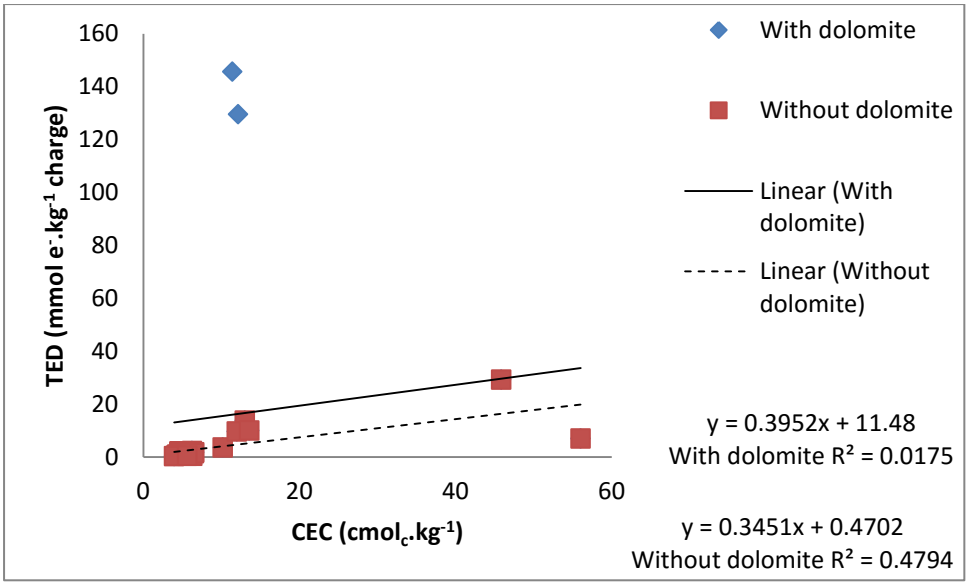

Figure 4.9: Correlation between cation exchange capacity and TED

A study by Reddy & Perkins (1974) provides a reason as to why CEC may not play a role in redox buffering. The study found an inverse relationship between CEC and Mn fixation (Reddy & Perkins, 1974). The less Mn available on the exchange complex, the lower the probability that CEC contributes to redox buffering. This would however have resulted in an inverse relationship, which was not seen. It is therefore assumed that the composition of the exchange complex does not lend itself to cations that act as electron acceptors.

4.3.2.2 The influence of clay content and organic carbon content on redox buffering

The other two soil properties that were looked at in terms of their influence on redox buffering in the soils investigated were clay content and organic carbon content. An increase in the amounts of both of these properties typically results in an increase in CEC and buffering capacity (McCauley, 2009; Fertilizer Industry Federation of Australia, 2006). Results shown in Figures 4.10 and 4.11, however, show that for both properties, there is a very poor correlation with TED and therefore neither appear to play a major role in redox buffering in the soils selected for this study. The reason for organic carbon not playing a major role could be that the organic matter is relatively stable and therefore does not participate in redox reactions in these soils. It is, however, difficult to determine the contribution that soil organic matter makes to redox buffering without information from an incubation study under water saturated conditions. This was beyond the scope of the study.

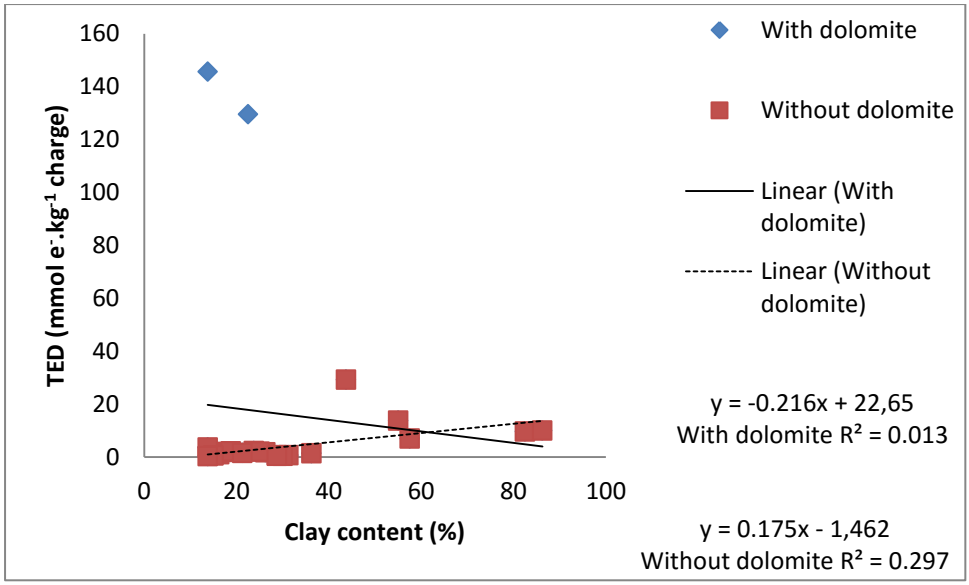

Figure 4.10: Correlation between clay content and TED

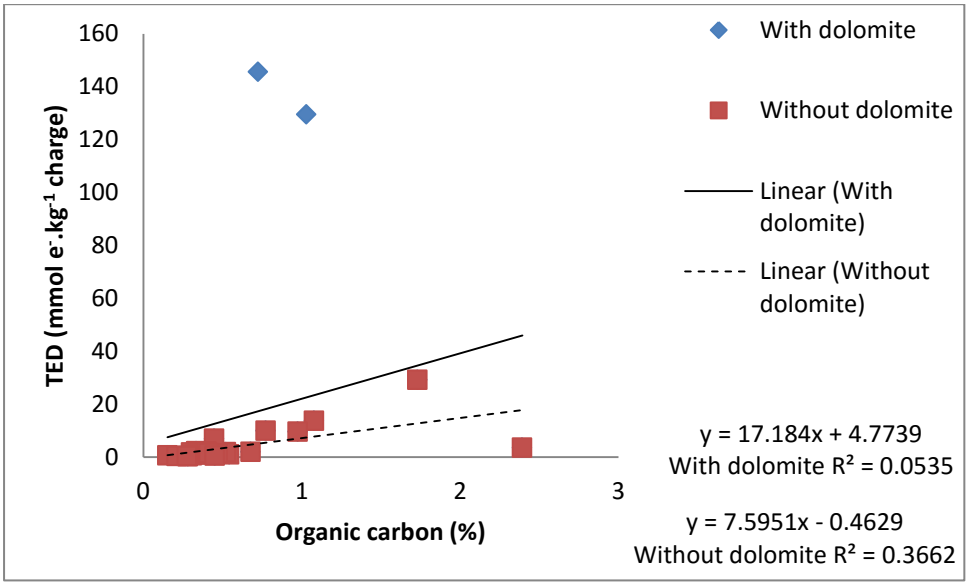

Figure 4.11: Correlation between organic carbon and TED

4.4 Summary

This chapter investigated the oxidizing capacity of the soils. Since MED was only measurable for three soil samples, TED was used as the index of redox buffering capacity of the soils. The samples with the highest Mn contents (dolomites, vertics and andesites) were the samples with the highest TED values. These are therefore the soils with the higher oxidizing capacities and with a propensity to "demand" electrons, resulting in redox buffering in these soils. Incidentally, the vertics show very poor mottle expression and the dolomites have a complete absence of redoximorphic features where they are expected to occur. The soils with the lowest TED values are the quartzite and granite soils, despite the high Fe

content of the quartzite sample. These soils therefore have weak redox buffering capacities and exhibit mottling, as expected for hydric soils.

Oxalate extractable and hydroxylamine extractable Mn appeared to have the strongest correlation with TED, followed by Fe, which shows a good relationship, and lastly Al, which exhibits a very weak relationship. It therefore appears that from these three elements, Mn is the major contributor to redox buffering in these soils. Removing the dolomite samples from the correlation increases the strength of the relationship for Fe and Al respectively with TED. This observation is more distinct with the correlation between Fe and TED. This is a result of Fe having the second best correlation with TED because Fe becomes the electron acceptor in the absence of Mn, following the sequence of electron acceptors. All other chemical extractions, oxalate, DC, CBD and hydroxylamine, showed the same trend as XRF with regards to the relationship between the three elements and TED with Mn having the best correlation with TED.

The soil properties correlated with TED were pH, titratable acidity, CEC and clay content. This was done in an attempt to verify if these soil properties, in addition to Mn, contribute to redox buffering. All soil properties showed poor relationships with TED and were therefore discounted as role players in redox buffering in these soils.

Chapter five: Exploratory investigations

This chapter will be dealt with in two parts. The first part is an exploratory investigation aimed to establish a quantitative relationship between the susceptibility of soil to chemical bleaching and redox buffering observed in the field (or lack thereof). The second part deals with the influence that soil matric potential and drying has on the oxidation and reduction of Mn in the soil. The importance of this investigation is that water is the driving force of redox reactions as well as mineral solubility.

5.1 Chemical induced bleaching as an indicator of redox buffering

5.1.1 Introduction

Soil colour and bleaching characteristics are used as a hydric soil indicator. A bleached soil horizon is an indication that reduction has occurred. Bleached soil colour is also a widely used determinant for soil processes as well as soil properties. One such soil property is Fe content. The colour of Fe-containing minerals in soils that undergo redox reactions can be a very useful determinant of the hydrological conditions of soil (Rossel et al., 2006). It is a morphological feature of reduction and is a hydric soil indicator (Vepraskas, 2001). The mechanism of soil bleaching is ferric iron reduction. Under conditions of saturation, an aerated soil becomes anaerobic and reducing conditions are induced. Under these conditions, Fe^{3+} is reduced to Fe^{2+}. Ferrous iron in its reduced form is mobile and can be transported out of the horizon or profile. Following this, the soil becomes grey in colour where the reduction has occurred. This grey, bleached colour is generally attributed to the colourless Fe^{2+} as well as the colour of the sand, silt and clay particles of the soil (Ottow, 1970; Vepraskas, 2001). The determination of soil colour is therefore imperative.

Soil colour is commonly measured using a Munsell soil colour chart (Rossel et al., 2006; Mouazen et al., 2007). This method however has limitations posed by the number of colour chips as well as the fact that it is a qualitative method. Errors are compounded by measurements under inappropriate light conditions as well as inexperienced observers (Mouazen et al., 2007). A study conducted comparing Munsell colour determinations by different soil scientists found that observers agreed only 52% of the time (Islam et at al., 2004). This led to a study by Islam et al. (2004) assessing the magnitude of variability in soil colour measurements among different observers, which concluded that errors were of a

sufficient magnitude to change the classification of a particular soil (Islam et at al., 2004). Such variability shows that this method is therefore highly subjected to human error, which has serious implications due to a lack of precision. All of these challenges posed led to the need to develop alternative methods to identify soil colour, in particular, more objective and quantitative approaches. One such technology is the use of spectrophotometers (Islam et al., 2004; Mouazen et al., 2007). The study by Islam et al., (2004) found that a diffuse reflectance spectrophotometer can be used to reliably measure soil colour in the laboratory.

Spectrophotometers make use of colour space models for the colour determinations. Colour space expresses colour of an object or light source using a form of notation, such as numbers (Konica Minolta, 2007). Colour space models have become an increasingly common method for the quantitative determination of soil colour (Rossel et al., 2006). Unlike the Munsell colour method, colour space models make use of the RGB (red, green, blue) system in which soil colour is related to reflectance. The latter method makes use of a set of orthogonal Cartesian coordinates related to soil spectral properties. (Doi & Ranamukhaarachchi, 2007). The red (630 – 690 nm), green (525 – 605 nm) and blue (450 – 515 nm) portions of the visible spectra are converted into Munsell notations. The colour space model chosen for this study is the commonly used L*a*b* colour space, also referred to as CIELAB. This was derived in 1976 in an effort to provide more uniform colour differences in relation to visual differences. The L* value indicates lightness and the a* and b* values are chromaticity coordinates (Konica Minolta, 2007).

Soil colour can therefore be a very useful indicator of reduction in soils. The problem arises when investigating a soil that shows visible signs of moisture, such as the dolomite derived soils in this study, where signs of wetness is absent. A previous study by Rabenhorst and Parikh (2000) investigated soils having problematic redoximorphic feature interpretations. They subjected problematic and non-problematic soils to CBD extraction and determined the Munsell colours of these soils thereafter. The aim was to establish a more objective test to interpret redoximorphic features. The study developed a colour change index from colour measurements using a digital colorimeter on soils treated with CBD at room temperature after one hour and 80°C after four hours. A CCPI (colour change propensity index) was derived from chroma index and hue index with a CCPI ≤ 30 being problematic and ≥ 40 being non-problematic soils in terms of redoximorphic feature interpretation (with 30-40 being

intermediate) (Rabenhorst & Parikh, 2000). Colours that fall in the intermediate index are therefore difficult to classify.

This exploratory study looks at the difference in extent of bleaching after subjecting soils to two extractants, CBD and DC, that both employ the strong electron donor dithionite to extract Fe by means of reductive dissolution of ferric oxides. The DC extraction induces more aggressive reducing conditions than the CBD extract. Samples that were subjected to DC and CBD extractions were subjected to colour determinations using a spectrophotometer. The reason for this was that visual differences were observed but a more accurate determination was necessary to verify this. In this investigation it is hypothesised that soils with high Mn contents will buffer the reduction of ferric iron, resulting in a decrease of CBD-induced bleaching in these soils as opposed to soils with low Mn contents. It is expected that the soils with a higher oxidizing capacity will buffer the reducing conditions that dithionite introduces. Evidence supporting this hypothesis is that soils with the highest Mn content will show the least amount of bleaching. An alternate hypothesis is that large reserves of Fe in the soil may prevent total reduction of all Fe in these soils. Supporting evidence for this hypothesis is that soils with the higher Fe content will have the least amount of bleaching. The net result of both these hypotheses is that these soils will show less dithionite bleaching by CBD and there would be a greater difference in soil colour between DC and CBD treated soils. The motivation behind this exploratory investigation was to explore this as a possible laboratory method to determine the oxidative capacity of a soil.

5.1.2 Methods and materials

Selected field moist samples were subjected to dithionite citrate (DC) and citrate-bicarbonate-dithionite (CBD) extractions. From previous experimentation (during data generation for Chapter three) it was observed that DC extraction provides almost complete reduction of soil samples, whereas CBD extraction in some samples, reduces the soil components to a lesser extent. This chapter aims to find a link between the difference between the soil colours after being extracted by the two different extractants and soil properties linked to redox buffering.

Samples were dried and ground to produce fine, homogenous samples. The dry samples were placed into a quartz sample holder and analysed using a Konica-Minolta CM 600d spectrophotometer. Values were obtained as L*a*b* values which were converted to Munsell colours. Software was programmed by using all the colour chips of the Munsell

colour chart in order to determine target values. Samples were measured using the spectrophotometer and colours were compared using this software in order to obtain the nearest target Munsell colour. Munsell colours indicated whether samples were bleached or not according to the South African Soil Taxonomy definition of bleached colours. The L*a*b* values were also compared between treated and untreated samples to determine the extent of the colour change between treatments (Konica Minolta, 2007).

The size of the colour difference was calculated by using the following formula:

$$\Delta E^*ab = \sqrt{(\Delta L)^2 + (\Delta a^*)^2 + (\Delta b^*)^2}$$

5.1.3 Results and discussion

This study was conceptualised during experimentation for the CBD analysis. From previous visual observations when conducting the CBD extraction, it appeared that the quartzite and granite soils were completely bleached after extraction with CBD while the dolomite and andesite soils were not completely bleached after extraction with CBD but were bleached to a larger extent after DC extraction. Incomplete bleaching suggests that not all of the Fe is removed from the soil. This is expected because the CBD extract does not contain enough electron donors, due to the small soil to solution ratio, to overcome the oxidizing tendency of the soil (Mn oxides in the case of the dolomite soils and the large reserves of Fe oxides in the quartzite and andesite soils). This would prevent the complete dissolution of iron oxides during the reaction time. An example of the differences seen between CBD and DC induced bleaching is shown in Figure 5.1. Only one photo is shown as an example because due to poor lighting, the quality of the photos in general were not very good.

Figure 5.1: Q1_Crest_A showing extensive bleaching after CBD and complete bleaching after DC reduction

The reason for the difference observed between the two extracts could be linked to the difference in pH between the two (the CBD extract has a pH of 7.3 and the DC extract has a pH of 7). The slightly higher pH of the CBD extract could cause the soils to resist reduction slightly more than they do when subjected to the DC extract. The lower pH of the DC extract could favour increased reduction of the Mn and Fe oxides, resulting in more complete bleaching of the soil particles. The more likely reason for the observed differences could be that the soil : extractant ratio was higher for the DC extract than the CBD extract. The DC extract method has a ratio of 0.5 g soil : 25 ml extractant (1:50) and the CBD extract has a ratio of 10 g soil : 37.5 ml extractant (1:3.75). The greater excess of reductant for the DC extract most likely ensured ferric oxide reduction was taken to completion, resulting in more complete bleaching of particles.

The different responses (in terms of colour change) of the soils to DC and CBD treatment led to the postulation that the magnitude of colour change after reductive dissolution by extraction could be used as a test for soils buffering against reduction. It is hypothesised that the higher the Mn content of the soil (and therefore TED), the greater the difference of bleaching between untreated and soil subjected to CBD extractions as well as untreated and DC extracted soils. Therefore, as a result, the differences in bleaching between DC and CBD

should increase with increasing redox buffering. Two approaches were followed to test these hypotheses:

1. A qualitative approach using the Munsell colour system
2. A quantitative approach using ΔE*ab values discussed in the introduction.

For the purpose of this exploratory investigation, samples were selected based on their total Fe (as determined by XRF) and easily reducible Mn (as determined by hydroxylamine extract) contents, as depicted in Table 5.1. The Fe content was important as ferric Fe reduction resulting in mottle formation is used as a soil wetness indicator. Different Fe contents could answer the question of whether it is just a large reserve of Fe in soil that prevents reduction of all ferric Fe by CBD. The Mn content was important in order to investigate if Mn plays a role in buffering against ferric Fe reduction. The Q_Crest samples were selected due to their high Fe content. The G_Bot samples were chosen as these occur closest to the wetland on this site and have a lower Fe content than the Q_Crest samples and exhibit redoximorphic features. The D_Bot sample was chosen as this was sampled at the point of moisture on this site and has a high Mn and Fe content and a lack of mottle expression. The andesite samples were chosen as these have the highest Fe contents and the Mn contents are higher than the quartzite and granite samples but lower than the dolomite sample.

Table 5.1: Total Fe and easily reducible Mn contents of selected soils (mmol.kg^{-1})

Sample	Total Fe	Easily Reducible Mn
Q_Crest_A	172	0.47
Q_Crest_B1	250	0.23
Q_Crest_B2	295	0.18
G_Bot_A	43	0.01
G_Bot_B1	88	< MDL
G_Bot_B2	40	< MDL
D_Bot_A	261	90.5
A_Mid_A	798	10.8
A_Mid_B1	1034	6.95
A_Mid_B2	1061	6.58

5.1.3.1 Qualitative approach using the Munsell colour system

The Munsell colours, which were generated from the L*a*b* values provided by the spectrophotometer, are shown in Table 5.2. Whether the samples are bleached or not, according to the South African Classification system, is also indicated.

Table 5.2: Soil Munsell colours as determined by spectrophotometry

Sample	Munsell colour		Munsell colour		Munsell colour	
	Untreated	Bleached/Not	After DC extraction	Bleached/Not	After CBD extraction	Bleached/Not
Q_Crest_A	5YR5/3	Not	10R6/1	Not	5Y6/1	Not
Q_Crest_B1	2.5YR5/4	Not	2.5Y7/1	Bleached	10YR6/2	Bleached
Q_Crest_B2	2.5YR5/4	Not	2.5Y7/1	Bleached	7.5YR6/3 10YR6/3*	Bleached
G_Bot_A	10YR5/2	Bleached	7.5YR6/1	Bleached	7.5YR6/1 5Y6/1*	Bleached
G_Bot_B1	10YR6/2	Bleached	7.5YR6/1	Bleached	2.5Y7/1	Bleached
G_Bot_B2	10YR6/3	Bleached	2.5Y7/1	Bleached	5Y6/1	Bleached
D_Bot_A	2.5YR4/1	Not	7.5YR6/1 10YR6/1*	Bleached	5YR5/2	Bleached
A_Mid_A	2.5YR5/3	Not	10YR6/1	Bleached	5YR5/2	Bleached
A_Mid_B1	2.5YR5/4	Not	5YR6/2 7.5YR5/2 7.5YR6/1	Bleached	5YR5/3	Not
A_Mid_B2	2.5YR5/3	Not	10YR6/2	Bleached	5YR5/3	Not

*This indicates that two of the three samples have this colour

For the DC treatments, all the samples had colours falling within the bleached range after this treatment. The value of 5Y6/1 is not found in the definition of bleached colours in the South African Classification system because it is not often encountered in South African soils, however the high value represents a bleached colour (Discussion with Johan van der Waals). The D_Bot_A and A_Mid_B1 samples had greater variation in colour for the different replicates. Originally, in order to keep the samples as close to field moisture as possible before extraction, grinding and sieving were not performed on them. The samples, however, needed to be homogenous for colour determination using the spectrophotometer. Spectroscopic colour measurements require ground, air-dry samples in order to ensure micro-topography (Rossel et al., 2006). Particularly for the andesite sample, the inner particle was not bleached and therefore there was non-uniformity in colour after samples were subjected to grinding. Grinding samples exposed ferric oxides that were not reached by the dithionite extraction on the samples. Due to the fact that samples were not air-dried and sieved before extraction, concretions remained in the sample. This could have happened to different extents in the different replicates resulting in the colour variation obtained. Even though the Munsell colours detected were not the same, they all still fell within the bleached category. Although new surfaces were exposed, therefore, the impact in terms of colour was not enough to create a "false" result.

The results for the soil colour after CBD extraction were not entirely as expected. It was thought that the dolomite and andesite samples would remain largely unbleached after extraction as this was suggested by visual observations. The spectrophotometer results, however, showed that the dolomite and A_Mid_A samples were bleached and the andesite subsoils, A_Mid_B1 and A_Mid_B2, were left unbleached after CBD extraction. This was possible due to the increase in concretions in these samples, resulting to a resistance in reduction, particularly the inner particles of the concretions. The fact that the dolomite and andesite topsoil samples appeared to be unbleached visually but were identified as bleached by the spectrophotometer proves that judgement of colour by the human eye can be deceiving. Comparisons were made between Munsell colours determined visually and spectroscopically and the results are shown in Table 5.3. The only Munsell value that was detected the same visually and spectroscopically is G3_Bot_A. The hue of about half of the samples appeared to be detected the same by both methods, however there was not much similarity in the values and chromas detected.

Table 5.3: Comparison of Munsell colour determined visually and by spectrophotometer before extractions

Sample	Munsell colour determined visually	Munsell colour determined spectroscopically
Q_Crest_A	7.5YR 4/6	5YR5/3
Q_Crest_B1	5YR 4/6	2.5YR5/4
Q_Crest_B2	5YR 4/6	2.5YR5/4
G_Bot_A	10YR 5/2	10YR5/2
G_Bot_B1	10YR 5/2	10YR6/2
G_Bot_B2	10YR 6/4	10YR6/3
D_Bot_A	7.5YR 3/3	2.5YR4/1
A_Mid_A	2.5YR 4/8	2.5YR5/3
A_Mid_B1	2.5YR 4/8	2.5YR5/4
A_Mid_B2	5YR 4/6	2.5YR5/3

5.1.3.2 Quantitative approach analysing colour spectrophotometrically

Since the Munsell colours did not prove to be conclusive, a more qualitative approach was followed by evaluating the magnitude of the difference in the colours measured between untreated samples and the two treatments respectively was determined. It was earlier stated that the hypothesis is that soils with high Mn contents will buffer the reduction of ferric iron, resulting in a decrease of CBD-induced bleaching in these soils. Alternatively it could be the large reserves of Fe in the soil that prevent total reduction of all Fe in these soils. This was tested by looking at three possible methods using **Δ**E*ab values:

1. The difference in colour change between untreated and after DC extraction ($\Delta E^*ab_{untreated-DC}$).
2. The difference in colour change between untreated and after CBD extraction ($\Delta E^*ab_{untreated-CBD}$).
3. The magnitude of the difference between $\Delta E^*ab_{untreated-DC}$ and $\Delta E^*ab_{untreated-CBD}$ ($\Delta E^*ab_{untreated-DC}$-$\Delta E^*ab_{untreated-CBD}$).

The magnitude of the colour difference between untreated samples and samples subjected to the reducing extractions is represented by ΔE^*ab values in Table 5.8. In line with the central hypothesis that soils with high Mn contents will have less CBD-induced bleaching, the hypothesis is that the quartzite and granite soils with low easily reducible Mn contents and low TED values, are not buffered and get bleached to more or less the same extent. It was therefore expected that the ΔE^*ab values would be largely unaffected by DC or CBD treatment. It was expected that the dolomite and andesite samples, with higher easily reducible Mn contents and higher TED values, would buffer reduction, particularly in the CBD extract, and not be bleached to the same extent as the DC extract. The ΔE^*ab values for untreated and DC and untreated and CBD should therefore be significant. The influence of the higher Fe contents was also investigated. It was expected that soils with high Fe contents, such as the quartzite and andesite samples, would have large enough Fe reserves for the ferric Fe in these soils to not be completely reduced by CBD. Table 5.4 shows the ΔE^*ab values as well as the significance of the differences.

Table 5.4: Colour comparison and significance of difference in colour between untreated and treated soils

Sample	Untreated			Dithionite Citrate (DC)			Citrate-Dithionite-Bicarbonate (CBD)			$\Delta E^*ab_{Untreated - DC}$	$\Delta E^*ab_{Untreated - CBD}$	p-value
	L^*	a^*	b^*	L^*	a^*	b^*	L^*	a^*	b^*			
Q_Crest_A	48	11	14	62	2	8	58	3	10	17	14	0.01*
Q_Crest_B1	49	15	17	67	3	10	61	5	15	23	15	<0.01**
Q_Crest_B2	49	16	18	70	2	10	63	7	16	26	17	<0.01**
G_Bot_A	56	4	10	61	3	8	60	3	9	6	4	0.21
G_Bot_B1	60	4	11	65	3	9	62	3	10	5	3	0.02*
G_Bot_B2	64	6	17	69	3	9	67	3	10	9	8	0.07
D_Bot_A	43	5	7	58	2	7	48	6	10	16	7	<0.01**
A_Mid_A	47	13	14	59	2	7	49	8	12	17	5	<0.01**
A_Mid_B1	47	14	14	57	5	10	48	11	14	13	3	0.03*
A_Mid_B2	47	13	13	63	3	10	51	13	16	19	4	<0.01**

For all of the samples, the magnitude of the colour difference between untreated samples and those subjected to DC extraction was larger than that between untreated samples and those subjected to CBD. Therefore the DC extraction did result in a larger extent of bleaching than the CBD extract, as expected. Significant differences were not expected to be detected between $\Delta E^*ab_{untreated\text{-}DC}$ and $\Delta E^*ab_{untreated\text{-}CBD}$ for the Q_Crest and G_Bot samples, however all except the G_Bot_A and G_Bot_B2 proved to be significant. This demonstrates the sensitivity of the instrument to detect small colour differences and detect slight degrees of change. The spectrophotometer, therefore, was found to be much more sensitive than the human eye. Differences detected in the granite samples were small because the samples were bleached before any reduction (as Table 5.2 demonstrated). Although the differences for the quartzite samples were significant with the ΔE*ab results for CBD extract being lower than the DC extract, the differences in ΔE*ab values were larger for the dolomite and andesite samples.

Correlations were drawn between several extracts and $\Delta E^*ab_{untreated\text{-}DC}$, however none of them revealed any relationship with $\Delta E^*ab_{untreated\text{-}DC}$. The correlation between $\Delta E^*ab_{untreated\text{-}DC}$ and total Fe as well as easily reducible Mn is given as an example. This was done in order to see if Fe or Mn is the major role player linked to the change in soil colour. The same was done for $\Delta E^*ab_{untreated\text{-}CBD}$. The results shown in Figures 5.2 and 5.3, however, indicates that total Fe and easily reducible Mn have a very poor relationship with the colour change observed for $\Delta E^*ab_{untreated\text{-}DC}$ and $\Delta E^*ab_{untreated\text{-}CBD}$.

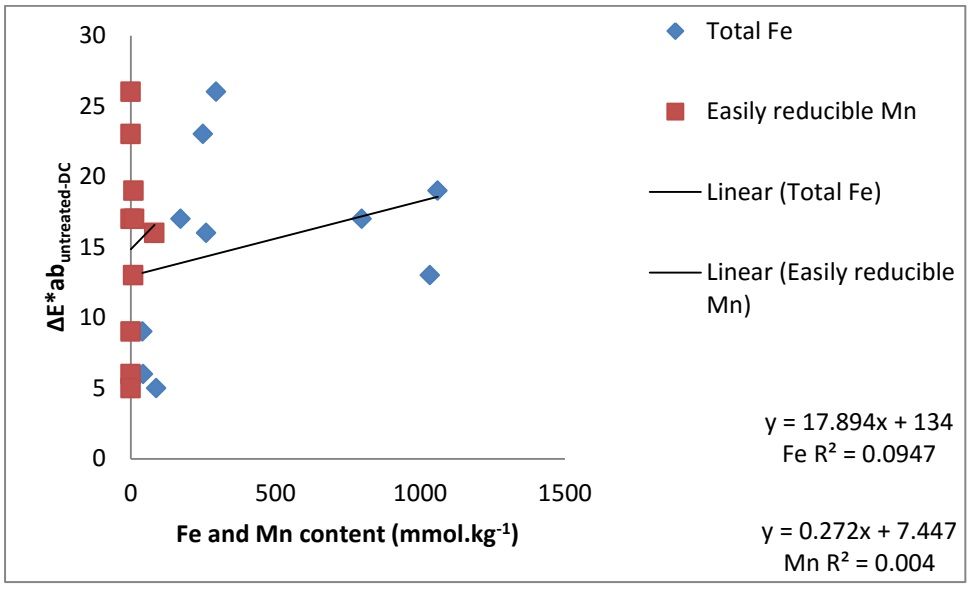

Figure 5.2: Relationship between $\Delta E^*ab_{untreated\text{-}DC}$ and total Fe as well as easily reducible Mn

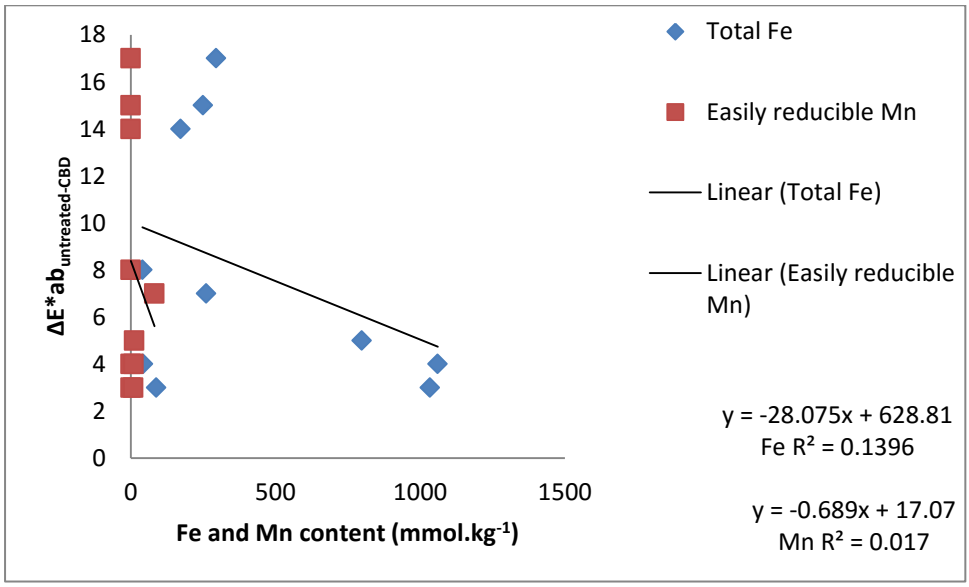

Figure 5.3: Relationship between $\Delta E^*ab_{untreated\text{-}CBD}$ and total Fe as well as easily reducible Mn

The next step was to look at the magnitude of the difference between $\Delta E^*ab_{untreated\text{-}DC}$ and $\Delta E^*ab_{untreated\text{-}CBD}$. The results are displayed in Table 5.5. The granite samples showed a very small difference between $\Delta E^*ab_{untreated\text{-}DC}$ and $\Delta E^*ab_{untreated\text{-}CBD}$, which can be explained by the low Fe and Mn contents of these soils. The Munsell colour analysis also showed that the granite samples were already bleached. They therefore bleached to more or less the same extent after treatment with the DC and CBD extractions respectively. The difference gets larger with the quartzite subsoil and dolomite samples. Both of these soils had higher Fe and Mn contents than the granite samples as well as the quartzite topsoil. The quartzite subsoil and dolomite samples had virtually the same difference between $\Delta E^*ab_{untreated\text{-}DC}$ and $\Delta E^*ab_{untreated\text{-}CBD}$. These soils had similar Fe contents but vastly different Mn contents. The andesite samples showed the largest difference between $\Delta E^*ab_{untreated\text{-}DC}$ and $\Delta E^*ab_{untreated\text{-}CBD}$. These samples had by far the highest Fe contents. With regards to Mn, they had higher values than the quartzites and granites but lower than the dolomite. It therefore appeared that Fe was the major role player in the difference in extent of bleaching and the oxidizing ability of Mn played a minor role. Figure 5.4 shows that this relationship is quite good.

Table 5.5: Magnitude of colour difference between ΔE*and $\Delta E^*ab_{untreated\text{-}CBD}$

Sample	$\Delta E^*ab_{Untreated\ -\ DC}$	$\Delta E^*ab_{Untreated\ -CBD}$	Difference between $\Delta E^*ab_{untreated\text{-}DC}$ and $\Delta E^*ab_{untreated\text{-}CBD}$
Q_Crest_A	17	14	3
Q_Crest_B1	23	15	8
Q_Crest_B2	26	17	9
G_Bot_A	6	4	2
G_Bot_B1	5	3	2
G_Bot_B2	9	8	1
D_Bot_A	16	7	9
A_Mid_A	17	5	12
A_Mid_B1	13	3	10
A_Mid_B2	19	4	15

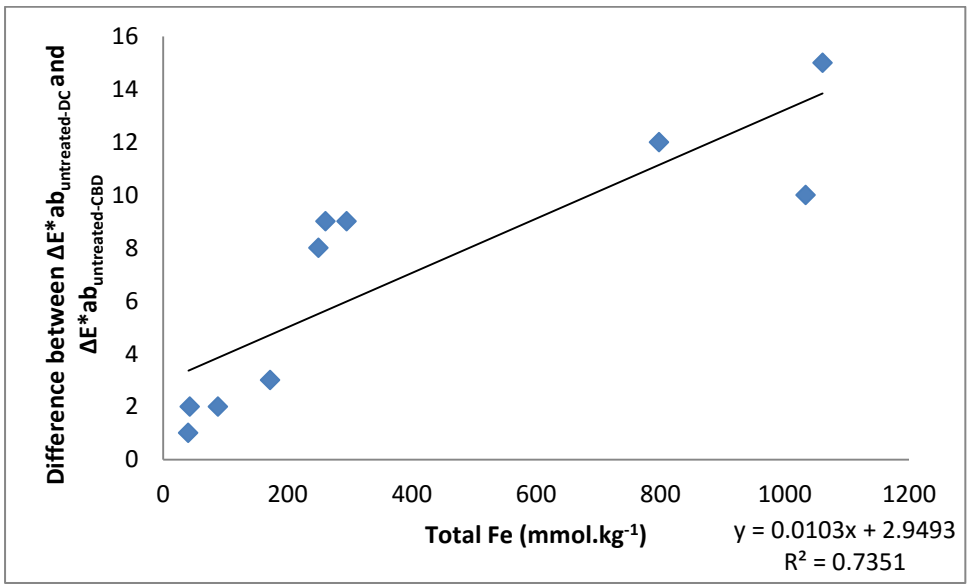

Figure 5.4: Correlation between total Fe and the difference between $\Delta E^*_{abuntreated\text{-}DC}$ and $\Delta E^*ab_{untreated\text{-}CBD}$

Reduction of soils can be buffered by the CBD extraction due to a large Fe content. This investigation does, however, show that bleaching cannot always be detected by the naked eye and measuring colour spectrophotometrically avoids bias and appears to be a more accurate measure of soil colour.

5.1.4 Summary

Selected samples were subjected to DC and CBD chemical extractions where DC was the more strongly reducing extract. The use of $\Delta E^*ab_{untreated\text{-}DC}$ and $\Delta E^*ab_{untreated\text{-}CBD}$ individually did not prove useful. An attempt was therefore made to use the difference in the extent of soil bleaching between the two as a measure of redox buffering. The results, showed that the higher the Fe content, the larger the difference between $\Delta E^*ab_{untreated\text{-}DC}$ and $\Delta E^*ab_{untreated\text{-}CBD}$.

It was therefore Fe and not Mn that played the dominant role in preventing the observed buffering against bleaching by CBD and differences in bleaching between DC and CBD. It was thus concluded that soil buffering against reduction by DC and CBD is not a reflection of buffering in the field. The reason is that the vast amount of electron donors (in the presence of an excess of electron donors) and the quantity of electron acceptors plays the determining role. The intensity (oxidation strength) is less important. Future studies, however, could evaluate the use of other extracts, such as oxalate and hydroxylamine. Bleaching with weaker reductants, such as these extracts, might yield more realistic results.

5.2 Effect of air drying and matric potential on manganese solubility and redox buffering

5.2.1 Introduction

5.2.1.1 Effect of air drying

The effect of drying on the increased solubility of Mn has been well documented (Bartlett & James, 1980; Berndt, 1988; Ross et al., 2001). It was discovered as early as 1913 that there is an increase in the soluble forms of Mn upon air drying of samples (Berndt, 1988). The reducing effect of even short-term air drying on soils, leading to an increase in exchangeable Mn (Mn^{2+}) is well documented (Negrac et al., 2005). Several studies have been conducted that demonstrate the increase in solubility of Mn with an increase in temperature. A study conducted by Bartlett & James (1979) showed an increase in the amount of Cr (III) oxidized by easily reducible Mn in field moist samples as opposed to the quantity oxidized by air-dried samples (Ross et al., 2001). Another study investigating chlorosis (a plant nutrient deficiency, most commonly arising from Mn induced Fe deficiency, associated with high soluble Mn content) in *Macadamia ternifolia* showed that the deficiency was more prevalent in hot dry summers than winters with greater rainfall (Fujimoto & Sherman, 1945). Solubility of Mn decreases under dry, more oxic conditions. A study conducted by Hardie et al. (2007) found that a period of extended drying followed by rewetting resulted in an increase in Mn^{2+} in soil water of some horizons. This is yet another indication of the effect that soil moisture regimes have on Mn release (Hardie et al., 2007).

Air drying favours the reductive dissolution of Mn^{3+} and Mn^{4+}, resulting in the formation of Mn^{2+}. An increase in Mn^{2+} and decrease in easily reducible Mn forms may lead to changes in the redox activity of Mn, thus affecting the redox buffering capacity of high Mn content soils. There are several explanations for this phenomenon. One explanation for this phenomenon comes from a study by Ross et al. (2001) which suggests that an intimate relationship exists between reduced organics and oxidized Mn, and drying facilitates this reaction. Studies have also shown that the oxidation of organic matter that leads to the slow reduction of Mn oxides results in an increase in soluble Mn (Berndt, 1988; Haynes & Swift, 1991; Ross et al., 2001). It is possible that upon drying, dissolved organic carbon concentrates at the mineral surface interface, creating more electron transfer (Discussion with PC de Jager). It is also plausible that upon drying, the volume of the soil solution decreases bringing the soil solution constituents closer together, resulting in closer contact of electron donors and acceptors

(Discussion with PC de Jager). Another possibility is that the structure and surface chemical properties of the oxide completely changes upon dehydration (Bartlett & James, 1980; Berndt, 1988; Haynes & Swift 1991). It is likely that under conditions when there is an increase in moisture, Mn may be fixed in non-exchangeable forms (Fujimoto & Sherman, 1945).

5.2.1.2 Effect of matric potential

The more unsaturated the soil, the lower the energy state and the more negative the matric potential becomes. This translates to a decrease in the chemical potential of water and will, therefore, result in a change of thermodynamic equilibrium for chemical reactions. It is therefore hypothesised that matric potential plays a role in the solubility of Mn and therefore redox buffering because matric potential decreases water potential, which in turn changes the activity of water and the activity of the dissolved constituents. The most dominant component of water potential in soil is the matric potential. Soil matric potential is an important indicator of water availability (Phene et al., 1973) for plants and microbes. It is an indication of the tendency for soil water to move and describes movement by forces of adhesion and cohesion (Foth, 1990). Soil matric potential also influences microbial activity, which is important for reduction processes in soil as well as for the shuffling of electrons. Studies have shown that microbial processes are rapid under conditions near field capacity but tend to slow down as the matric potential becomes more negative (drier environments) (Zak et al., 1999).

5.2.2 Methods and materials

The oxidation state of Mn can alter rapidly in response to environmental conditions (Negrac et al., 2005). When redox studies are undertaken, therefore, precautions must be taken to minimize the disruption of redox poise through sample handling and experimental protocols (Negrac et al., 2005). Special precaution was taken to keep samples for analysis at field moisture in plastic sample bags in a cold room at a constant temperature of 4°C. Sub-samples were air-dried for comparative analysis, representing the most extreme matric potential. The quantity of Mn extracted from field moist samples was compared to that extracted from air-dried samples (all samples done in triplicate). The extractions used for comparison were the hydroxylamine extract (to compare easily reducible Mn) and the KCl extract (to compare exchangeable Mn extracted). It was expected that the KCl extractable Mn would be dominated by Mn^{2+}. The methods were outlined in Chapter three.

Selected samples (in triplicate) were packed in rings on ceramic plates to a bulk density of 1200 kg.m^3 after which they were saturated with deionized water and left to equilibrate for 24 hours. The samples were transferred to the pressure plate extractors, which experiences atmospheric pressure from below and applied pressure from above. Various air pressures were applied to selectively remove water held at various energy states (or potentials). Samples were a left to equilibrate until water was no longer removed from the samples at the given pressure (determined visually). Samples were removed and weighed before and after drying (adapted from Dane & Hopmans, 2002). Sub-samples were taken straight off the pressure plate and analysed for easily reducible Mn using the acid hydroxylamine extractant (refer to Chapter three for method).

Pressures used were -100 J.kg^{-1} and -350 J.kg^{-1}. The reasoning for these chosen water potentials is as follows. Field capacity is between of -10 and -30 J.kg^{-1} and permanent wilting point occurs at around -1500 J.kg^{-1} (Brady & Weil, 2002). The pressure plate method is not always accurate below -100 J.kg^{-1} because the soil's water retention is strongly influenced by its structure and natural pore size distribution (Or & Wraith, 2002). Therefore the matric potential chosen to represent the point where the soil is unsaturated but still feels and appears moist was -100 J.kg^{-1}. It was therefore assumed that at this matric potential the results would be less affected by the packing of the samples. The matric potential of -350 J.kg^{-1}was selected to represent drier conditions. This represents a point where adsorbed water plays a large role. As this was an exploratory investigation, only these two matric potentials were selected.

5.2.3 Results and discussion

5.2.3.1 Effect of soil moisture on manganese solubility

The results of the comparison between the KCl extractable Mn (exchangeable Mn) from field moist and air-dried samples is shown in Table 5.6. The results are in accordance with literature with all of the samples having significantly higher exchangeable Mn^{2+} quantities in air-dried samples. It was also observed that topsoils had higher Mn^{2+} contents than subsoils for the air-dried samples. This is because subsoils do not reach the same level of dessication as topsoils, resulting in more easily reducible Mn in subsoils. It is also due to more organic material, and therefore electron donors, in the topsoil.

Table 5.6: Comparison of Mn extracted by KCl from air-dried and field moist samples

Sample	Mn (mmol.kg^{-1} soil)		p-value
	Air dry	Field moist	
G_Crest_A	0.08	0.01	<0.01**
G_Crest_B	0.07	0.01	< 0.01**
D_Crest_A	0.48	< MDL	< 0.01**
D_Bot_A	0.55	< MDL	< 0.01**
A_Mid_A	0.27	< MDL	< 0.01**
A_Mid_B1	0.09	< MDL	< 0.01**
A_Mid_B2	0.06	< MDL	< 0.01**

It was therefore expected that field moist soils not subjected to drying would have higher easily reducible Mn contents. Literature suggests that field moist soils will exhibit a higher redox buffer capacity due to the availability of more reactive Mn^{3+} and Mn^{4+} to act as electron acceptors. This, however, is subject to the amount of Mn in the soil because the impact will be much less in soils with very high amounts of Mn. The re-precipitation of these Mn species as a result of the greater accumulation and stability as well as regeneration capacity (the ability of Mn^{2+} to be continually reoxidized to Mn^{3+} and Mn^{4+}) of Mn in the subsoil where there is a decrease in electron donor availability would prevent the formation of redoximorphic features. In order to test this hypothesis, the easily reducible Mn contents of field moist soils were compared with their air-dried counterparts. The results are given in Table 5.7. The two methods looked at is the hydroxylamine method (soil to solution ratio 1:50) and the altered hydroxylamine method, as done for the speciation method in Chapter three (soil to solution ratio 1:25). The difference between the two is the sample size. For soil to solution ratio 1:50, 0.5 g of soil in 25 ml extractant was used and for soil to solution ratio 1:25, 1 g of sample in 25 ml extractant was used.

Table 5.7: Comparison of Mn extracted by acid hydroxylamine (mmol.kg^{-1}) from air-dried and field moist samples at two soil to solution ratios

Sample	Soil to solution 1:50 (0.5 g soil)			p-value	Soil to solution ratio 1:25 (1 g soil)			p-value
	Air Dry	Field Moist	Difference		Air Dry	Field Moist	Difference	
Q_Crest_A	0.31	0.47	0.15	0.09	0.54	0.43	0.11	0.35
Q_Crest_B1	0.22	0.23	0.01	0.86	0.27	0.24	0.03	0.63
Q_Crest_B2	0.18	0.18	0.00	0.50	0.20	0.16	0.03	0.16
Q_Mid_A	0.96	0.80	0.16	0.05*	1.27	0.98	0.28	0.04
Q_Mid_B1	0.58	0.68	0.10	0.01*	0.79	0.85	0.05	0.36
Q_Mid_B2	0.75	0.51	0.24	0.07	0.92	0.65	0.28	0.03*
Q_Foot_A	0.02	0.02	0.00	0.47	0.02	0.04	0.01	<0.01**
Q_Foot_B	0.03	0.03	0.00	0.88	0.03	0.03	0.00	0.33
Q_Bot_A	0.88	0.93	0.05	0.58	0.90	1.19	0.28	0.04*
V_Black	7.74	10.3	2.57	0.82	12.3	1.17	11.1	<0.01**
V_Brown	23.8	23.9	0.06	0.99	33.1	9.01	24.1	<0.01**
G_Crest_A	1.05	0.95	0.09	0.22	1.19	1.07	0.11	0.77
G_Crest_B	0.62	0.49	0.13	<0.01**	0.64	0.54	0.10	0.14
G_Mid_A	0.93	0.82	0.11	0.28	1.17	1.06	0.11	<0.01**
G_Mid_B	0.79	0.61	0.19	0.11	1.20	0.69	0.51	0.05
G_Bot_A	0.03	0.01	0.02	0.01*	0.05	0.02	0.02	<0.01**
G_Bot_B1	< MDL	< MDL	0.00	0.12	< MDL	< MDL	0.00	0.22
G_Bot_B2	0.01	< MDL	0.01	<0.01**	0.01	0.01	0.00	0.46
D_Crest_A	78.1	132	54.3	0.01*	101	95.2	6.1	0.06
D_Bot_A	88.3	90.5	2.19	0.89	85.1	71.1	14.0	0.10
A_Mid_A	11.9	10.8	1.13	0.10	8.43	9.03	0.61	0.30
A_Mid_B1	7.79	6.95	0.83	0.27	5.48	4.55	0.93	0.06
A_Mid_B2	8.47	6.58	1.88	<0.01**	5.38	6.10	0.71	0.61

Legend:
Supports literature and differences are statistically significant
Supports literature and differences are not statistically significant
Contradicts literature and differences are statistically significant
Contradicts literature and differences are not statistically significant
No highlight – values stayed the same

Significant differences were tested at $\alpha = 0.05$ and $\alpha = 0.01$. Looking at the 1:50 ratio first, from the 23 samples investigated, only 7 (30%) showed any significant difference in the easily reducible Mn content measured between the air-dried samples and their field moist counterparts. The 1:25 ratio is not much different with only 8 samples (35%) having significant differences in easily reducible Mn content between air-dried and field moist samples. The easily reducible Mn contents of most of the samples, therefore, appeared to be

unaffected by drying. It therefore seems that significant differences in easily reducible Mn might be dependent on the type of soil, more specifically the soil properties.

Samples that showed any significant differences in easily reducible Mn content between air-dried and field moist samples are highlighted in Table 5.7. Samples highlighted in green **supports literature** that a significantly higher easily reducible Mn content is observed in field moist samples. The samples highlighted in red show a significantly higher easily reducible Mn content in the air-dried samples. From the 15 samples that showed significant differences, only 4 show the expected increase in easily reducible Mn in the field moist samples. A decrease is seen for the rest of the samples. It was also seen that only two samples showed significant differences for both soil to solution ratio 1:50 and 1:25. The rest of the samples either had significant differences for ratio 1:50 or 1:25. Obtaining significant differences therefore also depends on the soil to solution ratio used.

A further investigation was conducted to determine whether certain soil properties may have any influence on differences between easily reducible Mn contents in air-dried and field moist samples. This was done for both soil to solution ratios. Correlations were drawn between the difference of air-dried and field moist samples for easily reducible Mn with pH, CEC and clay percentage. The results are given in Table 5.8.

Table 5.8: Linear correlation coefficients for the difference in easily reducible Mn between air-dried and field moist samples with selected soil properties

Soil property	Soil to solution ratio 1:50 (R^2)		Soil to solution ratio 1:25 (R^2)	
pH	0.42		0.56	
CEC	With vertics	Without vertics	With vertics	Without vertics
	0.31	0.71	0.62	0.25
Clay content (%)	0.35		0.03	

The dolomite soil, D_Crest_A had a much higher difference in easily reducible Mn between air-dried and field moist samples than any of the other samples for ratio 1:50. It was therefore excluded from the correlations in order to obtain the best possible fit. This was not the case for ratio 1:25 and therefore the dolomites were included in the correlations. The correlation between easily reducible Mn difference and pH appears to be average. It seems slightly better for ratio 1:25. The next comparison was with CEC. The reason that the correlation coefficient was calculated with and without the vertics for CEC is because these soils had a far higher CEC than any of the other samples and it was important to look at the

correlation without the dominant effect of the vertic soils. Another benefit of this omission was to see if a better correlation was obtained. A strong correlation was seen without the vertics for ratio 1:50, however a stronger correlation was observed with the vertics for ratio 1:25. The relationship appears to change with different soil to solution rations and evidence supporting the influence of CEC therefore appears to be inconclusive. A poor correlation was observed between easily reducible Mn difference and clay content, particularly using ratio 1:25. The extraction volume therefore appears to play a major role.

5.2.3.2 Effect of matric potential on manganese solubility

The two soils selected for this exploratory study were the G1 (granite samples upslope, topsoil and subsoil) and D samples (dolomite samples). The reason for this selection is because these soils have a stark contrast in Mn content, while both having relatively high Fe contents. The hypothesis is that the more negative the matric potential, the lower the amount of easily reducible Mn available. The aim is also to investigate the magnitude of change in easily reducible Mn as the matric potential changes. The results are shown in Table 5.9 and the significance of the differences between the samples are indicated in Table 5.10.

Table 5.9: Easily reducible Mn extracted from selected samples at varying matric potentials

Sample	Easily reducible Mn (mmol.kg^{-1} soil)		
	No P (Field Moist)	-100 J.kg^{-1}	-350 J.kg^{-1}
G_Crest_A	0.95	0.91	1.11
G_Crest_B	0.49	0.57	0.71
D_Crest_A	132	101	87.2
D_Bot_A	90.5	73	67.6

Table 5.10: Significance of differences between the same geology at different pressures

Sample	Statistical probability values (p-values)		
	No P & -100 J.kg^{-1}	No P & -350 J.kg^{-1}	-100 J.kg^{-1}& -350 J.kg^{-1}
G_Crest_A	0.26	0.46	0.07
G_Crest_B	0.04*	0.49	0.37
D_Crest_A	0.02*	0.21	0.01*
D_Bot_A	0.33	0.26	0.23

The general trend observed is that the amount of easily reducible Mn extracted decreased as the matric potential became more negative. This is expected based on literature which indicates that soluble Mn increases with drying, while easily reducible Mn decreases under these conditions. The results shown earlier, however, casted doubt on the clear relationship portrayed by literature. The results from the study showed that the only significant differences found were between no pressure applied and -100 J.kg^{-1} for the granite subsoil

and the dolomite sample upslope as well as between -100 $J.kg^{-1}$ and -350 $J.kg^{-1}$ for the dolomite upslope. These results will therefore be discussed.

The G1_Crest_B sample showed a small but constant increase in the quantity of Mn in the 3+ and 4+ valencies from the field moist sample to a matric potential of -100 $J.kg^{-1}$and a matric potential of -350 $J.kg^{-1}$. This difference was not, however, statistically significant. The organic carbon content of these soils were all very low, possibly resulting in more re-oxidation. Higher levels of dissolved organic matter may complex with Mn^{2+}, inhibiting re-oxidation to the easily reducible forms. It is possible that drying brings Mn^{2+} in solution closer to the Mn^{3+} and Mn^{4+} surfaces that re-oxidize it (Discussion with PC de Jager). The dolomite samples on the other hand showed a clear decrease in easily reducible Mn as the matric potential becomes more negative. This may be explained by the removal of Mn^{2+} with water during equilibration of the samples on the pressure plates.

Interesting to note is the trends observed in these samples are contrary to the observations made in the air-dried vs. field moist samples. While the granite samples in the matric potential investigation showed an increase in easily reducible Mn as the soil dries out, the investigation on the effect of drying exhibited a decrease in the air-dried samples. The same contradiction is observed for the dolomites. The matric potential study showed a decrease in easily reducible Mn as the soil dries but the effect of drying investigation showed an increase.

A challenge associated with this method is that it does not always provide a true representation of soil water. The actual matric potential may be higher than that of the pressure chamber. Several studies have also indicated that there is a lack of equilibration for measurements in the drier regions (Gubiani et al., 2012). Preliminary results show a relationship between matric potential and redox buffering however further investigations using a wider range of matric potentials would also be necessary to draw more decisive conclusions.

5.2.4 Summary

A comparison of field moist and air-dried samples from the Highveld subjected to the hydroxylamine extract were unaffected by drying, showing no significant decrease in the easily reducible Mn contents. This is contrary to what is generally reported in literature. The

significant differences that were found appeared to be dependent on soil properties as well as the soil to solution ratio used.

The study of the effect of soil moisture continued into the investigation of matric potential on redox buffering. The general trend for these specific soils tested was that as the soil dried and the matric potential became more negative, the easily reducible Mn content decreased. A low presence of Mn^{3+} and/or Mn^{4+} is associated with low TED values, therefore matric potential has an influence on soil redox buffering.

Chapter six: Synthesis

6.1 Summary

Wetland delineation is based on the interpretation of signs of wetness in a landscape. One of these determinants is the presence of redoximorphic features. The problem encountered, however, is that redox morphology is expressed differently in various geographical areas and these features are conspicuously absent in certain soils where they are expected to occur. It is therefore imperative to gain a deeper understanding of redoximorphic features, more importantly what causes the lack or suppression of these features in certain soils.

In order to investigate this phenomenon, soils were collected from various areas in the Pretoria, Midrand region. All samples except the andesite soil were sampled at wetland sites. The andesite soil provided an Mn content higher than the quartzite and granite but lower than the vertic and dolomite soils. The quartzite and granite soils showed the expected redoximorphic features indicating a fluctuating water table. Mottling in the vertic soils was poorly expressed and in the dolomite soils was completely suppressed. Analysis by XRF as well as chemical extractions revealed that the quartzite and granite soils had very low, almost negligible, Mn contents whereas the andesite soil had an appreciable Mn content. The vertic soils had a higher Mn content than these soils but lower than the dolomite which had by far the highest Mn content.

Total electron demand was used as an indicator of the oxidizing capacity of the soils and as the index of redox buffering. The dolomite, vertic and andesite soils, all with the highest Mn contents, had the highest TED. The granite and quartzite soils, with the lowest Mn contents, had the lowest TED. It is therefore the soils with higher Mn contents and higher Mn activity that experience redox buffering. This explains the lack of mottles in the dolomite soil where it was expected to occur.

It was important to investigate the influence of soil properties on chemical redox buffering in these soils. Several soil properties were correlated with TED and a very weak correlation for all properties was observed. This strengthens the validation that Mn is the major role player in redox buffering. It is possible, however, that correlations could have been missed due to the wide range of soils that were investigated.

An exploratory investigation looking at the effect of drying on Mn solubility and therefore redox buffering revealed that most soils were unaffected. Results showed that for many of the soils, there was no significant difference in the easily reducible Mn contents between field

moist and air dry soils. This contradicts literature where several investigations conclude that drying results in an increase in Mn^{2+} and decrease in the easily reducible forms of Mn. The difference in easily reducible Mn content observed in these soils sampled in the Highveld was due to differences in soil type and their associated soil properties.

The effect of matric potential revealed that as the soil dried out and matric potential became more negative, easily reducible Mn decreased. Samples with higher easily reducible Mn contents are associated with higher TED and therefore redox buffering. The results therefore indicate that soils are more susceptible to redox buffering in moist conditions than dry ones.

A possible lab method for redox buffering was attempted. This was done by using the difference in extent of soil bleaching as a measure of redox buffering. Visually, the DC extract resulted in complete or very close to complete bleaching of all soils, whereas the CBD extract resulted in incomplete bleaching for soils with higher Mn contents. Upon closer investigation spectrophotometrically using quantitative values, however, it was observed that high Fe contents was the major role player and not Mn as suspected. This was therefore not a useful lab method to predict redox buffering in soils.

The results of the study show that the manganiferous dolomite soil behaves differently to the other soils investigated due to the redox activity of Mn. It is therefore necessary for wetland delineation practices and guidelines to take this into consideration because redoximorphic features will not be expressed as expected and as they do in most soils. These results also have broader implications in the field of soil classification for pedogenic yellowing. By Mn preventing the reduction of ferric iron to ferrous iron, this inhibits the yellowing of soil. The influence of Mn on Fe reduction also has an impact in agriculture, nutrient management in particular. The prevention of Fe^{2+} formation inhibits its uptake by plants. This could result in Fe deficiency in plants grown on manganiferous soils. The influence of redox buffering therefore spans several applications and results of this study have contributed to the understanding of this phenomenon.

6.2 Conclusions

The dolomite soil showed a much greater oxidizing capacity as assessed by MED and, to a larger extent, TED measurements. TED correlated most strongly with hydroxylamine and

oxalate extractable Mn, followed by total Mn content as determined by XRF. The relationship between TED and Fe and Al, respectively, were weaker than they were with Mn. Correlations between the soil properties investigated (titratable acidity, CEC, clay content and organic carbon) and TED were all weak. Furthermore, soils with the lowest Mn contents and no measurable Mn activity levels (Q_Foot and G_Bot samples) expressed mottling where expected. The vertics, which had an appreciable Mn content, showed very poor mottle expression in their morphology. The dolomite soils, with the highest Mn contents and higher Mn activity levels than Fe, lacked mottles in their morphology. These soils were also enriched with Mn in the amorphous, reactive fraction of the soil, compared to Al and Fe. It was therefore concluded that Mn plays the dominant role in buffering redoximorphic features in wetland soils derived from the Malmani dolomites in Centurion. It is postulated that this buffering prevents the reduction of Fe^{3+} to Fe^{2+} and also reoxidizes Fe^{2+} to Fe^{3+}, which is the reason why mottling as a result of Fe reduction is not seen as expected in certain soils that are visibly wet. This phenomenon may not be specific to the Highveld region of South Africa. The dolomites stretch to areas such as Krugersdorp, Ventersdorp, Potchefstroom and Lichtenburg. Future studies should include these areas. The implication the results of this study has on wetland delineation is therefore not limited to Gauteng.

6.3 Recommendations for future research

Future studies could possibly investigate the formulation of TED categories to separate soils as having strong, medium or low oxidizing capacities. It is clear from the results of this study that MED did not work for the soils investigated and therefore could be problematic for highly weathered soils. Manganese concentration could also be linked to TED in order to categorize soils as being strongly or weakly buffering. Lastly a connection between organic matter accumulation and redox buffering in soils could be investigated.

Improvements that can be made to methods used in this study are as follows:

- Element extractability depends mainly on whether the element resides in oxides and hydroxides or in clay minerals. It is therefore crucial to carefully consider the choice of method for total elemental content as the effectiveness of different methods varies for elements. A deeper investigation into these methods (XRF, DC and CBD) and their effectiveness in removing Al, Fe and Mn is required in order to draw more conclusive evidence for the appropriate methods for specific applications. Results

from the study support the recommendation that DC be used for element extraction and not CBD.

- The MED method should be investigated for its suitability for highly weathered soils with high Fe content due to Fe oxides adsorbing iodide and possibly interfering with results.
- With regards to sample preparation, it was found that grinding concretions after drying affects the soil colour. Sieving and grinding can introduce artefacts into the sample. It affected the soil bleaching experiment as well because concretions when not sieved and ground did not bleach (the coating on concretions resisted reduction).
- Looking at the influence of soil moisture on redox buffering, the easily reducible Mn contents of a wider range of soil moisture conditions and matric potentials between field moist and permanent wilting point need to be studied in order to further investigate the relationship between soil moisture content and redox buffer capacity as well as the effect of matric potential on redox buffering.

REFERENCES

ABDEL-KHALEK EK, EL-MELIGY WM, MOHAMED EA, AMER TZ & SALLAM HA. 2008. Study of the relationship between electrical and magnetic properties and Jahn-Teller distortion in $R_{0.7}Ca_{0.3}Mn_{0.95}Fe_{0.05}O_3$Perovskites by Mossbauer effect. In: El Nadi LM (ed), *Modern Trends in Physics Research, Third International Conference on Modern Trends in Physics Research*. Cairo: World Scientific Publishing Co. pp 110-114.

ALEXANDER EB, COLEMAN RG, KELLER-WOLF T & HARRISON SP. 2007. *Serpentine geoecology of Western North America, geology, soils, and vegetation*. New York: Oxford University Press. pp 130.

ALOWAY BJ. 1995. Soil processes and the behaviour of heavy metals. In: Alloway BJ (ed.), *Heavy metals in soils*. Glasgow: Blackie Academic and Professional. pp 17.

ARSHAD MA, ST ARNAUD RJ & HUANG PM. 1971. Dissolution of tri-octahedral layer silicates by ammonium oxalate, sodium-dithionite-citrate-bicarbonate, and potassium pyrophosphate. *Canadian Journal of Soil Science*, 52(1): 19-26.

BAIZE D. 2009. Cadmium in soils and cereal grains after sewage-sludge application on French soils: A review. In: Lichtfouse E, Navarrete M, Debaeke P, Soucere V & Alberola C (eds). *Sustainable Agriculture, Volume One*. New York: Springer Science and Business Media. pp 847.

BARREIRO L & NAVES T. 2007. Content and language integrated learning (CLIL) materials in chemistry and English: Iodometric titrations. Students coursebook. Geralitat de Catalunya.

BARROW V & TORRENT J. 1987. Origin of red-yellow mottling in a Ferric Acrisol of southern Spain. *Z. Pflanzenerahr Bodenk*., 150: 308-313.

BARTLETT RJ & BRUCE RJ. 1996. Chromium. In: Sparks DL, Page AL, Helmke PA, Loeppert RH, Soltanpour PN, Tobatabai MA, Johnston CT & Summer MA(eds), *Methods of Soil Analysis. Part 3, Chemical Methods.* Madison: Soil Science Society of America. pp 695-696.

BARTLETT RJ & JAMES BR. 1980. Studying dried, stored soil samples – some pitfalls. *Soil Science Society of America Journal*, 444: 721-724.

BARTLETT RJ & JAMES BR. 1995. System for categorizing soil redox status by chemical field testing. *Geoderma*, 68: 211-218.

BARTLETT RJ. 1988. Manganese redox reactions and organic interactions in soils. In: Graham, R.D., Hannam, R.J.& Uren, N.C. (eds.), *Manganese in Soils and Plants*. The Netherlands: Kluwer Academic Publishers. pp 59-73.

BARTLETT RJ. 1999. Characterizing soil redox behaviour. In: Sparks DL (ed), *Soil Physical Chemistry, Second Edition*. Boca Raton: CRC Press. pp 393.

BERNDT GF. 1988. Effect of drying and storage conditions upon extractable soil manganese. *Journal of the Science of Food and Agriculture*, 45: 119-130.

BERTSCH PM & BLOOM PR. 1996. Aluminum. In: Sparks DL, Page AL, Helmke PA, Loeppert RH, Soltanpour PN, Tobatabai MA, Johnston CT & Summer MA (eds), *Methods of Soil Analysis. Part 3, Chemical Methods*. Madison: Soil Science Society of America. pp 678.

BOERO V & SCHWERTMANN U. 1987. Occurrence and transformations of iron and manganese in a colluvial Terra Rossa toposequence of Northern Italy. *Catena*, 14: 519-531.

BOUMA J. 1983. Hydrology and soil genesis of soils with aquic moisture regimes. In: Wilding LP, Smeck NE & Hall GF (eds.), *Pedogenesis and Soil Taxonomy, I, Concepts and Interactions*. Amsterdam: Elsevier Science Publishers. pp 253-281.

BRADY NC, WEIL RR. 2002. Nature and Properties of Soils, Thirteenth Edition. Prentice Hall. pp 187, 207-209, 376-391.

CHADWICK OA & CHOROVER J. 2001. The chemistry of pedogenic thresholds. *Geoderma*, 100: 321-353.

CHILDS CW & LESLIE DM. 1977. Interelement relationships in iron-manganese concretions from a catenary sequence of yellow-grey earth soils in loess. *Soil Science*, 123(6): 369-376

COURCHESNE F & TURMEL MC. 2007. Extractable Al, Fe, Mn and Si. In: Carter RM and Gregorich EG (ed.), *Soil Sampling and Methods of Analysis. Second Edition. Canadian Society of Soil Science*. Florida: CRC Press. pp 309-311.

COUTURE RA & SEITZ MG. 1983. Sorption of anions of iodine by iron oxides and kaolinte. *Nuclear and Chemical Waste Management*, 4: 301-306.

CUMMINGS DE, CACCAVO JR. F, FENDORF S & ROSENZWEIG RF. 1999. Arsenic mobilization by the dissimilatory Fe (III) – reducing bacterium *Shewanellaalga* BrY. *Environmental Science and Technology*, 33: 723 – 729.

DANE, J.H. & HOPMANS, J.W. 2002. The soil solution phase. In Dane JH & Topp GC (eds), *Methods of Soil Analysis. Part 4, Physical Methods*. Madison: Soil Science Society of America. pp 688.

DAVISON W & WOOF C. 1984. A Study of the cycling of manganese and other elements in a secondary anoxic lake, Rostherne Mere, UK. *Water Research*, 18(6): 727-734.

DE SCHAMPHELAIRE L, RABAEY K, BOON N & VERSTRAETA W. 2007. Minireview: The potential of enhanced manganese redox cycling for sediment oxidation. *Geomicrobiology Journal*, 24: 547-558.

DION HG, MANN PJG & HEINTZE SG. 1946. The 'easily reducible' manganese of soils. *Journal of Agricultural Science*, 37: 2-22.

DOI R & RANAMUKHAARACHCHI SL. 2007. Soil colour designation using Adobe Photoshop™ in estimating soil fertility restoration by *Acacia auriculiformis* plantation on degraded land. *Current Science*, 99(11): 1604-1609.

DOWDING CE & FEY MV. 2007. Morphological, chemical and mineralogical properties of some manganese-rich oxisols derived from dolomite in Mpumalanga province, South Africa. *Geoderma*, 141: 23-33.

DOWDING CE. 2004. Morphology, mineralogy and surface chemistry of manganiferous oxisols near Graskop, Mpumalanga Province, South Africa. MSc. dissertation, Stellenbosch University, South Africa. pp 31 - 32.

DOWLEY A, FITZPATRICK RW, CASS A & BESZ W. 1998. Measurement of redox potential (Eh) in periodically waterlogged viticultural soils. Proceedings of the International Soil Science Society Congress, Symposium No. 35, Montpellier, France, 20 -26 August 1998.

DWAF (Department of Water and Forestry). 2005. A practical field procedure for identification and delineation of wetlands and riparian areas. National Water Act, Edition 1.

ESSINGTON ME. 2004. *Soil and water chemistry, an integrative approach*. Boca Raton: CRC Press. pp131-133, 454.

FAULKNER SP, PATRICK JR WH & GAMBRELL RP. 1989. Field techniques for measuring wetland soil parameters. *Soil Science Society of America Journal*, 53(3): 883-890.

FERREIRA TO, OTERO XL, VIDAL-TORRADO P & MACIAS F. 2007. Redox processes in mangrove soils under *Rhizophora mangle* in relation to different environmental conditions. *Soil Science Society of America Journal*, 71: 484-491.

FERTILIZER INDUSTRY FEDERATION OF SOUTH AFRICA. 2006. *Australian soil fertility manual, third edition*. Collingwood: CSIRO Publishing. pp 13.

FEY MV. 1981. Hypothesis for the pedogenic yellowing of red soil materials. Proceedings of the 10th National Congress of Soil Science Society Southern Africa. East London. Tech. Comm. No. 180. Department of Agriculture. pp 130-136.

FEY MV. 2010. *Soils of South Africa. Profile descriptions and analytical data*. Cambridge: Cambridge University Press. pp 255.

FIEDLER S & SOMMER M. 2004. Water and redox conditions in wetland soils – their influence on pedogenic oxides and morphology. *Soil Science Society of America Journal*, 68: 326-335.

FIEDLER S, VEPRASKAS MJ & RICHARDSON JL. 2007. Soil redox potential: importance, field measurements, and observations. *Advances in Agronomy*, 94: 2-54.

FOTH HD. 1990. *Fundamentals of soil science, eighth edition*. New York: John Wiley & Sons. pp 59.

FRANZMEIER DP, YAHNER JE, STEINHARDT GC & SINCLAIR JR. HR. 1983. Colour patterns and water table levels in some Indiana soils. *Soil Science Society of America Journal*, 47: 1196-1202.

FRITSCH E, MORIN G, BEDIDI A, BONNIN D, BALAN E, CAQUINEAU S & CALAS G. 2005. Transformations of haematite and Al-poor goethite to Al-rich goethite and associated yellowing in a ferralitic clay soil profile in the middle Amazon Basin (Manus, Brazil). *European Journal of Soil Science*, 56: 575-588.

FROHNE T, RINKLEBE J, DIAZ-BONE RA & LAING GD. 2011. Controlled variation of redox conditions in a floodplain soil: Impact on metal mobilization and biomethylation of arsenic and antimony. *Geoderma*, 160: 414-424.

FUJIMOTO CK & SHERMAN GD. 1945. The effect of drying, heating, and wetting on the level of exchangeable manganese in Hawaiian soils. *Soil Science Society of America Proceedings*, 10: 107-112.

FUJIMOTO CK & SHERMAN GD. 1948. Behaviour of manganese in the soil and the manganese cycle. *Soil Science*, 66: 131-146.

GADDE RR & LAITINEN HA. 1974. Studies of heavy metal adsorption by hydrous iron and manganese oxides. *Analytical Chemistry*, 46(13): 2022-2026.

GAMBRELL RP. 1996.Manganese. In: Sparks DL, Page AL, Helmke PA, Loeppert RH, Soltanpour PN, Tobatabai MA, Johnston CT & Summer MA (eds), *Methods of soil analysis. Part 3, Chemical methods*. Madison: Soil Science Society of America. pp 678.

GILKES RJ & MCKENZIE RM. 1988. Geochemistry and mineralogy of manganese in soils. In: Graham RD, Hannam RJ & Uren NC (eds), *Manganese in Soils and Plants.* Dordrecht: Kluwer Academic Publishers. pp 23-95.

GLINSKI J, STAHR K, STEPNIEWSKA Z & BRZEZINSKA M. 1992. Changes of redox and pH conditions in a flooded soil amended with glucose and nitrate under laboratory conditions. *Z. Pflanzenerahr. Bodenk.*, 155: 13-17.

GOLDEN DC, DIXON JB & KANEHIRO Y. 1993. The manganese oxide mineral, lithiophorite, in an oxisol from Hawaii. *Australian Journal of Soil Research*, 31: 51-66.

GOTOH S & PATRICK JR. WH. 1972. Transformations of manganese in a waterlogged soil as affected by redox potential and pH. *Soil Science Society of America Journal*, 36(5): 738-742.

GROSSMAN RB & REINSCH TG. 2002. The solid phase. In: Dane JH & Topp GC (ed.), *Methods of Soil Analysis. Part 4, Physical methods*. Madison: Soil Science Society of America. pp 275-276, 281-282, 688.

GUBIANI PI, REICHERT JM, CAMPBELL C, REINERT DJ & GELAIN NS. 2012. Assessing errors and accuracy in dew-point potentiometer and pressure plate extractor measurements. *Soil Science Society of America Journal*, 77: 19-24.

HARDIE AM, HEAL KV & LILLY A. 2007. The influence of pedology and changes in soil moisture status on manganese release from upland catchments: soil core laboratory experiments. *Water Air Soil Pollut.*, 182: 369-382.

HARRIS RC & ADAMS JAS. 1966. Geochemical and mineralogical studies on the weathering of granitic rocks. *American Journal of Science*, 264: 146-173.

HAWKER LC & THOMPSON JG. 1988. Weathering sequence and alteration products in the genesis of the Graskop manganese residua, Republic of South Africa. *Clay and Clay Minerals*, 36(5): 448-454.

HAYNES RJ & SWIFT RS. 1991. Concentrations of extractable Cu, Zn, Fe and Mn in a group of soils as influenced by air- and oven- drying and rewetting. *Geoderma*, 49: 319-333.

HE J, SUNG Y, DOLLHOPF ME, FATHEPURE BZ, TIEDJE JM & LOFFLER FE. 2002. Acetate versus hydrogen as direct electron donors to stimulate the microbial reductive dechlorination process at chloroethene-contaminated Sites. *Environmental Science and Technology*, 36: 3945-3952.

HERBEL MJ, SUAREZ DL, GOLDBERG S & GAO S. 2007. Evaluation of chemical amendments for pH and redox stabilization in aqueous suspensions of three California soils. *Soil Science Society of America Journal*, 71(3): 927-939.

HUSSON O. 2013. Redox potential (Eh) and pH as drivers of soil/plant/microorganism systems: a transdisciplinary overview pointing to integrative opportunities for agronomy. *Plant Soil*, 362: 389-417.

ISLAM K, McBRATNEY AB & SINGH B. 2004. Estimation of soil colour from visible reflectance spectra. In: Australian New Zealand Soils Conference, 5-9 December 2004, University of Sydney, Australia.

JACOBS PM, WEST LT & SHAW JN. 2002. Redoximorphic features as indicators of seasonal saturation, Lowndes County, Georgia. *Soil Science Society of America Journal*, 66: 315-323.

JEANROY E, RAJOT JL,PILLON P & HERBILLION AJ. 1991. Differential dissolution of hematite and goethite in dithionite and its implication on soil yellowing. *Geoderma*, 50: 79-94.

KENNEDY CB, GAULT AG, FORTIN D, CLARK ID & FERRIS FG. 2011. Retention of iodide by bacteriogenic iron oxides. *Geomicrobiology Journal*, 28: 387-395.

KERSTEN M & FORSTNER U. 1990. Speciation of trace elements in sediments. In: Batley GE (ed), *Analytical Methods and Problems*. Boca Raton: CRC Press. pp 272-274.

KONICA MINOLTA, 2007. Precise color communication. Color control from perception to instrumentation, pp 57. 9242-4830-92, AJFIPK.

KUSUYAMA T, TANIMURA K & SATO K. 2002. Adsorptive properties of Mn-substituted goethite particles for aqueous solutions of lead, copper, and zinc. *Materials Transactions*, 43(3): 455-458.

LIN YS, CHEN YG, CHEN ZS & HSIEH ML. 2005. Soil morphological variations on the Taoyuan Terrace, Northwestern Taiwan: Roles of Topography and Groundwater. *Geomorphology*, 69: 138-151.

LINDBERG RD & RUNNELS DD. 1984. Ground water redox reactions: An analysis of equilibrium state applied to Eh Measurements and geochemical modeling. *Science*, 225(4665): 925 – 927.

LOUBSER M & VERRYN S.2008. Combining XRF and XRD analyses and sample preparation to solve mineralogical problems. *South African Journal of Geology* 111: 229-238.

LOVLEY DR & PHILLIPS EJP. 1988. Manganese inhibition of microbial iron reduction in anaerobic sediments. *Geomicrobiology Journal*, 6: 145-155.

MALO DD, BLUE RA, SCHUMACHER TE, DOOLITTLE JJ & LUND JJ. 2006. Redox development in soil materials as influenced by time, temperature and carbon level – Part A: morphological changes. Poster presented at the ASA – CSSA – SSSA 2006 International Annual Meetings. Indianapolis, November 12-16.

MANSFELDT T. 2003. *In situ* long-term redox potential measurements in a dyked marsh soil. *Journal of Plant Nutrition and Soil Science*, 166: 210-219.

MARTIN ST. 2005. Precipitation and dissolution of iron and manganese oxides. In: Grassian VH (ed), *Environmental Catalysis*. Boca Raton: Taylor and Francis Group. pp 61-82.

McCAULEY A, JONES C & JACOBSEN J. 2009. Soil pH and organic matter. Nutrient management module No. 8, 4449-8. Montana State University.

McKENZIE RM. 1972. The manganese oxides in soils - A review. *Z. Pflanzenerahr. Bodenk.* 131: 221-242.

McKENZIE RM. 1976. The Manganese oxides in soils. Presented at the proceedings of the 2nd International symposium on geology and geochemistry of manganese, 14-24 August, Sydney, Australia. pp 259-269.

McKENZIE RM. 1981. The surface charge of manganese dioxides. *Australian Journal of Soil Research*, 19: 41-50.

McKENZIE RM. 1989. Manganese oxides and hydroxides. In: Dixon JB & Weed SD (ed.), *Minerals in Soil Environments. Second Edition*. Madison: Soil Science Society of America. pp 439-460.

MEGONIGAL JP, PATRICK JR WH & FAULKNER SP. 1993. Wetland identification in seasonally flooded forest soils: Soil morphology and redox dynamics. *Soil Science Society of America Journal*, 57: 140-149.

MEHRA OP & JACKSON ML. 1960. Iron oxide removal from soils and clays by a dithionite-citrate system buffered with sodium bicarbonate. *Clays Clay Miner*. 7: 317-327

MOUAZEN AM, KAROUI R, DECKERS J, DE BAERDEMAEKER J & RAMON H. 2007. Potential of visible and near – infrared spectroscopy to derive colour groups utilising the Munsell soil colour charts. *Biosystems Engineering*, 97: 131-143.

MURRAY JW. 1974. The surface chemistry of hydrous manganese dioxide. *J. Colloid Interface Sci.*, 46: 357-371.

MYERS CR & NEALSON KH. 1988. Microbial reduction of manganese oxides: Interactions with iron and sulphur. *Geochimica et Cosmochimica Acta*, 52: 2727-2732.

NATH T, RAHA P & RAKSHIT A. 2010. Sorption and desorption behaviour of iodine in alluvial soils of Varanasi, India. *Agricultura*, 7: 9-14.

NEAMAN A, WALLER B, MOUELE F, TROLARD F & BOURRIE G. 2004. Improved methods for selective dissolution of manganese oxides from soils and rocks. *European Journal of Soil Science*, 55: 47-54.

NEGRAC C, ROSS DS & LANZIROTTI A. 2005. Oxidizing behaviour of soil manganese: Interactions among abundance, oxidation state, and pH. *Soil Science Society of America Journal*, 69: 87-95.

NELSON DW & SOMMERS LE. 1996. Total carbon, organic carbon, and organic matter. In: Sparks DL, Page AL, Helmke PA, Loeppert RH, Soltanpour PN, Tobatabai MA, Johnston CT & Summer MA (eds), *Methods of Soil Analysis. Part 3, Chemical Methods.* Madison: Soil Science Society of America. pp 995-996.

NEUE HU & BLOOM PR. 1987. Nutrient kinetics and availability in flooded rice soils. In: International Rice Research Institute (ed), *Progress in Irrigated Rice Research*. Proceedings of the International rice research conference, 21-25 September, Hangzhou, China.

NOGUEIRA MA, NEHLS U, HAMPP R, PORALA K & CARDOSO EJBN. 2007. Mycorrhiza and soil bacteria influence extractable iron and manganese in soil and uptake by soybean. *Plant Soil*, 298: 273-284.

NON-AFFILIATED SOIL ANALYSIS WORK COMMITTEE. 1990a. Organic carbon: Walkley-Black. In: Handbook of Standard Soil Testing Methods for Advisory Purposes. Pretoria: Soil Science Society of South Africa. pp 34/1-34/2.

NON-AFFILIATED SOIL ANALYSIS WORK COMMITTEE. 1990b. pH (KCl) and pH (H_2O). In: Handbook of Standard Soil Testing Methods for Advisory Purposes. Pretoria: Soil Science Society of South Africa. pp 2/1-3/2.

NON-AFFILIATED SOIL ANALYSIS WORK COMMITTEE. 1990c. Particle size distribution: Pipette. In: Handbook of Standard Soil Testing Methods for Advisory Purposes. Pretoria: Soil Science Society of South Africa. pp35/2 – 35/4.

OR D & WRAITH JM. 2002. Soil water content and Water potential relationships. In: Warrick AW (ed), *Soil Physics Companion*. Boca Raton: CRC Press LLC. pp 74.

OTTOW JCG. 1970. Iron reduction and gley formation by nitrogen-fixing clostridia. *Oecologia*, 6: 164-175.

OTTOW JCG. 1981. Mechanisms of bacterial iron-reduction in flooded soils. In: Instituite of Soil Science, Academia Sinica (ed.), *Proceedings of symposium on paddy soil*. Beijing: Science Press. pp 330.

PACK A, GUTZMER J, BEUKES NJ, VAN NIEKERK HS & HOERNES S. 2000. Supergene ferromanganese wad deposits derived from periman Karoo strata along the late cretaceous-mid-tertiary African land surface, Ryedal, South Africa. *Economic Geology*, 95: 203-220.

PANSU M & GAUTHEYROU J. 2007. *Handbook of soil analysis: Mineralogical, organic and inorganic Methods*. The Netherlands: Springer Science & Business Media. pp 187-188.

PHENE CJ, HOFFMAN GJ & AUSTIN RS. 1973. Controlling automated irrigation with soil matric potential sensors. In: Soil and Water Divison of ASAE (ed), *Transactions of the ASAE*, 16(4): 773-776.

PHILLIPS DH, AMMONS JT, LEE SY & LIETZKE DA. 1998. Deep weathering of calcareous sedimentary rock and the redistribution of iron and manganese in soils and saprolite. *Soil Science*, 163: 71-81.

PITTMAN JK. 2005. Managing the manganese: molecular mechanisms of manganese transport and homeostasis. *New Phytologist*, 167: 733-742.

PONNAMPERUMA FN. 1972. The chemistry of submerged soils. In: Brady NC (ed.), *Advances in Agronomy*. New York: Academic Press, Inc. pp 29-88.

POST JE. 1999. Manganese oxide minerals: Crystal structure and economic and environmental significance. *Proceedings of the National Academy of Sciences USA*, 96: 3447-3454.

RABENHORST MC & PARIKH S. 2000. Propensity of soils to Develop redoximorphic color changes. *Soil Science Society of America Journal*, 64: 1904-1910.

RAJAKUMAR GR, PATIL CV, PRAKASH SS, YELEDHALLI NA & MATH KK. 1996. Micronutrient distribution in paddy soils in relation to parent material and soil properties. *Karnataka Journal of Agricultural Sciences*, 9(2): 231-235.

RAYMONT GE & LYONS DJ. 2011. *Soil chemical methods – Australasia*. Collingwood: CSIRO Publishing. pp 364-365.

REDDY KR & DELAUNE RD. 2008. *Biogeochemistry of wetlands: Science and applications*. Boca Raton: CRC Press. pp 405-444.

REDDY KR & PERKINS HF. 1976. Fixation of manganese by clay minerals. *Soil Science*, 121(1): 21-24.

RELIC D, DORDEVIC D, POPOVIC A & BLAGOJEVIC, T. 2005. Speciation of trace metals in the Danube alluvial sediments within an oil refinery. *Environmental International*, 31: 661-669.

ROSS DS, HALES HC, SHEA-McCARTHY GC & LANZIROTTI A. 2001. Sensitivity of soil manganese oxides: Drying and storage cause reduction. *Soil Science Society of America Journal*, 65: 736-743.

ROSSEL RAV, MINASNY B, ROUDIER P & McBRATNEY AB. 2006. Colour space models for soil science. *Geoderma* 133: 320 – 337.

SCHULZE DG. 1984. The influence of aluminium on iron oxides, VIII. Unit cell dimensions of the Al-substituted goethites and estimation of Al from them. *Clay and Clay Minerals*, 32(1): 36-44.

SCHWERTMANN U. 1991. Solubility and dissolution of iron oxides. *Plant and Soil*, 130: 1-25.

SCHWERTMANN U. 2008. Iron oxides. In: Chesworth W (ed.), *Encyclopedia of Soil Science*. Dordrecht: Springer. pp 363.

SHANG C & ZELAZNY LW. 2008. Selective dissolution techniques for mineral analysis of soils and sediments. In: Ulery AL & Drees, LR (eds), *Methods of Soil Analysis. Part 5 – Mineralogical Methods*. Madison: Soil Science Society of America.

SINGH B & GILKES RJ. 1992. Properties and distribution of iron oxides and their association with minor elements in the soils of south-western Australia. *Journal of Soil Science*, 43: 77-98.

SINGH B & GILKES RJ. 1996. Nature and properties of iron rich glaebules and mottles from some South-west Australian soils. *Geoderma*, 71: 95-120.

SOIL CLASSIFICATION WORKING GROUP. 1991. Soil classification: A taxonomic system for South Africa. Pretoria: Department of Agricultural Development.

SPARROW LA & UREN NC. 1987. Oxidation and reduction of Mn in acidic soils: Effect of temperature and soil pH. *Soil Biology and Biochemistry*, 19(2): 143-148.

STEPNIEWSKI W, HORN R & MARTYNUIK S. 2002. Managing soil biophysical properties for environmental protection. *Agriculture, Ecosystems and Environment*, 88: 175-181.

STEPNIEWSKI W, STEPNIEWSKA Z. BENICELLI RP & GLINSKI J. 2005. Oxygenology in outline. Institute of Agrophysics PAS, Lublin, Report No. QLAM-2001-00428.

STRIGGOW B. 2013. Field measurements of oxidation-reduction potential (ORP). Report SESDPROC-113-R1, prepared for U.S. Environmental Protection Agency.

SWANEPOEL CM, MORGENTHAL TL, PRINSLOO HP & SCHOEMAN JL. 2008. Final report on wetland delineation. Report No.GW/A/2008/22. Pretoria: ARC-Institute for Soil, Climate, and Water.

TARDY I & NAHON D. 1985. Geochemistry of laterites, stability of Al –goethite, Al-hematite, and Fe^{3+} - kaolinite in bauxites and ferricretes: An approach to the mechanism of concretion formation. *American Journal of Science*, 285: 865-903.

THAMDRUP B, FOSSING H & JORGENSEN BB. 1994. Manganese, iron and sulphur cycling in a coastal marine sediment, Aarhus Bay, Denmark. *Geochimica et Cosmochimica Acta*, 58(23): 5115-5129.

THOMPSON A, CHADWICK OA, RANCOURT DG & CHOROVER J. 2006. Iron-oxide crystallinity increases during soil redox oscillations. *Geochimica et Cosmochimica Acta*, 70: 1710-1727.

TOWETT EK, SHEPHERD KD & CADISCH G. 2013. Quantification of total element concentrations in soils using total X-ray fluorescence spectroscopy (TXRF). *Science of the Total Environment*, 463-464: 374 -388.

TU S, RACZ GJ & GOH TB. 1994. Transformations of synthetic birnessite as affected by pH and manganese concentration. *Clays and Clay Minerals*, 4(3): 321-330.

VAN CAPPELLEN P & WANG Y. 1996. Cycling of iron and manganese in surface sediments: A general theory for the coupled transport and reaction of carbon, oxygen, nitrogen, sulphur, iron and manganese. *American Journal of Science*, 296: 197-243.

VAN HUYSSTEEN CW. 2008. A review of advances in hydropedology for application in South Africa. *South African Journal of Plant and Soil*, 125(4): 245-254.

VARADACHARI C, GOSWAMI G & GHOSH K. 2006. Dissolution of iron oxides. *Clay Research*, 25: 1-19.

VEPRASKAS MJ & BOUMA J. 1976. Model experiments on mottle formation simulating field conditions. *Geoderma*, 15: 217-230.

VERPRASKAS MJ. 2001. Morphological features of seasonally reduced soils. In: Vepraskas MJ, Craft CB & Richardson JL (eds), *Wetland Soils: Genesis, Hydrology, Landscapes, and Classification*. Florida: CRC Press. pp 165-166.

VODYANITSKII YN. 2009. Mineralogy and geochemistry of manganese: A review of publications. *Eurasian Soil Science*, 42(10): 1170-1178.

WALLMANN K, HENNIES K, KONIG J, PETERSON W & KNAUTH HD. 1993. New procedure for determining reactive Fe (III) and Fe (II) minerals in sediments. *Limnology and Oceanography*, 38(8): 1803-1812.

WHITE RE. 2006. *Principles and practice of soil science, the soil as a natural resource, fourth edition*. Oxford: Blackwell Publishing. pp 141-142.

WHITEHEAD DC. 1973. The sorption of iodide by soils as influenced by equilibrium conditions and soil properties. *Journal of the Science of Food and Agriculture*, 24: 547-556.

YAALON DH, JUNGREIS C & KOYUMDJISKY H. 1972. Distribution and reorganization of manganese in three catenas of Mediterranean soils. *Geoderma*, 7: 71-78.

YOON S, SANFORD RA & LOFFLER FE. 2013. *Shewanella* spp. use acetate as an electron donor for denitrification but not ferric iron or fumarate reduction. *Applied and Environmental Microbiology*, 79(8): 2818-2822.

ZAK DR, HOLMES WE, MACDONALD NW & PREGITZER KS. 1999. Soil temperature, matric potential, and the kinetics of microbial respiration and nitrogen mineralization. *Soil Science Society of America Journal*, 63: 575-585.

ZELAZNY LW, LIMINGM HE & VANWORMHOUDT AN. 1996. Charge analysis of soils and anion exchange. In: Sparks DL, Page AL, Helmke PA, Loeppert RH, Soltanpour PN, Tobatabai MA, Johnston CT & Summer MA (eds), *Methods of Soil Analysis. Part 3, Chemical Methods*. Madison: Soil Science Society of America. pp 1219, 1242-1243.

APPENDIX A – Figures relating to site descriptions in Chapter two

(a)  (b)  (c) 

Figure A1: Variation in soil colour moving down the quartzite catena with (a) representing the crest of the catena, (b) representing the midslope and (c) the valley bottom

Figure A2: Redoximorphic features present at Q_Mid indicating signs of wetness

(a)  (b)  (c) 

Figure A3: Variation in soil colour moving down the granite landscape (a) Soil collected at G_Crest (b) Soil sampled at G_Mid (c) Soil morphology at G_Bot with mottling present

Figure A4: Dolomite soil in the lower part of the landscape

(a)  (b) 

Figure A5:(a) Red andesite soil sampled (b) Cracks visible on the andesite soil

Figure A6: Ferromanganese wad mined in Ventersdorp

APPENDIX B – Supplementary data relating to Chapter three

Table B1: Elements (other than Mn, Fe and Al) detected by XRF

Sample	Ti	Mg	Ca	Na	K	P	Cr	Ni	V	Zr	Cu
Q1_Crest_A	40.6	2.48	1.78	3.23	13.5	5.11	1.84	2.42	0.54	1.33	0.69
Q1_Crest_B1	57.9	7.42	1.78	3.23	20.5	3.99	2.16	2.21	0.69	1.97	0.67
Q1_Crest_B2	68.9	11.4	1.78	3.23	21.8	3.87	2.54	2.48	0.80	2.47	0.70
Q2_Mid_A	43.7	2.48	1.78	3.23	18.9	3.52	1.54	1.87	0.45	1.69	0.57
Q2_Mid_B1	53.8	8.41	1.78	3.23	24.0	3.39	1.69	2.06	0.58	2.03	0.58

Q2_Mid_B2	60.2	12.8	1.78	3.23	27.5	3.19	3.32	2.26	0.81	2.18	0.67
Q3_Foot_A	47.2	2.48	1.78	3.23	17.8	2.38	1.59	1.66	0.48	1.87	0.50
Q3_Foot_B	61.4	12.6	1.78	3.23	28.0	2.61	2.28	2.25	0.68	2.17	0.60
Q4_Bot_A	38.5	2.48	1.78	3.23	15.0	3.33	1.46	1.45	0.55	1.54	0.50
V1_Black	107	803	998	25.7	57.0	3.41	6.70	4.40	2.16	1.10	1.85
V2_Brown	120	526	207	32.9	48.5	5.05	8.80	5.48	2.28	1.66	1.91
G1_Crest_A	38.2	10.5	1.78	8.42	340	4.09	0.80	1.53	0.39	1.64	0.58
G1_Crest_B	47.4	16.8	1.78	3.37	304	3.94	0.86	1.66	0.49	2.02	0.54
G2_Mid_A	38.8	2.48	1.78	3.23	220	3.45	0.88	1.51	0.38	1.87	0.48
G2_Mid_B	43.7	2.48	1.78	3.23	224	3.35	0.98	1.43	0.48	1.86	0.54
G3_Bot_A	28.4	2.48	1.78	3.23	151	3.00	0.82	1.39	0.36	1.28	0.54
G3_Bot_B1	43.6	2.48	1.78	3.23	160	3.18	0.97	1.61	0.50	1.82	0.52
G3_Bot_B2	27.6	2.48	1.78	3.23	157	2.75	1.15	1.26	0.39	1.13	0.44
D1_Crest_A	110	23.7	1.78	3.23	39.8	4.66	1.96	3.84	1.07	1.87	1.19
D2_Bot_A	79.2	21.0	1.78	3.23	172	5.71	1.34	2.04	0.82	1.87	0.68
A1_Mid_A	143	80.9	9.56	3.23	48.7	7.12	3.12	3.55	1.84	1.39	1.62
A1_Mid_B1	127	89.2	9.38	3.23	48.4	5.29	3.81	4.50	1.96	1.19	1.92
A1_Mid_B2	129	101	7.56	3.23	48.1	5.05	3.69	4.77	2.01	1.14	2.09
Mn Wad	13.5	14.4	4.39	3.23	31.9	7.83	2.09	3.49	0.96	0.41	0.77

Table B2: Significant Differences between Chemical Extractions and XRF Methods for Total Elemental Content - Fe

Sample	p-Values from T-Test for Significant Differences between Fe Contents		
	XRF & DC	XRF & CBD	DC & CBD
C3 0-20	$7.85*10^{-07**}$	$1.59*10^{-05**}$	0.04^{*}
C3 20-40	$1.77*10^{-08**}$	$6.65*10^{-08**}$	$1.55*10^{-03**}$
C3 40-60	$4.75*10^{-07**}$	$5.47*10^{-06**}$	$5.28*10^{-03**}$
D2 0-20	0.03^{*}	0.24	0.03^{*}
E 0-20	0.05	0.04^{*}	0.02^{*}
E 30-50	0.01^{*}	$5.57*10^{-04**}$	$3.25*10^{-03**}$
E 50-80	0.02^{*}	$9.09*10^{-03**}$	0.01^{*}

Table B3: Significant Differences between Chemical Extractions and XRF Methods for Total Elemental Content - Al

Sample	p-Values from T-Test for Significant Differences between Al Contents		
	XRF & DC	XRF & CBD	DC & CBD
C3 0-20	$7.21*10^{-10**}$	$3.84*10^{-08**}$	0.03*
C3 20-40	$1.84*10^{-10**}$	$4.56*10^{-10**}$	$4.33*10^{-03**}$
C3 40-60	$1.19*10^{-09**}$	$3.09*10^{-09**}$	$4.41*10^{-03**}$
D2 0-20	$2.25*10^{-07**}$	$1.83*10^{-08**}$	$3.02*10^{-04**}$
E 0-20	$1.43*10^{-06**}$	$6.56*10^{-09**}$	$1.83*10^{-03**}$
E 30-50	$2.24*10^{-06**}$	$5.14*10^{-09**}$	$2.11*10^{-03**}$
E 50-80	$6.2*10^{-07**}$	$2.11*10^{-09**}$	$4.11*10^{-04**}$

APPENDIX C - Semi-quantitative mineralogical soil analysis by XRD

Mn minerals were expected to be present, particularly in the dolomite and basalt derived vertic soils. This was due to the high Mn content detected in these soils by XRF. The mineralogical characterization, however, did not show any Mn oxides. It is not only the Mn oxides, however, that are of importance to reveal Mn in the soil. A study by Stiers & Schwertmann (1985) revealed that substitution of Mn (postulated to be in the trivalent state)

for Fe in goethite (α-FeOOH) increases the unit cell size of the mineral to approach that of groutite (α-MnOOH), thereby modifying the crystallinity of the structure. This substitution of Mn for Fe also appeared to increase the thermal stability of the mineral (Stiers & Schwertmann, 1985). Research conducted by Alvarez et al. (2006) concurred with this, revealing that Mn substituted goethite is thermally more stable than non-substituted goethite. The same effect was seen in Al substituted goethite (Alvarez et al., 2006). It is therefore possible that Mn substitution in Fe oxides has the same stabilizing effect that Al substitution provides. This would influence the reduction of Fe, having a direct effect on the formation of redoximorphic features in the soil.

Materials and method

Clay Preparation for XRD

There is no particular way to prepare samples for mineralogical analysis as each preparation technique will vary according to the analysis required (Moore & Reynolds, 1997). In order to minimise destruction of Mn oxides, the primary focus of the mineralogical study, no pre-treatments were conducted on the samples. In order to obtain the clay fraction, a similar procedure was followed to that of soil texture analysis. Stoke's law was used to determine the clay settling time. The sample was left for the pre-determined settling time and thereafter saturated with 1 M MgCl in order to flocculate the clay before analysis. The isolated clay fraction was dried and milled in a tungsten carbide vessel. Samples were then prepared according to the Panalytical backloading system. This preparation technique ensures that a nearly random distribution of the particles is achieved.

The use of chemical pre-treaments was avoided in an attempt to preserve the Mn oxides present in the samples. The suggested pre-treatment to concentrate Mn oxides involves the boiling of the soil samples with 5 M NaOH to remove kaolinite, followed by the removal of birnessite by washing the sample with unacidified hydroxylamine hydrochloride and lastly a CBD extraction to remove any remaining reducible oxides. Chemical pre-concentrations prior to mineralogical analysis, however, can create artefacts. A 5 M NaOH is fairly concentrated and can cause Mn minerals, such as lithiophorite, to become unstable and the crystallization of birnessite to be enhanced (Dowding, 2004). A study by Dowding & Fey (2007) using chemical pre-treatments still found that lithiophorite was not easily identified due to its poor crystallinity, even though it is the most stable Mn oxide in environments subjected to strong weathering.

XRD analysis

Samples were analysed using a PANalytical X'Pert Pro powder diffractometer in θ–θ configuration with an X'Celerator detector and variable divergence- and fixed receiving slits with Fe filtered Co-Kα radiation(λ=1.789Å). The phases were identified using X'Pert Highscore plus software. The relative phase amounts (weight %) were estimated using the Rietveld method (Autoquan Program). Errors were reported on the 3 sigma level. Amorphous phases, if present were not taken into consideration in the quantification.

Quartzite/Sandstone Geology (Q Samples)

Results in Table C1 reveal that the mineral that dominated these soils was kaolinite, which is a 1:1 clay mineral. This indicates that these soils are highly weathered. The amount of kaolinite increased as the position of sampling moves lower down the landscape. This is typical of a South African Highveld plinthic catena. As water moves further down the landscape, increased weathering is stimulated. This suggests that water movement occurs down the slope. Water also tends to carry weathering products downslope.

Table C1: Mineralogy of quartzite samples

Sample	Mineral	Chemical Formula	Weight %	3 σ error
Q_Crest_A	Anatase	TiO_2	3.07	0.33
	Goethite	FeOOH	10.2	0.75
	Hematite	Fe_2O_3	3.84	0.42
	Kaolinite	$Al_2(Si_2O_5)(OH)_4$	68.6	1.11
	Quartz	SiO_2	14.3	0.57
Q_Crest_B1	Anatase	TiO_2	6.12	0.78
	Goethite	FeOOH	15.9	1.68
	Hematite	Fe_2O_3	9.08	0.99
	Kaolinite	$Al_2(Si_2O_5)(OH)_4$	57.0	1.34

	Quartz	SiO_2	11.9	1.37
Q_Crest_B2	Anatase	TiO_2	2.87	0.33
	Goethite	FeOOH	10.2	0.90
	Hematite	Fe_2O_3	4.81	0.42
	Kaolinite	$Al_2(Si_2O_5)(OH)_4$	71.3	1.23
	Quartz	SiO_2	10.9	0.60
Q_Mid_A	Anatase	TiO_2	3.27	0.33
	Goethite	FeOOH	7.27	0.78
	Hematite	Fe_2O_3	1.18	0.39
	Kaolinite	$Al_2(Si_2O_5)(OH)_4$	78.2	1.32
	Quartz	SiO_2	10.1	0.93
Q_Mid_B1	Anatase	TiO_2	3.35	0.33
	Goethite	FeOOH	7,51	0.75
	Hematite	Fe_2O_3	0.79	0.36
	Kaolinite	$Al_2(Si_2O_5)(OH)_4$	72.4	1.02
	Quartz	SiO_2	16	0.51
Q_Mid_B2	Anatase	TiO_2	3.22	0.33
	Goethite	FeOOH	6.14	0.75
	Hematite	Fe_2O_3	0	0
	Kaolinite	$Al_2(Si_2O_5)(OH)_4$	79.2	0.99
	Quartz	SiO_2	11.4	0.54
Q_Foot_A	Kaolinite	$Al_2(Si_2O_5)(OH)_4$	78.1	1.32
	Muscovite	$KAl_2(AlSi_3O_{10})(OH)_2$	11.6	1.20
	Quartz	SiO_2	10.4	0.84
Q_Foot_B	Anatase	TiO_2	3.43	0.39
	Goethite	FeOOH	1.58	0.69
	Kaolinite	$Al_2(Si_2O_5)(OH)_4$	80.9	0.96
Q_Bot_A	Anatase	TiO_2	3.47	0.33
	Goethite	FeOOH	1.98	0.60
	Kaolinite	$Al_2(Si_2O_5)(OH)_4$	80.7	1.08
	Quartz	SiO_2	13.9	0.90

The second most abundant mineral in the Q_Crest and Q_Mid samples is goethite, which explains the high Fe content found in these samples, particularly Q_Crest. The Q_Foot_A sample has muscovite as its second most abundant mineral indicating a presence of potassium in the soil in this area. XRF determined a quantity of 17.8 mmol K per kg soil for this sample. The Q_Foot subsoils and Q_Bot sample have a considerable amount of quartz. This could be due to incomplete separation of silt from the clay fraction but it is possible that the quartz in these samples is organically bound. All samples, except Q_Foot_A, have a similar content of anatase, indicating a presence of titanium in these soils.

The kaolinite, goethite and anatase (in decreasing order of quantity) that are present in all samples is in accordance with a study conducted by Singh & Gilkes (1996). This also revealed that these minerals were the most abundant in the soil matrix and mottles. Hematite was also present in small amounts as is the case for the quartzite soils in this study. These

soils exhibit mottling, particularly the Q_Mid_B2 and Q_Foot_B samples, as did the soils studied by Singh & Gilkes (1996).

Basalt / Shale Geology (V Samples)

Both samples are dominated by kaolinite as seen in Table C2. The V_Black sample is black in colour while the V_Brown is brown. The higher amount of goethite as well as the presence of magnetite in the V_Brown sample explains the brown colour of V_Brown due to the higher Fe content in this sample. The Mn mineral that was expected in these samples is birnessite as this is a Ca containing mineral typically found in calcareous soils (Vodyanitskii, 2009) such as these. This expectation stems from the Ca present in the morphology of these samples, supported by the detection of 998 mmol.kg^{-1}Ca in the V_Black sample and 207 mmol.kg^{-1} in the V_Brown sample by XRF analysis. Neither birnessite nor any other Mn minerals is detected in the samples. It was also expected that smectite would be found in these samples, however this could not be identified. This is not unusual as the smectite peak of vertic clays is very large and often masks and encompasses adjoining small peaks (Murthy et al., 1999). An example of the diffractogram for the black vertic is provided in Figure C1. A clay mineral that was identified however was montmorillonite.

Table C2: Mineralogy of basalt (vertic) samples

Sample	Mineral	Chemical Formula	Weight %	3 σ error
V_Black	Anatase	TiO_2	2.72	0.57
	Goethite	FeOOH	2.63	1.11
	Hematite	Fe_2O_3	0	0
	Kaolinite	$Al_2(Si_2O_5)(OH)_4$	74.9	1.83
	Quartz	SiO_2	19.8	1.50
V_Brown	Goethite	FeOOH	7.66	0.90
	Kaolinite	$Al_2(Si_2O_5)(OH)_4$	72.5	1.35
	Magnetite	Fe_3O_4	3.40	0.45
	Quartz	SiO_2	14.2	1.05
	Zircon	$ZrSiO_4$	2.23	0.39

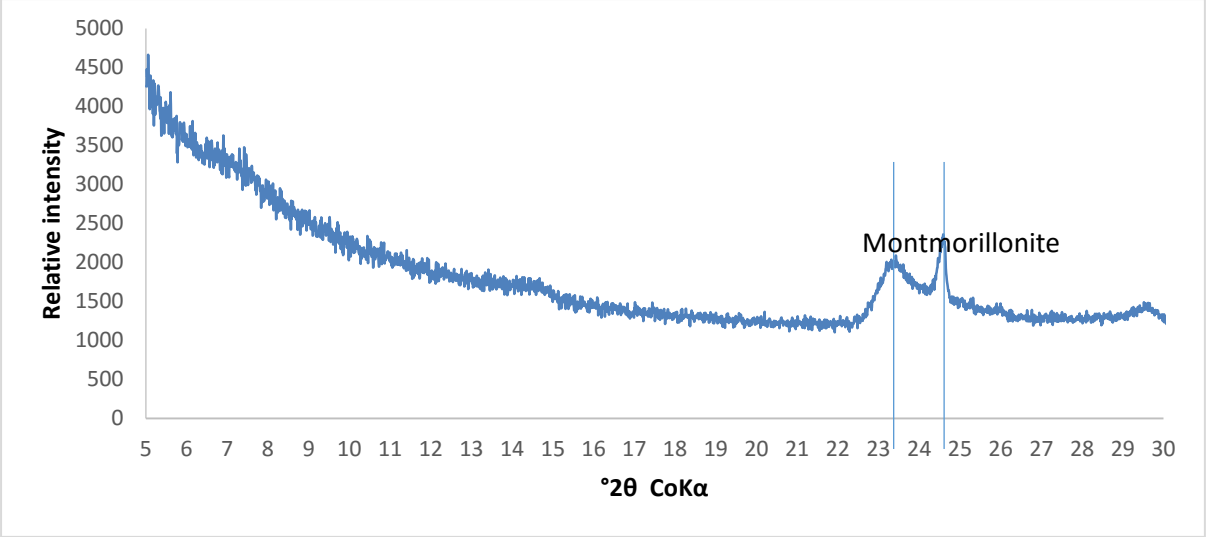

Figure C1: Diffractogram for V_Black

Granite Geology (G Samples)

The kaolinite present, as shown in Table C3, is indicative of the highly weathered nature of the soils but could also explain the high amount of Al found in these soils. In all samples, kaolinite is the most abundant mineral. The G_Crest_B and G_Mid_B have about 10% muscovite, a mineral commonly associated with granite soils. The G_Bot samples contain rutile, which is a polymorph of the anatase titanium dioxide (Nolan et al., 1987). Less hematite is detected in the granite samples than the quartzite samples. This explains the higher Fe content in the quartzite samples. The amount of hematite in the granite samples appears to decrease downslope, which is in accordance with the loss of red colour from the summit to the bottom of the catena. The G_Bot samples, that exhibit mottling, have rutile present in small amounts, which is in accordance with a study conducted by Singh & Gilkes (1996) investigating iron rich glaebules and mottles in Australian soils that also found rutile in the samples containing mottles.

Table C3: Mineralogy of granite samples

Sample	Mineral	Chemical Formula	Weight %	3 σ error
G_Crest_A	Hematite	Fe_2O_3	2.14	0.36
	Kaolinite	$Al_2(Si_2O_5)(OH)_4$	81.6	1.17
	Muscovite_2M1	$KAl_2(AlSi_3O_{10})(OH)_2$	10.4	0.99
	Quartz	SiO_2	5.84	0.45
G_Crest_B	Hematite	Fe_2O_3	2.03	0.39
	Kaolinite	$Al_2(Si_2O_5)(OH)_4$	80.4	1.14
	Muscovite	$KAl_2(AlSi_3O_{10})(OH)_2$	9.64	0.99
	Quartz	SiO_2	7.98	0.39
G_Mid_A	Anatase	TiO_2	2.99	0.39
	Hematite	Fe_2O_3	0.66	0.42
	Kaolinite	$Al_2(Si_2O_5)(OH)_4$	85.6	1.17
	Quartz	SiO_2	10.7	0.99
G_Mid_B	Anatase	TiO_2	3.41	0.36
	Hematite	Fe_2O_3	0.17	0.42
	Kaolinite	$Al_2(Si_2O_5)(OH)_4$	76.2	1.44
	Muscovite	$KAl_2(AlSi_3O_{10})(OH)_2$	10.3	1.02
	Quartz	SiO_2	9.91	0.87
G_Bot_A	Anatase	TiO_2	3.10	0.36
	Kaolinite	$Al_2(Si_2O_5)(OH)_4$	80.2	1.05
	Quartz	SiO_2	15.7	0.93
	Rutile	TiO_2 *(similar structure to MgF_2)*	1.07	0.33
G_Bot_B1	Anatase	TiO_2	3.06	0.36
	Kaolinite	$Al_2(Si_2O_5)(OH)_4$	83.8	1.02
	Quartz	SiO_2	12.3	0.87
	Rutile	TiO_2 *(similar structure to MgF_2)*	0.91	0.33
G_Bot_B2	Anatase	TiO_2	3.19	0.36
	Kaolinite	$Al_2(Si_2O_5)(OH)_4$	87.3	0.87
	Quartz	SiO_2	9.51	0.78

Dolomite Geology (D Samples)

Table C4 shows that both samples were dominated by kaolinite. The hematite detected explains the Fe content in the samples, however, the low values suggest that much of the Fe is probably amorphous and poorly crystalline. This is in accordance with results from the ammonium oxalate extract, which indicates that the dolomite soils have a very high amorphous Fe content. There is a lack of Mn oxides in the mineralogy of these soils.

Table C4: Mineralogy of dolomite samples

Sample	Mineral	Chemical Formula	Weight %	3 σ error
D_Crest_A	Anatase	TiO_2	2.96	0.36
	Hematite	Fe_2O_3	8.25	0.60
	Kaolinite	$Al_2(Si_2O_5)(OH)_4$	79.4	1.23
	Quartz	SiO_2	9.36	0.93
D_Bot_A	Anatase	TiO_2	3.08	0.36
	Hematite	Fe_2O_3	6.96	0.54
	Kaolinite	$Al_2(Si_2O_5)(OH)_4$	83.0	0.84
	Quartz	SiO_2	6.98	0.48

Andesite Geology (A Samples)

As with the other soil samples, these soils are characterized by a dominance of kaolinite, which is seen in Table C5. The hematite explains the red colour observed in these soils as well as the Fe content. Similar to the dolomite sample, the low hematite content detected suggests that a large fraction of the Fe is in the non-crystalline phase. The goethite present in the sample explains the prevalence of Al in these soils due to isomorphous substitution of Al^{3+} for Fe^{3+}, which is a commonly occurring phenomenon in goethite in soils. The morphology of these soils demonstrates a large number of concretions. Due to the Mn concretions observed in these soils, it was anticipated that Mn minerals would be found in these soils, Fe-containing vernadite in particular. This mineral is commonly found in Fe-Mn nodules and is generally well contained centrally in the nucleus of these nodules. This feature provides a high resistance to reduction (Vodyanitskii, 2009). This would have explained the considerable Mn content in the soil. There are no Mn oxides, however, detected in these samples.

Table C5: Mineralogy of andesite samples

Sample	Mineral	Chemical Formula	Weight %	3 σ error
A_Mid_A	Hematite	Fe_2O_3	6.33	0.57
	Kaolinite	$Al_2(Si_2O_5)(OH)_4$	91.6	0.72
	Quartz	SiO_2	2.12	0.42
A_Mid_B1	Anatase	TiO_2	2.82	0.33
	Goethite	FeOOH	6.97	0.78
	Hematite	Fe_2O_3	5.86	0.45
	Kaolinite	$Al_2(Si_2O_5)(OH)_4$	82.1	1.02
	Quartz	SiO_2	2.24	0.42
A_Mid_B2	Anatase	TiO_2	2.82	0.33
	Goethite	FeOOH	7.21	0.75
	Hematite	Fe_2O_3	5.49	0.45
	Kaolinite	$Al_2(Si_2O_5)(OH)_4$	82.4	1.02
	Quartz	SiO_2	2.05	0.39

Ferromanganese Wad

The mineralogy of the wad, shown in Table C6, is dominated by hematite (more than 50% of the sample). This is expected due to the naturally high Fe content of these minerals. Goethite is also prevalent, constituting approximately 20% of the sample. Kaolinite is detected to a lesser extent with a small amount of quartz also analysed. Similarly to the high Mn containing dolomite soils, no Mn oxides could be detected in the wad.

Table C6: Mineralogy of Mn wad

Sample	Mineral	Chemical Formula	Weight %	3 σ error
Mn wad	Goethite	FeOOH	19.8	1.23
	Hematite	Fe_2O_3	58.9	1.86
	Kaolinite	$Al_2(Si_2O_5)(OH)_4$	13.4	1.89
	Muscovite	$KAl_2(AlSi_3O_{10})(OH)_2$	2.24	1.89
	Quartz	SiO_2	5.6	0.66

Summary of Mn (IV) oxides

It was expected that Mn oxides would be detected in many of these samples, especially those derived from dolomite, basalt and andesite as well as the ferromanganese wad due to the high Mn content, however, none were detected. This could be the result of Mn oxides having poor crystallinity (Tokashiki et al., 1986; Zhang & Karthanasis, 1997; Post, 1999). It could also be a function of the Mn oxides being non-stoichiometric with disordered structures and having small crystal sizes as well as lack of single crystals, qualities making their detection difficult (Gilkes & McKenzie, 1988; Post, 1999).

A further complication could be the insensitivity of XRD for weakly diffracting but crystalline Mn oxides (Gilkes & McKenzie, 1988) due to diffuse XRD patterns as well as coincidence of diagnostic diffraction peaks with associated minerals (Tokashiki et al., 1986; Post, 1999). The X-ray lines of silicate phases are often confused with those of Mn oxides (Potter & Rossman, 1979). It is often difficult to detect the commonly occurring mineral, birnessite, in the presence of kaolinite ($Al_2(Si_2O_5)(OH)_4$) due to the similar intensity of the peaks (Taylor et al., 1964). Other examples of coincidence are the similar d-spacings of todokorite to mica and gibbsite ($Al(OH)_3$) as well as the similar major peaks of nsutite ($(Mn^{4+}, Mn^{2+})(O, OH)_2$) to that of maghemite ($Fe_2O_3$) (Dowding, 2004).

Yet another complication of studying Mn mineralogy is that Mn forms a vast amount of oxides and hydroxides where substitution of Mn^{2+} and Mn^{3+} for Mn^{4+} occurs extensively (McKenzie, 1972; Post, 1999). This can happen frequently as Mn oxides have a large surface area and can therefore readily participiate in many redox and cation exchange reactions (Post, 1999). The complexity of studying Mn mineralogy is also explained by the wide range of structures they can exist in, many of which can readily accommodate several other metal cations (Post, 1999). It is important to take into consideration that factors such as cation substitution, non-stoichiometry, crystal disorder and small crystal size all result in changes in unit cell dimensions and line broadening making positive identification of Mn oxides very

difficult to analyze by XRD (McKenzie, 1989). All of these reasons contribute to why data on Mn minerals is sparse and was often excluded in the past from soil mineralogical analysis as dissolvable impurities (Golden et al., 1993).

The lack of detection of Mn peaks in this study could also have been a result of experimental error with ineffective removal of Si causing the quartz to block the expression of Mn peaks. Another possibility is the loss of Mn oxides with the removal of the silt fraction. It has been identified that many Mn compounds in soil have an affinity for the silt faction due to their negative charge (as a result of their generally low point of zero net charge) in the typical pH range of most soils (Vodyanitskii, 2009).

A possible way that the detection of Mn oxides could have been improved is by the removal of kaolinite. This would have been useful for the soils in this study as they are all dominated by the presence of kaolinite. It therefore appears that the avoidance of pre-treatments in an attempt to preserve the natural state of the Mn oxides in the soils did not prove useful for their detection and pre-treatments are necessary. Since this was beyond the scope of this study this was not further investigated.

Recent developments in analytical procedures have improved Mn mineralogy identification (Golden et al., 1993). Coupling XRD with other techniques such as transmission electron microscopy (TEM), infra-red (IR) spectroscopy, Rietveld refinement using powder diffraction data, extended X-ray absorption fine-structure microscopy, electron microprobe analysis, as well as single crystal studies using charge-coupled device detectors and synchrotron sources have helped overcome many of the challenges associated with studying Mn mineralogy (Post, 1999). In-depth mineralogical analysis was beyond the scope of the study and therefore no further analysis was conducted.

APPENDIX D -Scanning electron microscopy of Mn wad

Materials and method:

Samples were embedded and left to set for a week. Thereafter, the samples were ground down and polished in order to obtain a smooth surface. This procedure was followed by the carbon coating of the samples. The samples were then analysed using a JEOL JSM 5800 LSV SEM, JEOL, Japan machine with a Thermo Scientific detector. The software used was NSS 2.3. The images produced were secondary electron images and backscatter electron imaging. The quantitative results were obtained by EDS spectral imaging and point and shoot analysis. The acceleration voltage used was 20 kV and the working distance was 10 mm.

Results and discussion:

Scanning electron microscopy (SEM) is a well established method for obtaining chemical and micromorphological data (Sparks, 2003; Buol et al., 2011; Schaetzl & Anderson, 2005). Its application in clay mineralogy is common (Markgraf, 2006). SEM is more useful than other optical methods because it provides a larger depth of field (the range of distance that appears in acceptably sharp focus) as well as greater resolution (Schaetzl & Anderson, 2005).

This technique makes use of a high-energy focused electron beam that scans across a sample in a pattern of parallel lines (raster). Once contact is made between the beam and the sample, secondary (backscattered) electrons are captured by a detector. The detector primarily captures electrons at the surface of the samples and is used to produce a map of the sample surface. A useful tool that can be coupled with SEM is EDS (energy dispersive spectroscopy). This provides the location and non-destructive quantitative analysis of elements within a sample. It also enables the identification of the sites where a specific element is dominant (Schaetzl & Anderson, 2005).

Figure D1 below shows SEM images of the Mn wad sample. The highly porous nature of the sample can be clearly seen in these images.

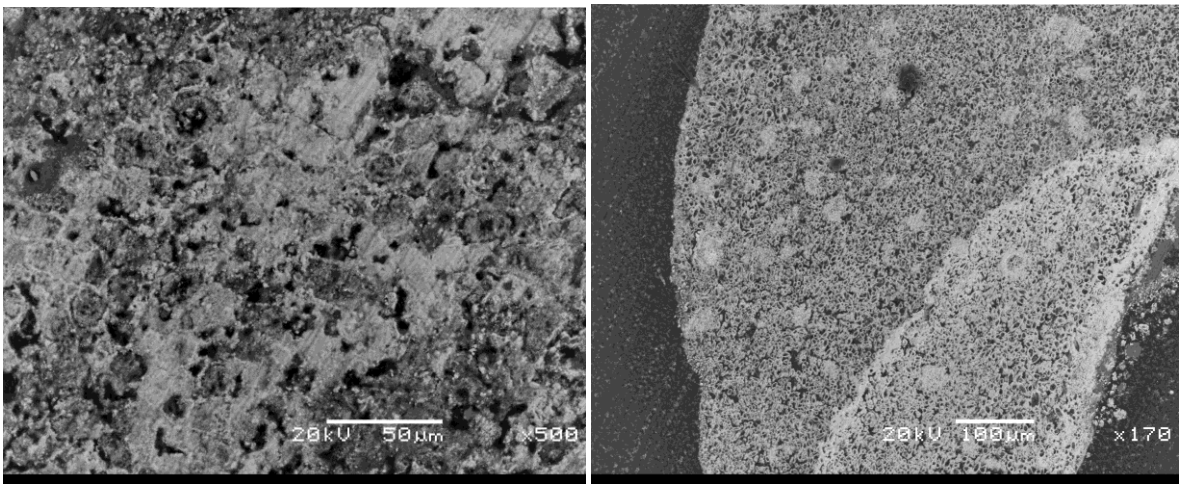

Figure D1: SEM images of Mn wad sample

The spectral image of the wad is illustrated in Figure D2. The entire scanned area appears to be dominated by Fe and O to a lesser extent. The lighter areas on the grey scale image appear to be dominated by Mn. It is the Fe, Mn and O that therefore interact with each other, which is expected of a ferro-manganese wad. The elements associated with wad include O, Si, Cl, Mn, Fe, Al, K, F, Ba, Mg, Ca and Ti. Much of this can be explained by the XRD results for this sample (refer to Appendix C). Oxygen is present in all of the minerals that were picked up in the wad. The Si results from the quartz, kaolinite and muscovite minerals detected by XRD. The prevalence of Fe comes from the hematite and goethite that dominate the mineralogy (59% and 20% of the mineral respectively). The Al present comes from the kaolinite and muscovite with K present also generated from the latter mineral. The Cl present could have come from several environmental sources as explained for the dolomite sample. There is less Cl picked up in the wad than the dolomite. The results obtained for this study are similar to the results from the mineralogical analysis that was conducted by Pack et al., (2000). Not all of the minerals picked up by Pack et al. (2000) however, were picked up by XRD analysis. It is therefore possible that improper sample preparation resulted in many minerals not being detected for the Mn wad sample.

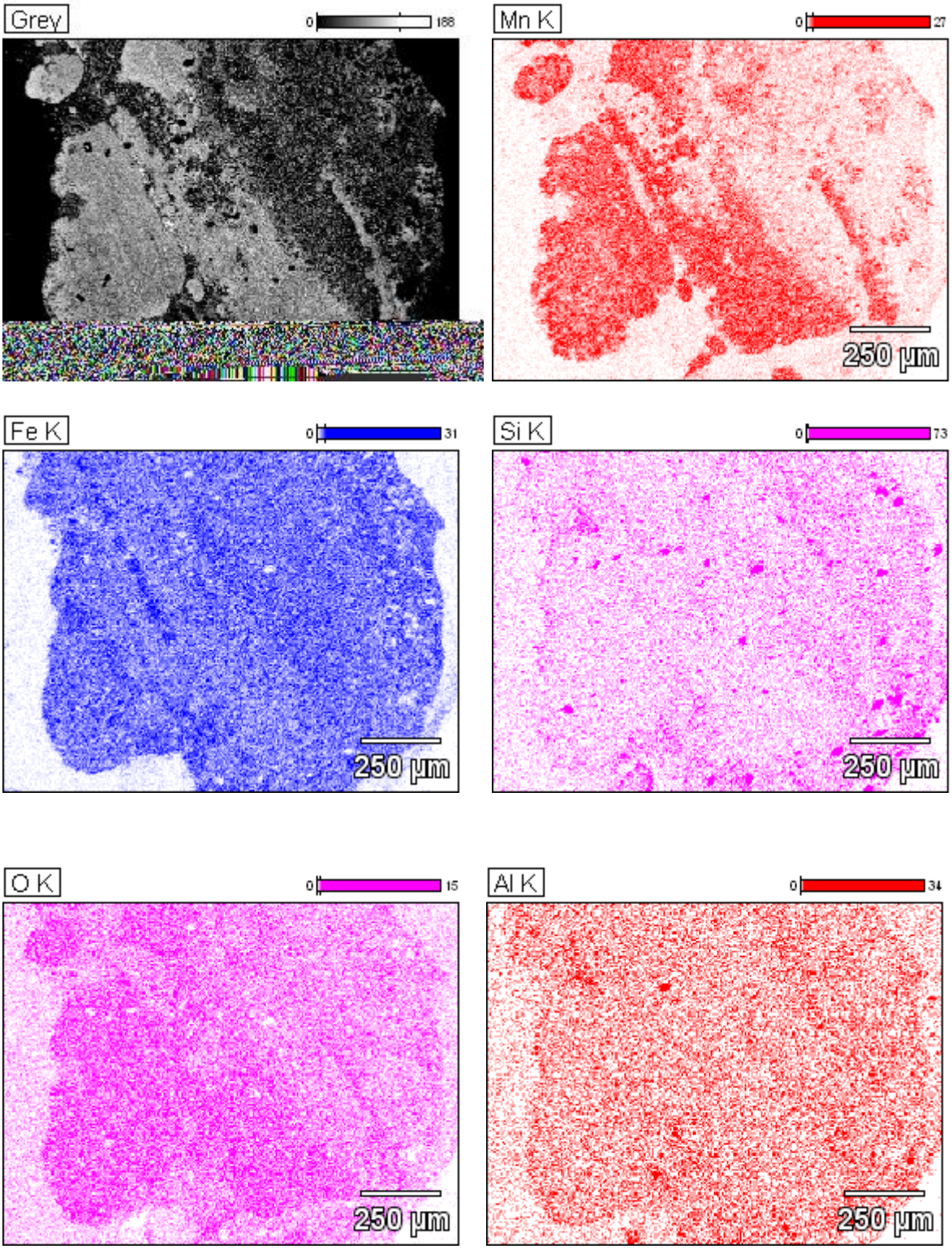

Figure D2: Map of the distribution and relative proportion (intensity) of elements in the wad sample at a magnification of 90 and acceleration voltage of 20 kV

The mineralogical study by Pack et al. (2000) revealed the following minerals that could explain their presence in the SEM analysis of the wad sample. The TiO_2 found in the

mineralogy could explain the Ti detected by SEM and the Fe and Mn carbonates detected could explain the Ca from the SEM analysis. The trace quantities of Ba could be explained by Ba-poor romanecite with the formula $(Ba_{0.38-0.39}K_{0.14-0.19}Na_{0.04-011})Mn_{7.74-7.76}O_{16}\cdot 2.57H_2O$ detected by Pack et al. (2000). The SEM analysis shows a high quantity of Mn, which is picked up by XRF but no Mn minerals are detected by XRD. Pack et al. (2000) found cryptomelane ($KMn^{4+}{}_6Mn^{2+}{}_2O_{16}$), nsutite ($\gamma$-$MnO_2$) and trace amounts of lithiophorite ($LiAl_2[Mn(IV)_2Mn(III)]O_6(OH)_6$). All three are considered important Mn oxide minerals (Post, 1999). It's possible that errors in sample preparation prevented XRD analysis from detecting these minerals. It is also possible that in the particular sample analysed the Mn could not be detected in the crystal structure due to the highly amorphous nature of it.

The first portion of the Mn wad scanned is Mn wad_1 as seen in Figure C9. Results for the first portion of the Mn wad sanned are given in Table D1. For all points and areas scanned, Fe is the dominant element. The only exception is point 3 where Mn dominates. Mn is the second most abundant element in the areas and points scanned, followed by O. Unlike the dolomite sample, Al is found in trace quantities, comparable to the other trace elements found in the sample.

Table D1: Weight percentage elemental composition at different points for Mn wad_1

	O	F	Mg	Al	Si	Cl	K	Ca	Ti	Mn	Fe	Co	Sr	Ba
Base(9)_pt1	14.4			1.1	0.5	1.1	0.9	0.2		36.9	42.8			2.1
Base(9)_pt2	13.3	0		2	2.6	3.4				13.4	65.4			
Base(9)_pt3	10.1		0.5	1.3	0.3	0.5	1.6		0.4	68.2	14.7			2.4
Base(9)_pt4	12.7		0.3	1	0.3	0.8	0.8			32.8	50	0		1.3
Base(9)_pt5	9.8			2.5	3	3.4				17.5	63.7			
Base(9)_pt6	0	0		2	2.5	3.7				9	82.9			
Base(9)_pt7	10.9	0		2	2.2	4.2				13.2	67.2		0.4	
Base(9)_pt8	9.1		0.2	1	1	2.1	0.4			19	66.5			0.8
Base(9)_pt9	13.3	0		1.9	2.1	2.3	0.6			24.3	55.5			

A second portion of the Mn wad was investigated and the results are provided in Table D2. The results are very similar to that of the first area scanned (Table D1), with the only difference being that in this particular area there is much less Mn and the ratio of Fe:Mn is larger than in the first area scanned. There are also fewer trace elements, which could suggest that trace elements have a higher affinity for Mn oxides than Fe oxides.

Table D2: Weight percentage elemental composition at different points for Mn wad_2

	O	Al	Si	Cl	Mn	Fe
Base(3)_pt1	17.7	0	1.2	5.7	3	72
Base(3)_pt2	24.6	1	1.2	0.5	2	71.2
Base(3)_pt3	24.8	0	1.2	1.4	2.5	69.8

Analysis of the Mn wad shows a strong interaction between Fe, Mn and O. It is therefore possible that Mn oxides have an affinity for Fe and could possible poise redox reactions by oxidizing Fe^{2+} in its reduced form and incorporate it in its crystal structure. The problem that SEM poses is that it only permits analysis of a very small section of the sample being observed (Brodowski, 2005) and therefore does not cover the heterogeneity of the mineral being examined. Therefore not all of the elements in the sample could be identified.

REFERENCES FOR APPENDICES

ALVAREZ M, RUEDA EH & SILEO EE. 2006. Structural characterization and chemical reactivity of synthetic Mn – goethites and hematites. *Chemical Geology*, 231: 288-299.

BRODOWSKI S, AMELUNG W, HAUMAIER L, ABETZ C & ZECH W. 2005. Morphological and chemical properties of black carbon in physical soil fractions as revealed by scanning electron microscopy and energy-dispersive X-ray spectroscopy. *Geoderma*, 128: 116-129.

BUOL SW, SOUTHARD RJ, GRAHAM RC & McDANIEL PA. 2011. *Soil genesis and classification, sixth edition*. Oxford: Wiley – Blackwell. pp 80.

DOWDING CE. 2004. Morphology, mineralogy and surface chemistry of manganiferous oxisols near Graskop, Mpumalanga Province, South Africa. MSc. dissertation, Stellenbosch University, South Africa. pp 31 - 32.

DOWDING CE & FEY MV. 2007. Morphological, chemical and mineralogical properties of some manganese-rich oxisols derived from dolomite in Mpumalanga province, South Africa. *Geoderma*, 141: 23-33.

GILKES RJ & MCKENZIE RM. 1988. Geochemistry and mineralogy of manganese in soils. In: Graham RD, Hannam RJ & Uren NC (eds), *Manganese in Soils and Plants.* Dordrecht: Kluwer Academic Publishers. pp 23-95.

GOLDEN DC, DIXON JB & KANEHIRO Y. 1993. The manganese oxide mineral, lithiophorite, in an oxisol from Hawaii. *Australian Journal of Soil Research*, 31: 51-66.

MARKGRAF W. 2006. Microstructural changes in soils, rheological investigations in soil mechanics. PhD thesis, Christian-Albrechts-Universitatzu Kiel, Germany.

McKENZIE RM. 1972. The manganese oxides in soils - A review. *Z. Pflanzenerahr. Bodenk.* 131: 221-242.

McKENZIE RM. 1989. Manganese oxides and hydroxides. In: Dixon JB & Weed SD (ed.), *Minerals in Soil Environments. Second Edition*. Madison: Soil Science Society of America. pp 439-460.

MOORE DM & REYNOLDS RC. 1997. *X-Ray diffraction and the identification and analysis of clay minerals*. New York: Oxford University Press. pp 204-226.

MURTHY ILYN, DATTA SC, SASTRY TG &RATTAN RK. 1999. Nature and relative abundance of smectite in clays of Vertisols derived from different parent materials. *Agropedology*, 9: 47-53.

NOLAN RP, LANGER AM, WEISMAN I & HERSON GB. 1987. Surface character and membranolytic activity of rutile and anatase: two titanium dioxide polymorphs. *Br. J. Ind. Med*., 44(10): 687-698.

PACK A, GUTZMER J, BEUKES NJ & VAN NIEKERK HS. 2000. Supergene ferromanganese wad deposits derived from permian Karoo strata along the late cretaceous – mid – tertiary African land surface, Ryedal, South Africa. *Economic Geology*, 95: 203-220.

POST JE. 1999. Manganese oxide minerals: Crystal structures and economic and environmental significance. *Proceedings of the National Academy of Sciences USA*, 96: 3447-3454.

POTTER RM & ROSSMAN GR. 1979. The tetravalent manganese oxides: identification, hydration, and structural relationships by infrared spectroscopy. *American Mineralogist*, 64: 1199-1218.

SCHAETZL RJ & ANDERSON S. 2005. *Soils, genesis and geomorphology*. New York: Cambridge University Press. pp 26-29.

SINGH B & GILKES RJ. 1996. Nature and properties of iron rich glaebules and mottles from some South-west Australian soils. *Geoderma*, 71: 95-120.

SPARKS DL. 2003. *Environmental Soil Chemistry, Second Edition*. California: Academic Press. pp 41.

STIERS W & SCHWERTMANN U. 1985. Evidence for manganese substitution in synthetic goethite. *Geochimica et Cosmochimica Acta*, 49: 1909-1911.

TAYLOR RM, McKENZIE RM & NORRISH K. 1964. The mineralogy and chemistry of manganese in some Australian soils. *Australian Journal of Soil Research*, 2: 235-248.

TOKASHIKI Y, DIXON JB & GOLDEN DC. 1986. Manganese oxide analysis in soils by combined x-ray diffraction and selective dissolution methods. *Soil Science Society of America Journal*, 50: 1079-1084.

VODYANITSKII YN. 2009. Mineralogy and geochemistry of manganese: A review of publications. *Eurasian Soil Science*, 42(10): 1170-1178.

ZHANG M & KARTHANASIS AD. 1997. Characterization of iron – manganese concretions in Kentucky Alfisols with perched water tables. *Clay and Clay Minerals*, 45(3): 428-439.